This dissertation has been
microfilmed exactly as received 68-13,345

KURZENBERGER, John Lewis, 1936-
THE USE OF CONSTRAINTS TO IMPROVE NUMERICAL INTEGRATION OF TRAJECTORIES ON DIGITAL COMPUTERS.

The University of Michigan, Ph.D., 1968
Engineering, aeronautical

University Microfilms, Inc., Ann Arbor, Michigan

THE USE OF CONSTRAINTS TO IMPROVE NUMERICAL INTEGRATION OF TRAJECTORIES ON DIGITAL COMPUTERS

by

John Lewis Kurzenberger

A dissertation submitted in partial fulfillment
of the requirements for the degree of
Doctor of Philosophy in
The University of Michigan
1968

Doctoral Committee:

Doctor Laurence E. Fogarty, Co-Chairman
Professor Donald T. Greenwood, Co-Chairman
Professor Harm Buning
Professor Robert M. Howe
Doctor Lynn E. Wolaver, Wright-Patterson Air Force Base

Abstract

THE USE OF CONSTRAINTS TO IMPROVE NUMERICAL INTEGRATION OF TRAJECTORIES ON DIGITAL COMPUTERS

By John Lewis Kurzenberger

The purpose of this study is twofold. First, it is desired to develop a method for computing orbits under the influence of small perturbing forces which is similar in complexity to the simple integration of the standard translational equations of motion. Such a method will be applicable to the use of small to moderate size digital computers with relatively simple integration routines. Second, it is desired that the resulting equations be free from many of the singularities encountered in the standard variation of orbital elements technique so that they can be used to consider the full range of orbital trajectories.

The method developed makes use of five quantities which result from the three components of the angular momentum vector, referred to a rotating coordinate system, and two components of the eccentricity vector, referred to an inertial coordinate system. The five quantities thus obtained vary slowly under the influence of small perturbing forces and can therefore be obtained accurately using relatively large integration step sizes and simple integration routines. A sixth variable of integration is selected to be an angle measured from the intersection of the instantaneous plane of motion with an inertial plane to the position vector from the center of the earth. At each integration step, the vehicle radial position and inertial velocity components are constrained to be consistent with the six variables of integration. As the only significant singularity contained within these equations arises for cases when angular momentum approaches zero, the equations can be used without adjustment to consider the full range of circular, elliptic, parabolic, and hyperbolic trajectories, including transitions from one to another.

Solutions are obtained with this method for a number of orbital problems including the cases of non-perturbed Keplerian trajectories, a radial perturbing force, oblate earth perturbations, and atmospheric drag. A special case of terminal re-entry, for which the angular momentum becomes small, is also treated and suggestions are made to alleviate the problems which are encountered for this case. The solutions obtained with this method are compared to solutions obtained by integrating the standard equations of motion referred to a rotating coordinate system and with exact solutions for the cases where such solutions exist.

For the problems considered, the large step size solutions obtained with this method are considerably more accurate than those obtained using the standard equations of motion referred to a rotating coordinate system. This increase in accuracy is found to be even more significant if angular location in the orbit, rather than time, is treated as the independent variable. From the standpoint of program complexity and use of computer time, this method compares favorably with that resulting from simple integration of the standard equations of motion.

ACKNOWLEDGEMENTS

I would like to sincerely thank Dr. Laurence E. Fogarty and Prof. Robert M. Howe for their invaluable guidance and encouragement during the preparation of this dissertation. The helpful suggestions and interest of all the committee members are greatly appreciated.

I would also like to express my appreciation to the United States Air Force for giving me the opportunity to pursue this graduate work and to the Digital Computation Division, Directorate of Computation Services, Aeronautical Systems Division, Wright-Patterson Air Force Base, Ohio, whose facilities were used extensively in this investigation.

Finally, I wish to thank my wife who typed this dissertation and provided encouragement throughout the period of its preparation.

John Lewis Kurzenberger

TABLE OF CONTENTS

	Page
ACKNOWLEDGEMENTS	ii
TABLE OF CONTENTS	iii
LIST OF TABLES	v
LIST OF FIGURES	vii
LIST OF APPENDICES	xii
LIST OF SYMBOLS	xiii
CHAPTER 1. INTRODUCTION	1
1.1 Cowell's Method	2
1.2 Encke's Method	3
1.3 Variation of Parameters Method	3
1.4 Trajectory Computation Using Constraints	4
CHAPTER 2. AXIS SYSTEMS AND VEHICLE EQUATIONS OF MOTION	6
2.1 Axis Systems	6
2.2 Vehicle Equations of Motion Referred to the $\vec{e}_r$, $\vec{e}_n$, $\vec{e}_h$ Axis System	8
2.3 Discussion of Equations of Motion	11
CHAPTER 3. CONSTRAINED EQUATIONS	14
3.1 Development of Variables	15
3.2 Discussion of Constrained Equations	22
CHAPTER 4. COMPUTER SOLUTIONS FOR NON-PERTURBED ORBIT TRAJECTORIES	27
4.1 Orbit Eccentricity, 0.5	28
4.2 Estimate of Time Difference $\Delta\hat{t}$, and Correction Technique for Path Angle Difference, Δu, Between Computer Solutions at Two Different Integration Step Sizes	38
4.3 Orbit Eccentricity, 0.05	41
4.4 Orbit Eccentricity, 1.0 (Parabolic Trajectory)	49

Page

CHAPTER 5. RADIAL PERTURBING FORCE 57

5.1 Development of Equations 57
5.2 Computer Solutions for Radial Perturbing Force . . . 60
5.2.1 0.5 Nondimensional Step Size, $K_1 = 5x10^{-4}$ . . 61
5.2.2 1.0 Nondimensional Step Size, $K_1 = 5x10^{-4}$ . . 61
5.2.3 1.0 Nondimensional Step Size, $K_1 = 5x10^{-2}$ . . 67

CHAPTER 6. OBLATE EARTH PERTURBING FORCES 71

6.1 Oblate Earth Perturbations 71
6.2 Computer Solutions 74
6.2.1 0.5 Eccentricity Orbit 75
6.2.2 0.05 Eccentricity Orbit 87

CHAPTER7. PERTURBING FORCES RESULTING FROM AERODYNAMIC DRAG . . 99

7.1 Development of Equations 99
7.2 Computer Solutions for Small Eccentricity Orbit . . . 101
7.3 Computer Solutions for Terminal Re-entry 107

CHAPTER 8. CONCLUSIONS 122

APPENDICES 125

BIBLIOGRAPHY 168

LIST OF TABLES

Table		Page
5-1	0.5 Step Size Constrained Solutions Compared to Exact Solutions for Radial Perturbing Force, $K_1 = 5x10^{-4}$ . . .	62
5-2	0.5 Step Size Unconstrained Solutions Compared to Exact Solutions for Radial Perturbing Force, $K_1 = 5x10^{-4}$	63
5-3	1.0 Step Size Constrained Solutions Compared to Exact Solutions for Radial Perturbing Force, $K_1 = 5x10^{-4}$ . . .	65
5-4	1.0 Step Size Unconstrained Solutions Compared to Exact Solutions for Radial Perturbing Force, $K_1 = 5x10^{-4}$	66
5-5	1.0 Step Size Constrained Solutions Compared to Exact Solutions for Radial Perturbing Force, $K_1 = 5x10^{-2}$ . . .	68
5-6	1.0 Step Size Unconstrained Solutions Compared to Exact Solutions for Radial Perturbing Force, $K_1 = 5x10^{-2}$	69
A-1	0.2 Step Size Constrained Solutions Compared to Exact Solutions for Non-Perturbed 0.5 Eccentricity Case	126
A-2	0.2 Step Size Unconstrained Solutions Compared to Exact Solutions for Non-Perturbed 0.5 Eccentricity Case	127
A-3	0.8 Step Size Constrained Solutions Compared to Exact Solutions for Non-Perturbed 0.5 Eccentricity Case	128
A-4	0.8 Step Size Unconstrained Solutions Compared to Exact Solutions for Non-Perturbed 0.5 Eccentricity Case	129
A-5	0.2 Step Size Constrained Solutions Compared to Exact Solutions for Non-Perturbed 0.05 Eccentricity Case . . .	130
A-6	0.2 Step Size Unconstrained Solutions Compared to Exact Solutions for Non-Perturbed 0.05 Eccentricity Case	131
A-7	0.8 Step Size Constrained Solutions Compared to Exact Solutions for Non-Perturbed 0.05 Eccentricity Case . . .	132

Table		Page
A-8	0.8 Step Size Unconstrained Solutions Compared to Exact Solutions for Non-Perturbed 0.05 Eccentricity Case	133
A-9	0.2 Step Size Constrained Solutions Compared to Exact Solutions for Non-Perturbed 1.0 Eccentricity Case	134
A-10	0.2 Step Size Unconstrained Solutions Compared to Exact Solutions for Non-Perturbed 1.0 Eccentricity Case	135
A-11	0.8 Step Size Constrained Solutions Compared to Exact Solutions for Non-Perturbed 1.0 Eccentricity Case	136
A-12	0.8 Step Size Unconstrained Solutions Compared to Exact Solutions for Non-Perturbed 1.0 Eccentricity Case	137
A-13	0.125 Step Size Constrained Solutions Compared to Exact Solutions for Non-Perturbed 0.05 Eccentricity Case - 50th Orbit	138
A-14	0.125 Step Size Unconstrained Solutions Compared to Exact Solutions for Non-Perturbed 0.05 Eccentricity Case - 50th Orbit	139
B-1	Comparison of Differences Between 0.8 and 0.2 Step Size Constrained Solutions and Those Obtained from Sterne's Equations at Corresponding Values of Path Angle	155
C-1	Actual Per Step Error Compared to Predicted Per Step Truncation Error for the 0.8 Step Size Unconstrained Solutions for the 0.5 Eccentricity Orbit Under the Influence of Oblate Earth Perturbations	164
C-2	Computer Solutions at Times $\hat{t}_1 = 5.6$ and $\hat{t}_2 = 6.4$ for 0.5 Eccentricity Orbit with Oblate Earth Perturbations	165
C-3	Computer Solutions at Times $\hat{t}_1 = 11.2$ and $\hat{t}_2 = 12.0$ for 0.5 Eccentricity Orbit with Oblate Earth Perturbations	166
C-4	Computer Solutions at Times $\hat{t}_1 = 19.2$ and $\hat{t}_2 = 20.0$ for 0.5 Eccentricity Orbit with Oblate Earth Perturbations	167

LIST OF FIGURES

Figure		Page
2-1	Coordinate systems used in development of trajectory equations (X, Y, Z inertial system, $\vec{e}_r$, $\vec{e}_n$, $\vec{e}_h$ rotating system).	7
4-1	Nondimensional error in time $\hat{\epsilon}_t$ versus path angle u for 0.8 step size constrained and unconstrained computer solutions for non-perturbed 0.5 eccentricity orbit (computer solutions subtracted from exact solutions).	31
4-2	Nondimensional error in radius $\hat{\epsilon}_r$ and path angle ϵ_u versus nondimensional time for 0.8 step size constrained computer solutions for non-perturbed 0.5 eccentricity orbit (0.2 constrained solutions subtracted from 0.8 constrained solutions).	33
4-3	Nondimensional error in radial velocity $\hat{\epsilon}_{v_r}$ and normal velocity $\hat{\epsilon}_{v_n}$ versus nondimensional time for 0.8 step size constrained computer solutions for non-perturbed 0.5 eccentricity orbit (0.2 constrained solutions subtracted from 0.8 constrained solutions).	33
4-4	Nondimensional error in radius $\hat{\epsilon}_r$ and path angle ϵ_u versus nondimensional time for 0.8 step size unconstrained computer solutions for non-perturbed 0.5 eccentricity orbit (0.2 constrained solutions subtracted from 0.8 unconstrained solutions).	34
4-5	Nondimensional error in radial velocity $\hat{\epsilon}_{v_r}$ and normal velocity $\hat{\epsilon}_{v_n}$ versus nondimensional time for 0.8 step size unconstrained computer solutions for non-perturbed 0.5 eccentricity orbit (0.2 constrained solutions subtracted from 0.8 unconstrained solutions).	34
4-6	Nondimensional error in radius $\hat{\epsilon}_r$, radial velocity $\hat{\epsilon}_{v_r}$, and normal velocity $\hat{\epsilon}_{v_n}$ versus path angle u for 0.8 step size unconstrained computer solutions for non-perturbed 0.5 eccentricity orbit (0.8 unconstrained solutions subtracted from exact solutions).	36
4-7	Nondimensional error in time $\hat{\epsilon}_t$ versus path angle u for 0.8 step size constrained and unconstrained computer solutions for non-perturbed 0.05 eccentricity orbit (computer solutions subtracted from exact solutions).	45

Figure		Page
4-8	Nondimensional error in radius $\hat{\epsilon}_r$, radial velocity $\hat{\epsilon}_{v_r}$, and normal velocity $\hat{\epsilon}_{v_n}$ versus path angle u for 0.8 step size unconstrained computer solutions for non-perturbed 0.05 eccentricity orbit (0.8 unconstrained solutions subtracted from exact solutions). . .	45
4-9	Nondimensional error in radius $\hat{\epsilon}_r$, radial velocity $\hat{\epsilon}_{v_r}$, and normal velocity $\hat{\epsilon}_{v_n}$ versus nondimensional time for 0.8 step size constrained computer solutions for non-perturbed 0.05 eccentricity orbit (0.2 constrained solutions subtracted from 0.8 constrained solutions).	47
4-10	Error in path angle ϵ_u (in radians) versus nondimensional time for 0.8 step size constrained computer solutions for non-perturbed 0.05 eccentricity orbit (0.2 constrained solutions subtracted from 0.8 constrained solutions).	47
4-11	Nondimensional error in radius $\hat{\epsilon}_r$, radial velocity $\hat{\epsilon}_{v_r}$, and normal velocity $\hat{\epsilon}_{v_n}$ versus nondimensional time for 0.8 step size unconstrained computer solutions for non-perturbed 0.05 eccentricity orbit (0.2 constrained solutions subtracted from 0.8 unconstrained solutions).	48
4-12	Error in path angle ϵ_u (in radians) versus nondimensional time for 0.8 step size unconstrained computer solutions for non-perturbed 0.05 eccentricity orbit (0.2 constrained solutions subtracted from 0.8 unconstrained solutions).	48
4-13	Nondimensional error in time $\hat{\epsilon}_t$ versus path angle u for 0.8 step size constrained and unconstrained computer solutions for non-perturbed parabolic trajectory (computer solutions subtracted from exact solutions). . . .	51
4-14	Error in path angle ϵ_u (in radians) versus nondimensional time for 0.8 step size constrained and unconstrained computer solutions for non-perturbed parabolic trajectory (0.8 solutions subtracted from 0.2 constrained solutions).	53
4-15	Nondimensional error in normal velocity $\hat{\epsilon}_{v_n}$ versus nondimensional time for 0.8 step size constrained and unconstrained computer solutions for non-perturbed parabolic trajectory (0.8 solutions subtracted from 0.2 constrained solutions).	53

Figure		Page
4-16	Nondimensional error in radius $\hat{\epsilon}_r$ versus nondimensional time for 0.8 step size constrained and unconstrained computer solutions for non-perturbed parabolic trajectory (0.8 solutions subtracted from 0.2 constrained solutions).	54
4-17	Nondimensional error in radial velocity $\hat{\epsilon}_{v_r}$ versus nondimensional time for 0.8 step size constrained and unconstrained computer solutions for non-perturbed parabolic trajectory (0.8 solutions subtracted from 0.2 constrained solutions).	54
4-18	Nondimensional error in radius $\hat{\epsilon}_r$ versus path angle u for 0.8 step size unconstrained computer solutions for non-perturbed parabolic trajectory (0.8 unconstrained solutions subtracted from exact solutions).	56
4-19	Nondimensional error in radial velocity $\hat{\epsilon}_{v_r}$ and normal velocity $\hat{\epsilon}_{v_n}$ versus path angle u for 0.8 step size unconstrained computer solutions for non-perturbed parabolic trajectory (0.8 unconstrained solutions subtracted from exact solutions).	56
6-1	Nondimensional error in radius $\hat{\epsilon}_r$ and path angle ϵ_u versus nondimensional time for 0.8 step size constrained computer solutions for oblate earth perturbed 0.5 eccentricity orbit (0.2 constrained solutions subtracted from 0.8 constrained solutions).	77
6-2	Nondimensional error in radial velocity $\hat{\epsilon}_{v_r}$ and normal velocity $\hat{\epsilon}_{v_n}$ versus nondimensional time for 0.8 step size constrained computer solutions for oblate earth perturbed 0.5 eccentricity orbit (0.2 constrained solutions subtracted from 0.8 constrained solutions). . . .	77
6-3	Nondimensional error in radius $\hat{\epsilon}_r$ and path angle ϵ_u versus nondimensional time for 0.8 step size unconstrained computer solutions for oblate earth perturbed 0.5 eccentricity orbit (0.2 constrained solutions subtracted from 0.8 unconstrained solutions).	78
6-4	Nondimensional error in radial velocity $\hat{\epsilon}_{v_r}$ and normal velocity $\hat{\epsilon}_{v_n}$ versus nondimensional time for 0.8 step size unconstrained computer solutions for oblate earth perturbed 0.5 eccentricity orbit (0.2 constrained solutions subtracted from 0.8 unconstrained solutions). . .	78

Figure		Page
6-5	Nondimensional error in radial velocity $\hat{\epsilon}_{v_r}$ versus nondimensional time for 0.5 step size constrained computer solutions for oblate earth perturbed 0.05 eccentricity orbit (0.125 constrained solutions subtracted from 0.5 constrained solutions).	89
6-6	Nondimensional error in radius $\hat{\epsilon}_r$ and normal velocity $\hat{\epsilon}_{v_n}$ versus nondimensional time for 0.5 step size constrained computer solutions for oblate earth perturbed 0.05 eccentricity orbit (0.125 constrained solutions subtracted from 0.5 constrained solutions).	89
6-7	Error in path angle ϵ_u (in radians) versus nondimensional time for 0.5 step size constrained computer solutions for oblate earth perturbed 0.05 eccentricity orbit (0.125 constrained solutions subtracted from 0.5 constrained solutions).	89
6-8	Nondimensional error in radius $\hat{\epsilon}_r$, radial velocity $\hat{\epsilon}_{v_r}$, and normal velocity $\hat{\epsilon}_{v_n}$ versus nondimensional time for 0.5 step size unconstrained computer solutions for oblate earth perturbed 0.05 eccentricity orbit (0.125 constrained solutions subtracted from 0.5 unconstrained solutions).	90
6-9	Error in path angle ϵ_u (in radians) versus nondimensional time for 0.5 step size unconstrained computer solutions for oblate earth perturbed 0.05 eccentricity orbit (0.125 constrained solutions subtracted from 0.5 unconstrained solutions).	90
6-10	Nondimensional error in radius $\hat{\epsilon}_r$ versus nondimensional time for 0.5 step size constrained and unconstrained computer solutions for 50th orbit of oblate earth perturbed 0.05 eccentricity orbit (0.125 constrained solutions subtracted from 0.5 solutions).	92
6-11	Nondimensional error in radial velocity $\hat{\epsilon}_{v_r}$ versus nondimensional time for 0.5 step size constrained and unconstrained computer solutions for 50th orbit of oblate earth perturbed 0.05 eccentricity orbit (0.125 constrained solutions subtracted from 0.5 solutions). . .	92
6-12	Nondimensional error in normal velocity $\hat{\epsilon}_{v_n}$ versus nondimensional time for 0.5 step size constrained and unconstrained computer solutions for 50th orbit of oblate earth perturbed 0.05 eccentricity orbit (0.125 constrained solutions subtracted from 0.5 solutions). . .	93

Figures

		Page
6-13	Error in path angle ϵ_u (in radians) versus nondimensional time for 0.5 step size constrained and unconstrained computer solutions for 50th orbit of oblate earth perturbed 0.05 eccentricity orbit (0.125 constrained solutions subtracted from 0.5 solutions). . .	93
7-1	Nondimensional error in radius $\hat{\epsilon}_r$, radial velocity $\hat{\epsilon}_{v_r}$, and normal velocity $\hat{\epsilon}_{v_n}$ versus nondimensional time for 0.5 step size constrained computer solutions for 10th orbit of drag perturbed small eccentricity orbit (0.125 constrained solutions subtracted from 0.5 constrained solutions).	104
7-2	Error in path angle ϵ_u (in radians) versus nondimensional time for 0.5 step size constrained computer solutions for 10th orbit of drag perturbed small eccentricity orbit (0.125 constrained solutions subtracted from 0.5 constrained solutions).	104
7-3	Nondimensional error in radius $\hat{\epsilon}_r$, radial velocity $\hat{\epsilon}_{v_r}$, and normal velocity $\hat{\epsilon}_{v_n}$ versus nondimensional time for 0.5 step size unconstrained computer solutions for 10th orbit of drag perturbed small eccentricity orbit (0.125 constrained solutions subtracted from 0.5 unconstrained solutions).	105
7-4	Error in path angle ϵ_u (in radians) versus nondimensional time for 0.5 step size unconstrained computer solutions for 10th orbit of drag perturbed small eccentricity orbit (0.125 constrained solutions subtracted from 0.5 unconstrained solutions).	105

LIST OF APPENDICES

Appendix		Page
A	COMPUTER SOLUTIONS COMPARED TO EXACT SOLUTIONS FOR NON-PERTURBED KEPLERIAN TRAJECTORIES	125
B	PROOF OF CORRESPONDENCE BETWEEN THE CONSTRAINED VARIABLES $\hat{r}$, $\hat{v}_r$, $\hat{v}_n$ AND u FOR 0.5 ECCENTRICITY ORBIT WITH OBLATE EARTH PERTURBING FORCES	140
	B.1 Use of Sterne's Equations to Verify Correspondence of Constrained Solutions with Path Angle	146
	B.2 Use of Sterne's Equations to Verify Linear Correction Technique	152
C	DEVELOPMENT OF EQUATIONS FOR THE DETERMINATION OF TRUNCATION ERROR OCCURRING OVER AN INTEGRATION STEP	156
	C.1 Development of Equations	156
	C.2 Application of Truncation Error Test	161

LIST OF SYMBOLS

$\vec{a}$ Vehicle acceleration vector with respect to inertial space

A, B, C, D, L, T, G, N, S — Elements of transformation matrix relating rotating unit vectors $\vec{e}_r$, $\vec{e}_n$, $\vec{e}_h$ to inertial unit vectors $\vec{i}$, $\vec{j}$, $\vec{k}$ (See Chapter 3)

A_r Vehicle characteristic area (e.g. frontal area or wing area)

c_d Drag coefficient

$\vec{e}_r$, $\vec{e}_n$, $\vec{e}_h$ — Unit vectors along the three axes of the rotating reference frame (See Chapter 2)

$\vec{E}$ Instantaneous orbit eccentricity vector (a vector with magnitude equal to orbit eccentricity and with direction from focus to the instantaneous periapsis)

E Magnitude of instantaneous orbit eccentricity vector $\vec{E}$

E_e Eccentricity of a rotated ellipse forming an oblate spheroid used to represent earth's equatorial bulge (See Chapter 6)

$\vec{F}_P$ External perturbation force vector (e.g. includes all forces except central force field gravity for spherical earth)

F_r, F_n, F_h — Components of external perturbation force vector $\vec{F}_p$ referred to rotating $\vec{e}_r$, $\vec{e}_n$, $\vec{e}_h$ coordinate system

g_o — Acceleration due to the central force field gravity component at a reference distance r_o from the center of the earth

$\vec{H}$ — Angular momentum vector of vehicle center of mass about the origin of the inertial X, Y, Z coordinate system

H — Magnitude of angular momentum vector $\vec{H}$

h — Altitude of vehicle above the surface of the earth

$\vec{i}$, $\vec{j}$, $\vec{k}$ — Unit vectors along the three axes of the inertial reference frame (X, Y, Z, respectively)

I — Angle of inclination between instantaneous plane of motion and X, Y inertial plane

J_2, J_3 — Coefficients of first two zonal harmonics for oblate earth perturbation potential (See Chapter 6)

K — Reference gravitational constant, $K = g_o r_o^2$

K_1 — Coefficient to adjust magnitude of radial perturbing force (See Chapter 5)

m — Vehicle mass

$\vec{M}$ — Moment vector of perturbation force $\vec{F}_p$ about origin of inertial X, Y, Z coordinate system

P, Q, R — Components of absolute angular velocity vector $\vec{W}$ of rotating coordinate system referred to rotating system ($\vec{e}_r$, $\vec{e}_n$, $\vec{e}_h$ respectively)

$P_k(x)$ kth Legendre polynomial (See Chapter 6)

$\vec{r}$ The radius vector from the center of the earth to the vehicle center of mass

r Magnitude of radius vector $\vec{r}$

r_o A convenient constant reference radius for r

r_e Radius of earth

R_o An initial value of radius used in development of exact solution for radial perturbing force (See Chapter 5)

s Integration step size

t Time

t_o A convenient reference time scale, $t_o = \sqrt{\frac{r_o}{g_o}}$

u Path angle measured in instantaneous plane of motion from nodal axis ξ to position vector $\vec{r}$

$\vec{v}$ Vehicle velocity vector with respect to inertial space

v_r, v_n Components of vehicle velocity vector $\vec{v}$ referred to rotating coordinate system ($\vec{e}_r$, $\vec{e}_n$ respectively)

V Total potential function of earth including both central force field and oblateness effects

V_p Perturbation potential of earth due to first zonal harmonic (See Chapter 6)

$\vec{W}$ Absolute angular velocity vector of the $\vec{e}_r$, $\vec{e}_n$, $\vec{e}_h$ rotating coordinate system

$\mathbb{D}$ Drag-weight parameter, $\mathbb{D} = \frac{A_r c_d}{m g_o}$

X, Y, Z A right hand set of cartesian axes denoting inertial reference frame

y_i A general state variable (variables such as r, v_r, v_n, etc.)

α, γ, η — Components of eccentricity vector $\vec{E}$ referred to inertial coordinate system (X, Y, Z respectively)

β — Scale height for atmospheric density (See Chapter 7)

δ_1, δ_2, δ_3, δ_4 — Weighting parameters for Runge-Kutta (See Chapter 7)

ϵ_i — Error between numerical solution and a solution considered to be exact for a general state variable (e.g. ϵ_r indicates error in numerical solution for r)

θ — Instantaneous latitude (See Chapter 6)

ξ — Axis denoting intersection of instantaneous plane of motion with X, Y inertial plane

ρ — Atmospheric density

ρ_b — Atmospheric base density

σ — Undisturbed true anomaly (See Appendix B)

σ' — Disturbed true anomaly (See Appendix B)

τ — Orbital period

Φ — Increment function in numerical integration (See Chapter 7)

Ψ — Flight path angle, $\tan \Psi = \frac{v_r}{v_n}$

Ω — Nodal angle measured from inertial X axis to ξ (corresponds to orbital element termed longitude of ascending node)

ω — Elliptical orbital element, argument of perifocus (See Appendix B)

$\hat{}$ — Accent circumflex (denotes a nondimensional quantity, e.g. $\hat{r} = \frac{r}{r_o}$, $\hat{t} = \frac{t}{t_o}$, $\hat{v} = \frac{v}{\sqrt{g_o r_o}}$)

CHAPTER I

INTRODUCTION

The standard two-body Keplerian relations give convenient approximations for use in preliminary orbit computations. Among the many texts which cover these approximate methods are those of Baker and Makemson[1], Moulton[2], Thomson[3], Escobal[4], Danby[5], Brouwer and Clemence[6], Goldstein[7], Synge and Griffith[8], and Greenwood[9]. In order to obtain precise earth satellite orbits, however, the various perturbing factors which give rise to accelerations (in addition to that of the central force field) and cause the motion to deviate from pure conic form must be considered. These perturbative accelerations are due to the mass asymmetry of the earth, the gravitational attraction of other bodies, atmospheric drag, electromagnetic drag, radiation pressure, etc. All of these factors affect the motion of the satellite to a varying degree depending on the shape and mass of the satellite and the type of trajectory.

Methods of orbit prediction or computation which include the above-mentioned perturbing factors are generally referred to as methods of perturbations. It is customary to distinguish between two classes of perturbation methods called general perturbations and special perturbations. The former class includes methods of calculating perturbative effects by series expansions and term by term integration. The latter class, with which this study is concerned, involves the formulation of the differential equations of motion in such a manner that the computation of the orbit is achieved by direct numerical integration. The three special perturbation methods currently used for computing

satellite orbits are discussed briefly below. For a more detailed discussion of these methods the reader is referred to the many classical references on this subject which include Moulton[2], Baker[10], Battin [11], Conte[12], Pines, Payne, and Wolf[13], Krause[14], Baker, Westrom, et. al.[15], Pines[16], and Herrick[17].

1.1 Cowell's Method

In this method the total acceleration, central as well as perturbative, acting on a satellite is integrated directly by some numerical integration technique. The equations of motion which must be integrated twice to obtain position coordinates are of the form

$$\frac{d^2X}{dt^2} = -\frac{KX}{r^3} + \sum_{i=1}^{n} \frac{FX_i}{m} \qquad (X \rightarrow Y,Z).$$

The first term on the right represents the central force term in the X direction and the second term represents the total perturbative term in the X direction due to asphericity, drag, thrust, attraction of other bodies, etc.

These equations are symmetrical in the rectangular coordinates and are simple in form; they apply to elliptic, parabolic, and hyperbolic orbits, and require no conversion from one coordinate system to another.

A disadvantage of the method is the large number of places which must be carried because of the large central force term to prevent loss of significance for the small perturbations[18]. Also, since the total acceleration, which is subject to fairly rapid changes, is being integrated, it is necessary to use a smaller integration step size to maintain a given accuracy[10]. This requires an increase in the number of

integration steps and the inherent roundoff error accumulation. Cowell's method is especially useful when the perturbation forces, such as thrust or drag, are of the same order as the central force[11].

1.2 Encke's Method

In the Encke method, only the deviations of the actual motion from a reference orbit, which is assumed to be reasonably close to the actual orbit, are integrated. Usually a two-body reference orbit is used since the position at any time on this orbit can be determined analytically. These deviations are then added on to the coordinates of the satellite as found from the two-body equations to obtain the actual position of the satellite. When the deviations exceed a certain limit, the integration process is stopped and a new reference orbit is computed based upon the last calculated values of position and velocity. This process is termed rectifying the reference orbit.

Since the deviations are much smaller than the total coordinates and velocities, and therefore need not be determined as accurately, it is possible to maintain a given accuracy with larger integration steps. As a consequence of the large integration steps, there is less danger of serious roundoff accumulation.

Although the roundoff error is less, Encke's method involves expressions that are much more complicated than Cowell's simple formulas. In addition, both the necessity of solving the two-body formulas at every step and the possible need for frequent rectification introduce sources of error[18].

1.3 Variation of Parameters Method

The variation of parameters or variation of orbital elements method differs from the Encke method in that there is a continuous set of elements for the reference orbit. The perturbed motion of the

satellite may thus be described by a conic section, the elements of which change continuously. The variable Keplerian orbit is tangent to the actual orbit at all times, and the velocity at any time is the same in both orbits.

The essential characteristic of this method is that the integration is carried out on parameters which are much more slowly changing functions of time than rectangular coordinates. Since they vary slowly, much larger integration steps can be taken for a given accuracy.

A disadvantage of this method is that the programing and numerical analysis involved in this method are the most complicated of the three methods discussed[18]. In addition, since the parameters used consist of elliptical elements, there are a number of bothersome singularities in the standard variation of parameters methods which lead to special difficulties on low eccentricity orbits as well as hyperbolic and parabolic orbits. Such cases all require special consideration, particularly with respect to the relation between true anomaly and time, thus detracting from the usefulness of this method.

The universal variable approach discussed by Baker[10] and Battin [11] alleviates the above mentioned singularities by treating the initial position and velocity vectors as orbital elements. The resulting equations, however, are long and algebraically complex and as pointed out by Pitkin[19] the solution of the generalized Kepler's equation is not straightforward.

1.4 Trajectory Computation Using Constraints

The purpose of the present study is twofold. First, it is desired to develop a method for computing orbits under the influence of small perturbing forces similar in complexity to the simple integration of the

equations of motion so that it will be applicable to the use of small to moderate size digital computers with relatively simple integration routines. Second, it is desired that the method have superior accuracy to Cowell's method without having many of the singularities encountered in the standard variation of parameters methods so that the resulting equations can be used to consider the full range of trajectories.

The method developed makes use of the angular momentum vector and the Runge or eccentricity vector, both of which vary slowly under the influence of small perturbing forces and can therefore be obtained accurately using relatively large integration step sizes. At each integration step, the satellite position and velocity are constrained to be consistent with these accurately determined quantities. In addition, the method allows the full range of circular, elliptic, parabolic, and hyperbolic trajectories to be considered without the necessity of modifying the equations.

Solutions are obtained with this method for the cases of non-perturbed orbits, a radial perturbing force, oblate earth perturbations, and atmospheric drag. These solutions are compared to the solutions obtained by integrating the equations of motion expressed in polar coordinates and with exact solutions for the cases where such solutions exist.

CHAPTER 2

AXIS SYSTEMS AND VEHICLE EQUATIONS OF MOTION

When numerical integration of vehicle equations of motion is required, the selection of appropriate axis systems is important. The accuracy of numerical integration is dependent upon proper scaling of the system variables, and these variables are in turn dependent upon the axis system selected.

2.1 Axis Systems

For this study the axis systems selected for purposes of developing the vehicle equations of motion are shown in Fig. 2-1. The motion of the vehicle with respect to "inertial" space is referred to a nonrotating X, Y, Z coordinate system with origin located at the center of the earth. The corresponding unit vectors are denoted by $\vec{i}$, $\vec{j}$, and $\vec{k}$. Although the origin of this frame describes a near circular motion about the sun which produces a "reversed effective force" on the vehicle, it can be shown that this force is almost exactly cancelled by the sun's gravitational force for near earth orbits, and therefore it is valid to use the center of the earth as the origin of an inertial frame for the problems considered in this study.

The location of the vehicle center of mass in the instantaneous plane of motion is given by a position vector $\vec{r}$ in the plane of motion, and an angle u measured in the plane of motion from the nodal axis ξ to the position vector $\vec{r}$. The location of the instantaneous plane of motion is given by an angle Ω measured from the inertial X axis to the nodal axis; and an inclination angle I measured from the X, Y inertial plane to the instantaneous plane of motion.

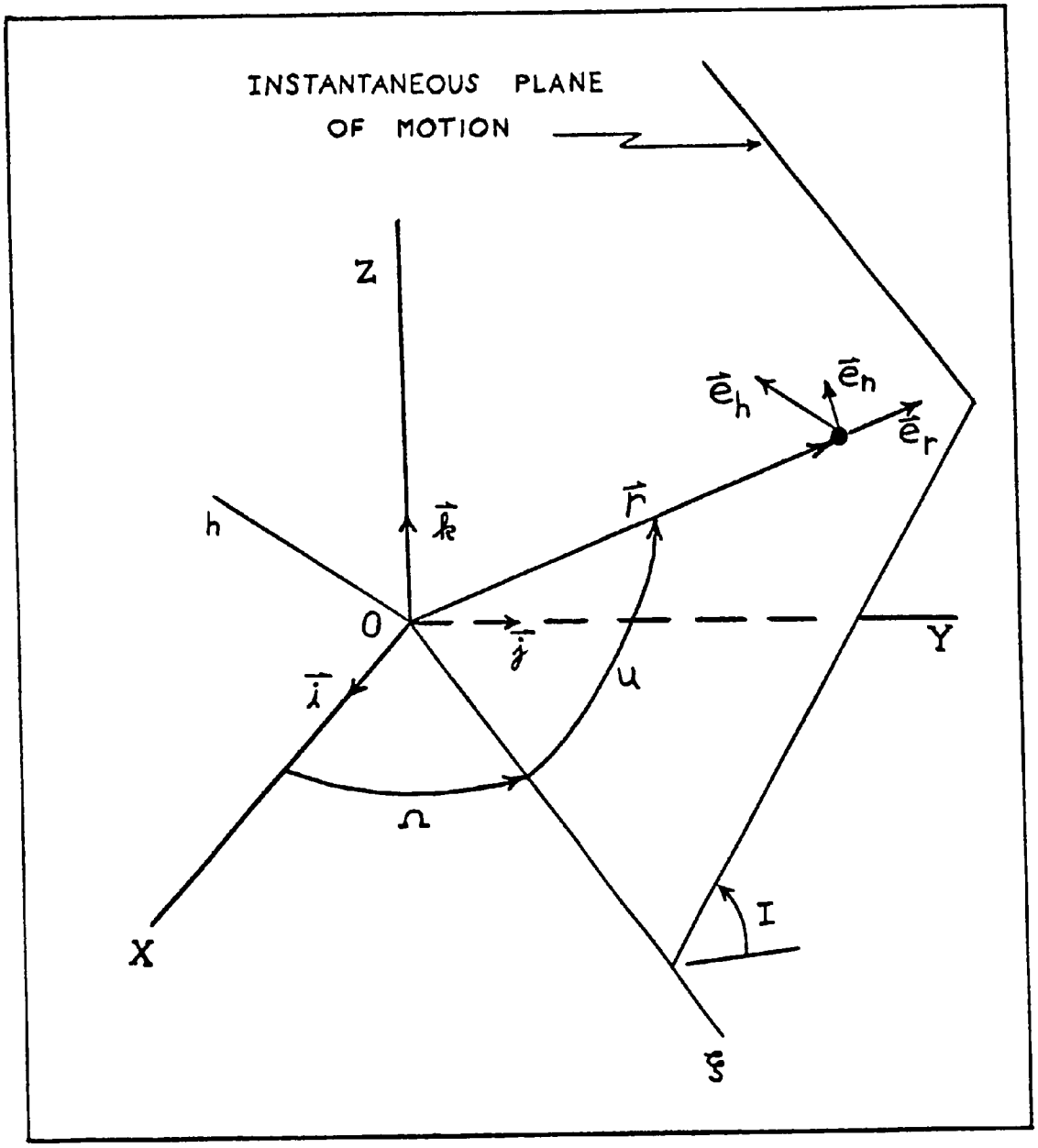

Fig. 2-1: Coordinate systems used in development of trajectory equations (X, Y, Z inertial system, $\vec{e}_r$, $\vec{e}_n$, $\vec{e}_h$ rotating system).

Knowledge of the system variables r, u, Ω, and I specifies the location of the vehicle center of mass. The unit vector triad $\vec{e}_r$, $\vec{e}_n$, and $\vec{e}_h$ forms an orthogonal set with $\vec{e}_r$ directed outward along the position vector $\vec{r}$, $\vec{e}_n$ in the instantaneous plane of motion perpendicular to $\vec{e}_r$ with positive direction in the direction of increasing path angle u, and $\vec{e}_h$ perpendicular to the instantaneous plane of motion. The $\vec{e}_r$, $\vec{e}_n$, $\vec{e}_h$ axis system is similar to the H frame coordinate system used by Fogarty and Howe[20].

Although the purpose of this study is to develop equations which accurately describe the motion of the vehicle center of mass, the $\vec{e}_r$, $\vec{e}_n$, $\vec{e}_h$ triad would be a suitable reference frame from which a set of modified Euler angles could be measured to describe the orientation of the vehicle in space.

2.2 Vehicle Equations of Motion Referred to the $\vec{e}_r$, $\vec{e}_n$, $\vec{e}_h$ Axis System

The conventional equations of motion, referred to the $\vec{e}_r$, $\vec{e}_n$, $\vec{e}_h$ coordinate system are developed in this section. Although the form of these equations is well known, their derivation is included here for completeness and because computer solution of these equations will be used as a basis of comparison for the constrained equations to be developed later.

The absolute angular rate of the $\vec{e}_r$, $\vec{e}_n$, $\vec{e}_h$ vector triad is given by

$$\vec{W} = P\vec{e}_r + Q\vec{e}_n + R\vec{e}_h \tag{2-1}$$

where

$$P = \frac{d\Omega}{dt} \sin I \sin u + \frac{dI}{dt} \cos u \tag{2-2}$$

$$Q = \frac{d\Omega}{dt} \sin I \cos u - \frac{dI}{dt} \sin u \tag{2-3}$$

$$R = \frac{d\Omega}{dt} \cos I + \frac{du}{dt} \tag{2-4}$$

The absolute velocity vector of the vehicle center of mass must lie in the instantaneous plane of motion and can be expressed in terms of the $\vec{e}_r$, $\vec{e}_n$, $\vec{e}_h$ system as

$$\vec{v} = v_r\vec{e}_r + v_n\vec{e}_n \tag{2-5}$$

where v_r represents the radial velocity of the vehicle and v_n represents the local horizontal component of velocity.

The absolute acceleration of the vehicle center of mass may be expressed as

$$\vec{a} = \dot{v}_r\vec{e}_r + \dot{v}_n\vec{e}_n + \vec{W} \times \vec{v} \tag{2-6}$$

or

$$\vec{a} = (\dot{v}_r - Rv_n)\vec{e}_r + (\dot{v}_n + Rv_r)\vec{e}_n + (Pv_n - Qv_r)\vec{e}_h \tag{2-7}$$

The total force acting on the particle can be expressed as

$$\vec{F} = (-\frac{Km}{r^2} + F_r)\vec{e}_r + F_n\vec{e}_n + F_h\vec{e}_h \tag{2-8}$$

where the term $-\frac{Km}{r^2}$, represents the standard inverse square gravitational attraction force for a spherical earth with $K = g_o r_o^2$, where g_o is the acceleration due to the central force gravity component at a constant reference distance, r_o, from the center of the earth. The terms F_r, F_n, and F_h represent any other forces which may be acting on the particle. These forces may include the effects of an oblate earth, atmospheric drag, thrust, attraction of other bodies, etc.

Equating the components of mass times Eq. (2-7) with those of Eq. (2-8) yields:

$$m(\dot{v}_r - Rv_n) = -\frac{Km}{r^2} + F_r \tag{2-9}$$

$$m(\dot{v}_n + Rv_r) = F_n \tag{2-10}$$

$$m(Pv_n - Qv_r) = F_h \tag{2-11}$$

To evaluate the relationships between the angular rates P, Q, and R and the forces, we can make use of the relationship between the time rate of change of angular momentum about 0 and the moment of the external forces about 0. The angular momentum about 0 is given by

$$\vec{H} = m\vec{r} \times \vec{v} = mrv_n\vec{e}_h \tag{2-12}$$

and the moment of the external forces about 0 is given by

$$\vec{M} = \vec{r} \times \vec{F} = rF_h\vec{e}_n + rF_n\vec{e}_h \tag{2-13}$$

Differentiating $\vec{H}$ yields

$$\frac{d\vec{H}}{dt} = mrv_nQ\vec{e}_r - mrv_nP\vec{e}_n + m(v_rv_n + r\dot{v}_n)\vec{e}_h \tag{2-14}$$

Equating components of Eqs. (2-13) and (2-14) yields

$$m(v_rv_n + r\dot{v}_n) = rF_n \tag{2-15}$$

$$mrv_nQ = 0 \tag{2-16}$$

$$mrv_nP = rF_h \tag{2-17}$$

Therefore,

$$P = \frac{F_h}{mv_n} \tag{2-18}$$

$$Q = 0 \tag{2-19}$$

and by comparing Eqs. (2-15) and 2-10) we have

$$R = \frac{v_n}{r} \tag{2-20}$$

Finally, by making use of the relationships given by Eqs. (2-2), (2-3), and (2-4) and those given by (2-18), (2-19), and (2-20) we can write the complete set of differential equations for the system as

$$\frac{dr}{dt} = v_r \tag{2-21}$$

$$\frac{dv_r}{dt} = \frac{v_h^2}{r} - \frac{K}{r^2} + \frac{F_r}{m} \tag{2-22}$$

$$\frac{dv_n}{dt} = -\frac{v_r v_n}{r} + \frac{F_n}{m} \tag{2-23}$$

$$\frac{du}{dt} = \frac{v_n}{r} - \frac{F_h}{mv_n} \frac{\sin u \cos I}{\sin I} \tag{2-24}$$

$$\frac{d\Omega}{dt} = \frac{F_h}{mv_n} \frac{\sin u}{\sin I} \tag{2-25}$$

$$\frac{dI}{dt} = \frac{F_h}{mv_n} \cos u \tag{2-26}$$

2.3 Discussion of Equations of Motion

At this point it is of interest to examine the advantages and disadvantages, with respect to numerical integration, which result from using the equations of motion referred to the $\vec{e}_r$, $\vec{e}_n$, $\vec{e}_h$ axis system as

opposed to the simpler approach of expressing the trajectory equations of motion directly in terms of a rectangular cartesian inertial frame with the origin at the center of the earth.

In the X, Y, Z inertial system it is apparent that the X, Y, Z coordinates will be ranging through distances on the order of twice the apogee radius from the center of the earth, the X, Y, Z velocity components will be undergoing changes on the order of twice the orbital velocity, and the X, Y, Z acceleration components will be undergoing changes on the order of twice the gravitational acceleration.

On the other hand, when the equations of motion are referred to the $\vec{e}_r$, $\vec{e}_n$, $\vec{e}_h$ coordinate system, the distance ranges only over the difference between apogee and perigee, the velocity ranges over the difference between apogee and perigee velocities, and the acceleration ranges over only the difference between gravitational acceleration at apogee and at perigee. A disadvantage when the equations of motion are referred to the $\vec{e}_r$, $\vec{e}_n$, $\vec{e}_h$ system does occur if the inclination angle, I, becomes small. This is evident from the form of Eqs. (2-24) and (2-25) since a singularity occurs when sin I approaches zero. This disadvantage, however, represents only a minor inconvenience since the orientation of the X, Y plane from which the inclination angle is measured is arbitrary. Therefore, if it is desired to study near-equatorial orbits, the orientation of the X, Y plane may be selected such that it does not coincide with the earth's equatorial plane.

Although the selection of equations of motion referred to the $\vec{e}_r$, $\vec{e}_n$, $\vec{e}_h$ coordinate system yields a distinct advantage over equations of motion referred to the X, Y, Z system from the standpoint of computer scaling, certain disadvantages for the case of small perturbing forces

still remain. This subject is discussed in the following chapter and a new set of variables is developed which helps to alleviate this problem.

CHAPTER 3

CONSTRAINED EQUATIONS

Suppose we consider the forces represented by F_r, F_n and F_h to consist only of small perturbing forces such as those which would result from an oblate earth, the presence of other bodies, micro thrust, small aerodynamic forces, or solar pressure. From Eqs. (2-21) through (2-26) it can be seen that all but the last two equations of motion (2-25 and 2-26) contain terms on the right side other than those involving functions of the perturbing forces F_r, F_n, and F_h. Due to the relative sizes of these other terms, a large number of digits must be carried in performing numerical integration to prevent loss of significance of the small perturbations. Also, since the relatively large total time rates of change of the system variables are being integrated it would be necessary to use smaller integration step sizes to maintain a given accuracy which in turn requires an increase in the number of integration steps and with it the inherent accumulation of roundoff error. In fact, detection of very small perturbation effects such as those caused by radiation pressure may be impossible due to roundoff and truncation error[18].

On the other hand, Eqs. (2-25) and (2-26) for Ω and I consist of functions involving only the perturbing force F_h, and in the absence of this force Ω and I would be constants. Even if the small perturbing force is present, the time rates of change of Ω and I will be very small and relatively large integration step sizes can be taken while maintaining accuracy. With this in mind, we can pursue the idea of finding other variables whose time rates of change are dependent on functions

involving only the perturbing forces and which do not suffer from many of the singularities encountered in the standard variation of orbital elements technique.

3.1 Development of Variables

The equations for the rates of change of Ω and I came about from the expression for the time rate of change of the angular momentum vector. If we return to Eq. (2-15) and write it in the form of the scalar time rate of change of angular momentum, we have $\frac{dH}{dt} = rF_n$; and therefore angular momentum is a quantity which varies slowly in the presence of a perturbing force F_n, and which is constant in the absence of this perturbing force. In effect, we have made use of the three components of the time rate of change of the vector $\vec{H}$ and from it we have obtained the equations

$$\frac{dI}{dt} = \frac{F_h}{mv_n} \cos u \tag{3-1}$$

$$\frac{d\Omega}{dt} = \frac{F_h}{mv_n} \frac{\sin u}{\sin I} \tag{3-2}$$

$$\frac{dH}{dt} = rF_n \tag{3-3}$$

Next, consider the eccentricity vector or Rünge's vector[28] which lies in the instantaneous plane of motion, in the direction from the focus to the instantaneous periapsis and has a magnitude E equal to the instantaneous eccentricity. This vector can be expressed as

$$K\vec{E} = \vec{v} \times \frac{\vec{H}}{m} - \frac{K\vec{r}}{r} \tag{3-4}$$

From Eqs. (2-5) and (2-12) for $\vec{v}$ and $\vec{H}$, Eq. (3-4) can be expressed in terms of the $\vec{e}_r$, $\vec{e}_n$, $\vec{e}_h$ coordinate system as

$$\vec{KE} = (rv_n^2 - K)\vec{e}_r - rv_r v_n \vec{e}_n \tag{3-5}$$

From Eq. (3-4) the time rate of change of the vector $\vec{KE}$ becomes

$$\frac{d}{dt}(\vec{KE}) = \dot{\vec{v}} \times \frac{\vec{H}}{m} + \vec{v} \times \frac{\dot{\vec{H}}}{m} - \frac{K\dot{\vec{r}}}{r} + \frac{K\vec{r}}{r^2} v_r \tag{3-6}$$

But

$$\dot{\vec{r}} = \vec{v} = v_r \vec{e}_r + v_n \vec{e}_n \tag{3-7}$$

$$\vec{e}_n = \frac{\vec{H} \times \vec{r}}{Hr} = \frac{\vec{H} \times \vec{r}}{mr^2 v_n} \tag{3-8}$$

$$\dot{\vec{v}} = -\frac{K}{r^3}\vec{r} + \frac{\vec{F}_P}{m} \tag{3-9}$$

and $$\dot{\vec{H}} = \vec{M} = \vec{r} \times \vec{F}_P \tag{3-10}$$

where $\vec{F}_P$ consists only of the perturbing forces or

$$\vec{F}_P = F_r \vec{e}_r + F_n \vec{e}_n + F_h \vec{e}_h \tag{3-11}$$

From Eqs. (3-7) and (3-8) the velocity $\dot{\vec{r}}$ can be expressed as

$$\dot{\vec{r}} = \vec{v} = v_r \frac{\vec{r}}{r} + \frac{\vec{H}}{m} \times \frac{\vec{r}}{r^2} \tag{3-12}$$

Using Eqs. (3-9), (3-10), and (3-12) the first three terms of Eq. (3-6) become

$$\dot{\vec{v}} \times \frac{\vec{H}}{m} = -\frac{K}{r^3}\vec{r} \times \frac{\vec{H}}{m} + \frac{\vec{F}_P}{m} \times \frac{\vec{H}}{m} \tag{3-13}$$

$$\vec{v} \times \frac{\dot{\vec{H}}}{m} = \vec{v} \times (\vec{r} \times \frac{\vec{F}_P}{m}) \tag{3-14}$$

$$\frac{K\dot{\vec{r}}}{r} = \frac{K\vec{v}}{r} = Kv_r \frac{\vec{r}}{r^2} + \frac{K}{r^3} \frac{\vec{H}}{m} \times \vec{r} \tag{3-15}$$

Substituting Eqs. (3-13), (3-14), and (3-15) into Eq. (3-6) yields

$$\frac{d}{dt} (K\vec{E}) = \frac{\vec{F}_P}{m} \times \frac{\vec{H}}{m} + \vec{v} \times (\vec{r} \times \frac{\vec{F}_P}{m}) \tag{3-16}$$

From Eq. (3-16) we see that the time rate of change of the $\vec{E}$ vector is a function of only the perturbing forces, and that $\vec{E}$ would be constant in the absence of these perturbing forces. In terms of the $\vec{e}_r$, $\vec{e}_n$, and $\vec{e}_h$ unit vectors, Eq. (3-16) becomes

$$\frac{d}{dt} \left\{ (rv_n^2 - K)\vec{e}_r - rv_r v_n \vec{e}_n \right\} = 2rv_n \frac{F_n}{m} \vec{e}_r$$

$$- r(v_r \frac{F_n}{m} + v_n \frac{F_r}{m})\vec{e}_n - rv_r \frac{F_h}{m} \vec{e}_h \tag{3-17}$$

Although it would appear that we now have three additional equations available to us we actually have only two. Since $\vec{H}$ is perpendicular to the plane of the motion and $\vec{E}$ is in the plane of motion, $\vec{E}$ and $\vec{H}$ are perpendicular and are therefore not independent. In addition, it can be seen that Eq. (3-17) in its present form is not very useful for if we try to solve for the time rates of change of the quantities $(rv_n^2 - K)$ and $(rv_r v_n)$, we will obtain terms other than those which involve only the perturbing forces due to the fact that the unit vectors $\vec{e}_r$ and $\vec{e}_n$ have time rates of change. If, however, we resolve Eq. (3-17) into components along the X, Y, and Z directions of the inertial reference frame

we can find quantities whose time rates of change are only functions of the perturbing forces.

We start with the transformation matrix which relates the $\vec{e}_r$, $\vec{e}_n$, $\vec{e}_h$ unit vectors to the inertial unit vectors $\vec{i}$, $\vec{j}$, and $\vec{k}$. This transformation may be expressed as

$$\begin{bmatrix} \vec{e}_r \\ \vec{e}_n \\ \vec{e}_h \end{bmatrix} = \begin{bmatrix} A & B & C \\ D & L & T \\ G & N & S \end{bmatrix} \begin{bmatrix} \vec{i} \\ \vec{j} \\ \vec{k} \end{bmatrix} \tag{3-18}$$

where

$$\begin{aligned} A &= \cos u \cos \Omega - \sin u \sin \Omega \cos I \\ B &= \cos u \sin \Omega + \sin u \cos \Omega \cos I \\ C &= \sin u \sin I \\ D &= -\sin u \cos \Omega - \cos u \sin \Omega \cos I \\ L &= -\sin u \sin \Omega + \cos u \cos \Omega \cos I \\ T &= \cos u \sin I \\ G &= \sin \Omega \sin I \\ N &= -\cos \Omega \sin I \\ S &= \cos I \end{aligned} \tag{3-19}$$

Applying the above transformation to Eq. (3-17) and equating the resulting $\vec{i}$, $\vec{j}$, and $\vec{k}$ components yields

$$\frac{d}{dt}\left\{A(rv_n^2 - K) - Drv_r v_n\right\} = 2rv_n \frac{F_n}{m} A$$

$$- r(v_r \frac{F_n}{m} + v_n \frac{F_r}{m}) D - rv_r \frac{F_h}{m} G \tag{3-20}$$

we can find quantities whose time rates of change are only functions of the perturbing forces.

We start with the transformation matrix which relates the $\vec{e}_r$, $\vec{e}_n$, $\vec{e}_h$ unit vectors to the inertial unit vectors $\vec{i}$, $\vec{j}$, and $\vec{k}$. This transformation may be expressed as

$$\begin{bmatrix} \vec{e}_r \\ \vec{e}_n \\ \vec{e}_h \end{bmatrix} = \begin{bmatrix} A & B & C \\ D & L & T \\ G & N & S \end{bmatrix} \begin{bmatrix} \vec{i} \\ \vec{j} \\ \vec{k} \end{bmatrix} \tag{3-18}$$

where

$$\begin{aligned} A &= \cos u \cos \Omega - \sin u \sin \Omega \cos I \\ B &= \cos u \sin \Omega + \sin u \cos \Omega \cos I \\ C &= \sin u \sin I \\ D &= -\sin u \cos \Omega - \cos u \sin \Omega \cos I \\ L &= -\sin u \sin \Omega + \cos u \cos \Omega \cos I \\ T &= \cos u \sin I \\ G &= \sin \Omega \sin I \\ N &= -\cos \Omega \sin I \\ S &= \cos I \end{aligned} \tag{3-19}$$

Applying the above transformation to Eq. (3-17) and equating the resulting $\vec{i}$, $\vec{j}$, and $\vec{k}$ components yields

$$\frac{d}{dt}\left\{A(rv_n^2 - K) - Drv_r v_n\right\} = 2rv_n \frac{F_n}{m} A$$

$$- r(v_r \frac{F_n}{m} + v_n \frac{F_r}{m}) D - rv_r \frac{F_h}{m} G \tag{3-20}$$

$$\frac{d}{dt}\left\{B(rv_n^2 - K) - Lrv_rv_n\right\} = 2rv_n \frac{F_n}{m} B$$

$$- r(v_r \frac{F_n}{m} + v_n \frac{F_r}{m})L - rv_r \frac{F_h}{m} N \qquad (3\text{-}21)$$

$$\frac{d}{dt}\left\{C(rv_n^2 - K) - Trv_rv_n\right\} = 2rv_n \frac{F_n}{m} C$$

$$- r(v_r \frac{F_n}{m} + v_n \frac{F_r}{m})T - rv_r \frac{F_h}{m} S \qquad (3\text{-}22)$$

If we define quantities α, γ, and η such that

$$\alpha = A(rv_n^2 - K) - Drv_rv_n \qquad (3\text{-}23)$$

$$\gamma = B(rv_n^2 - K) - Lrv_rv_n \qquad (3\text{-}24)$$

and

$$\eta = C(rv_n^2 - K) - Trv_rv_n \qquad (3\text{-}25)$$

we see that the time rates of change of the variables α, γ, and η are functions of the perturbing forces and that they are constants in the absence of these perturbing forces. Since we are only free to select two of the above three variables due to the dependency between $\vec{H}$ and $\vec{E}$, let us select α and γ for purposes of discussion.

In this case we now have five quantities, I, Ω, H, α, and γ which vary slowly with time and can therefore be accurately determined even with relatively large integration step sizes. If we now solve explicitly for r, v_r, and v_n in terms of these quantities we are, in effect, constraining the radial position and the velocities v_r and v_n to satisfy the quantities H, α, and γ which can be determined accurately through

numerical integration. In addition, the location of the instantaneous orbit plane may also be accurately determined through the variables I and Ω.

Before proceeding with the discussion it is beneficial from the standpoint of computer scaling to nondimensionalize the equations. To do this we define a reference radius, r_o, and a reference acceleration, g_o, which represents the local acceleration due to the standard inverse square force field at the reference radius, r_o. With these definitions, the nondimensional variables of position, velocity, angular momentum, time and force become

$$\hat{r} = \frac{r}{r_o} \tag{3-26}$$

$$\hat{v} = \frac{v}{\sqrt{g_o r_o}} \tag{3-27}$$

$$\hat{H} = \frac{H}{m\sqrt{g_o r_o^3}} \tag{3-28}$$

$$\hat{t} = t\sqrt{\frac{g_o}{r_o}} \tag{3-29}$$

$$\hat{F}_P = \frac{F_P}{mg_o} \tag{3-30}$$

In terms of these nondimensional quantities, the constrained equations become

$$\frac{d\hat{H}}{d\hat{t}} = \hat{r}\hat{F}_n \tag{3-31}$$

$$\frac{dI}{d\hat{t}} = \frac{\hat{F}_h}{\hat{v}_n}\cos u \tag{3-32}$$

$$\frac{d\Omega}{d\hat{t}} = \frac{\hat{F}_h}{\hat{v}_n} \frac{\sin u}{\sin I} \tag{3-33}$$

$$\frac{d\hat{\alpha}}{d\hat{t}} = 2\hat{r}\hat{v}_n\hat{F}_n A - \hat{r}(\hat{v}_r\hat{F}_n + \hat{v}_n\hat{F}_r)D - \hat{r}\hat{v}_r\hat{F}_h G \tag{3-34}$$

$$\frac{d\hat{\gamma}}{d\hat{t}} = 2\hat{r}\hat{v}_n\hat{F}_n B - \hat{r}(\hat{v}_r\hat{F}_n + \hat{v}_n\hat{F}_r)L - \hat{r}\hat{v}_r\hat{F}_h N \tag{3-35}$$

$$\frac{du}{d\hat{t}} = \frac{\hat{v}_n}{\hat{r}} - \frac{\hat{F}_h}{\hat{v}_n} \frac{\sin u \cos I}{\sin I} \tag{3-36}$$

where r, v_r, and v_n are constrained to agree with the quantities H, α, and γ through Eqs. (2-12), (3-23), and (3-24) yielding the nondimensional expressions

$$\hat{v}_n = \frac{1}{\hat{H}} \left(1 + \frac{\hat{\alpha}L - \hat{\gamma}D}{\cos I}\right) \tag{3-37}$$

$$\hat{v}_r = \frac{1}{\hat{H}} \left(\frac{\hat{\alpha}B - \hat{\gamma}A}{\cos I}\right) \tag{3-38}$$

$$\hat{r} = \frac{\hat{H}}{\hat{v}_n} \tag{3-39}$$

The conventional equations of motion given in Chapter 2 by Eqs. (2-21) through (2-26) can also be put into nondimensional form with the above definitions of reference radius and acceleration. If this is done, the nondimensional conventional equations of motion become

$$\frac{d\hat{r}}{d\hat{t}} = \hat{v}_r \tag{3-40}$$

$$\frac{d\hat{v}_r}{d\hat{t}} = \frac{\hat{v}_n^2}{\hat{r}} - \frac{1}{\hat{r}^2} + \hat{F}_r \tag{3-41}$$

$$\frac{d\hat{v}_n}{d\hat{t}} = -\frac{\hat{v}_r\hat{v}_n}{\hat{r}} + \hat{F}_n \tag{3-42}$$

$$\frac{du}{d\hat{t}} = \frac{\hat{v}_n}{\hat{r}} - \frac{\hat{F}_h}{\hat{v}_n}\,\frac{\sin u \cos I}{\sin I} \tag{3-43}$$

$$\frac{d\Omega}{d\hat{t}} = \frac{\hat{F}_h}{\hat{v}_n}\,\frac{\sin u}{\sin I} \tag{3-44}$$

$$\frac{dI}{d\hat{t}} = \frac{F_h}{\hat{v}_n}\cos u \tag{3-45}$$

For the remainder of this report, Eqs. (3-31) through (3-39) will be referred to as the constrained equations while Eqs. (3-40) through (3-45) will be referred to as the unconstrained equations.

3.2 Discussion of Constrained Equations

From Eqs. (3-31) through (3-36) it can be seen that we now have five variables whose time rates of change are only functions of the perturbing forces. Even with large integration step sizes, these variables can be determined accurately through numerical integration.

The time rate of change of the remaining variable, u, involves a term other than the perturbing force and therefore it would be expected that large integration step sizes would cause some error in the determination of u with time. In order to place a constraint on this remaining variable some equivalent of Kepler's equation would be required. Although this can be done, Kepler's equation is difficult to

implement and in the conventional orbital elements techniques has different forms depending upon whether it is applied to elliptical, parabolic, or hyperbolic trajectories. A generalized form of Kepler's equation is given in Reference[11]; however, the resultant equations are long and algebraically complex and it is still necessary to use an iterative procedure for its solution.

In view of the above, we might consider an alternate approach. Since the angle u varies smoothly it would not be expected that the error between u and time would be very large for moderate integration step sizes using an integration scheme of the fourth-order Runge-Kutta type. The time rates of change of the other five variables are very small in the presence of small perturbing forces and would therefore be essentially correct even if u is slightly in error with time. Expressing this another way, we could expect the values of I, Ω, $\hat{\mathrm{H}}$, $\hat{\alpha}$, and $\hat{\gamma}$ to be essentially constant over any small variation in u. Therefore, since the expressions for $\hat{v}_n$ and $\hat{v}_r$ given by Eqs. (3-37) and (3-38) involve trigonometric functions of u, we could expect the explicit solutions for $\hat{r}$, $\hat{v}_r$, and $\hat{v}_n$ to be correct with respect to u, even though u is slightly in error with time. In addition, since at each integration step the time rate of change of u is corrected to correspond to the constrained values of $\hat{v}_n$ and $\hat{r}$ which are correct with the last computed value of u, it could be expected that the error between u and time would not be as large as one resulting from integration of the standard equations of motion where we have, in effect, six open ended integrations being performed with no constraints being enforced between the six variables. Therefore, if one can accept a small error between time and u with the assurance that velocity and radial position

are correct with respect to the path angle u, then it is not neccessary to use some form of Kepler's equation and the constrained equations can be used with no adjustments to consider the full range of orbital trajectories.

If small errors between u and time cannot be accepted, then of course the integration step size must be reduced. However, even in this case, the enforcement of the constraints will alleviate the problem of performing six open ended integrations.

At this point, it is also of interest to compare the constrained equations with those arising from the standard orbital elements approach with respect to possible singularities. In the conventional variation of orbital elements approach, singularities can occur for the cases of small inclination, low eccentricity orbits, parabolic trajectories, and hyperbolic trajectories. As a result, different forms of these equations must be used depending upon the type of orbit to be considered in order to avoid these singularities.

From Eqs. (3-31) through (3-36) it can be seen that a singularity will arise if the inclination angle I approaches zero. However, as discussed previously, this singularity can be easily eleminated by a redefinition of the reference X, Y, Z coordinate system.

From Eqs. (3-37) through (3-39) we see that there is a possibility of two additional singularities. The first occurs if the inclination angle approaches $\pm$ 90 degrees. Although this singularity could also be eliminated by a redefinition of the X, Y, Z reference frame, an alternate approach is possible. In developing Eqs. (3-31) through (3-39) we arbitrarily selected the variables $\hat{\alpha}$ and $\hat{\gamma}$ from the three possible choices of variables given by the Rünge-vector. We could have selected the variable $\hat{\eta}$ in place of either $\hat{\alpha}$ or $\hat{\gamma}$ in which case either Eq. (3-34) or

Eq. (3-35) would be replaced by

$$\frac{d\hat{\eta}}{d\hat{t}} = 2\hat{r}\hat{v}_n\hat{F}_n C - \hat{r}(\hat{v}_r\hat{F}_n + \hat{v}_n\hat{F}_r)T - \hat{r}\hat{v}_r\hat{F}_h S \tag{3-46}$$

If we had selected to use the variables $\hat{\alpha}$ and $\hat{\eta}$, Eqs. (3-37) and (3-38) would be replaced by

$$\hat{v}_n = \frac{1}{\hat{H}}\left(1 + \frac{\hat{\alpha}T - \hat{\eta}D}{\cos\Omega \sin I}\right) \tag{3-47}$$

$$\hat{v}_r = \frac{1}{\hat{H}}\left(\frac{\hat{\alpha}C - \hat{\eta}A}{\cos\Omega \sin I}\right) \tag{3-48}$$

If we had selected to use the variables $\hat{\gamma}$ and $\hat{\eta}$, Eqs. (3-37) and (3-38) would be replaced by

$$\hat{v}_n = \frac{1}{\hat{H}}\left(1 + \frac{\hat{\gamma}T - \hat{\eta}L}{\sin\Omega \sin I}\right) \tag{3-49}$$

$$\hat{v}_r = \frac{1}{\hat{H}}\left(\frac{\hat{\gamma}C - \hat{\eta}B}{\sin\Omega \sin I}\right) \tag{3-50}$$

The choice as to which set of equations is to be used does not need to be determined prior to trajectory computation. All of the above equations can be included in the computer program along with two simple comparison tests on the values of I and Ω. Suppose, for example, that solutions are being obtained through the use of Eqs. (3-31) through (3-39). If at some time during computation the value of I approaches some specified value near 90 degrees and the value of Ω is within some specified value near zero degrees, the computer can be programed to

automatically compute the value of $\hat{\eta}$ at the last computed point, replace Eq. (3-35) by Eq. (3-46) and Eqs. (3-37) and (3-38) by Eqs. (3-47) and (3-48) and proceed with integration to the next point thus avoiding the region within which a singularity might occur.

It should be noted, that for the case of small perturbing forces, the rate of change of I will be very small. Therefore, a proper choice of orientation for the X, Y, Z reference frame would in all probability eliminate the need of automatically changing equations unless the integration is carried out over a large number of orbits.

The last singularity to be dealt with is the case for which the angular momentum $\hat{H}$ approaches zero. The situations for which this would become of practical importance in considering earth satellites are those of the early boost phase and terminal re-entry for the idealized case of a non-rotating planet. Both of these cases involve very large perturbing forces and are not representative of the type of problems for which the constrained equations were developed. Since the perturbing forces are large, the time rates of change of the variables $\hat{H}$ and $\hat{E}$ will also be large and there is no longer any advantage in using these variables in place of the standard unconstrained equations of motion. This particular case will be discussed in greater detail in Chapter 7.

In summary, for the case of small perturbing forces, the primary singularity occuring in the constrained equations involves only the inclination angle, and this singularity is easily eliminated by a redefinition of the reference X, Y, Z coordinate system.

CHAPTER 4

COMPUTER SOLUTIONS FOR NON-PERTURBED ORBIT TRAJECTORIES

As an initial check on the relative accuracy of the constrained equations given by Eqs. (3-31) through (3-39) versus the conventional equations of motions (unconstrained) developed in Chapter 2 and given in their nondimensional form in Chapter 3 by Eqs. (3-40) through (3-45), the motion of a point mass in a central force field was investigated. For this case the perturbing forces $\hat{F}_r$, $\hat{F}_n$, and $\hat{F}_h$ were set equal to zero. The two sets of equations were programed on an IBM 1620 digital computer using a fixed-step fourth-order Runge-Kutta integration scheme. Solutions were obtained using two different integration step sizes for three different trajectories corresponding to orbit eccentricities of 0.5, 0.05, and 1.0. In addition, exact solutions were also obtained as functions of the path angle, u, to obtain a precise standard of comparison.

For purposes of converting the nondimensional computer solutions to dimensional values, the reference radius r_o was selected to be that of the earth and the corresponding reference acceleration g_o was taken to be 32.2 ft./sec.^{2}. With these values the characteristic values of distance, velocity, and time become

$$r_o = 20.9 \times 10^6 \text{ ft.}$$

$$v_o = 25{,}950 \text{ ft./sec.}$$

$$t_o = 810 \text{ sec.}$$

Multiplication of the nondimensional computer solutions of $\hat{r}$, $\hat{v}_r$, $\hat{v}_n$ and $\hat{t}$ by their corresponding characteristic values yields dimensional results.

4.1 Orbit Eccentricity, 0.5

The 0.5 eccentricity trajectory considered had the following orbit parameters:

$\hat{r}_p$ = radius at perigee = 1.5 earth radii

$\hat{r}_a$ = radius at apogee = 4.5 earth radii

$\hat{v}_{np}$ = nondimensional normal velocity at perigee = 1.0

$\hat{v}_{na}$ = nondimensional normal velocity at apogee = 1/3

$\hat{\tau}$ = nondimensional orbital period = 32.648387 which corresponds to a dimensional time of 7.34589 hours.

Initial conditions were as follows:

$\hat{r} = 1.5$

$\hat{v}_n = 1.0$

$\hat{v}_r = 0.0$

$u = 0.0$, u corresponds to true anomaly for this case

$I = 0.78539816$ radians

$\Omega = 0.0$

The nondimensional computer integration step sizes used were 0.2 and 0.8 which correspond to dimensional increments of time of 2.7 minutes and 10.8 minutes respectively. These step sizes correspond to approximately 163 and 41 integration steps per orbit.

Tables A-1 and A-2 of Appendix A present comparisons between the constrained and unconstrained 0.2 step size computer solutions and those obtained using the exact two-body Keplerian equations for selected points over one orbit. These tables were generated by first obtaining the constrained and unconstrained computer solutions and then obtaining the exact solutions of time, radius, and velocity components for the values of path angle u obtained from each of the computer solutions. This

method of comparison allows for a correlation between path angle u and time and also for a comparison of the variables $\hat{r}$, $\hat{v}_r$, and $\hat{v}_n$ versus path angle for both the computer solutions and the exact solutions.

For example, entering Table A-1 with a value of u = 4.0816313 radians yields an exact solution of time for this angle of $\hat{t}$ = 26.400001. The corresponding value of time for the computer solution at the same value of u yields a time of 26.40. The error between u and time for the constrained computer solution is therefore $\hat{\epsilon}_t = 1 \times 10^{-6}$. For the same value of u, the values of $\hat{r}$, $\hat{v}_r$, and $\hat{v}_n$ are in agreement between the exact and constrained computer solutions except for a few digits in the eighth significant figure.

A similar entry into Table A-2 with a value of computer output time of 26.40 indicates the unconstrained computer solution of u at this time to be u = 4.0816408. The exact value of time for this angle is $\hat{t}$ = 26.400066 indicating an error in time of $\hat{\epsilon}_t = 66 \times 10^{-6}$. A comparison of the variables $\hat{r}$, $\hat{v}_r$, and $\hat{v}_n$ between the unconstrained solution and the exact solution for this value of u are also in good agreement, however, the values of $\hat{v}_r$ agree exactly only to the sixth significant digit.

Both the constrained and unconstrained solutions yield values of sufficient accuracy for a fixed-step single-precision computation routine and the order of magnitude of the differences between solutions is not sufficient to lead to a clear preference for one method over the other for the 0.2 integration step size solutions. Certain trends; however, can be observed. The enforcement of the constraints has some effect on the error between time and path angle. From a comparison between the exact time and the computer output time at corresponding values of u in Tables A-1 and A-2, the maximum error in time for the constrained

solutions occurs at a value of u = 2.4281613 and has a value of $\hat{\epsilon}_t$ = $2\text{x}10^{-6}$, while the maximum error in time for the unconstrained solutions occurs at u = 4.0816408 and has a value of $\hat{\epsilon}_t = 66\text{x}10^{-6}$. For all points, the error between u and time is less for the constrained solutions than for the unconstrained solutions. In addition, a comparison between the exact values of $\hat{r}$, $\hat{v}_r$, and $\hat{v}_n$ and the computer solutions at corresponding values of u shows that the constrained solutions agree with the exact values to at least seven significant digits and in many cases eight significant digits, while the unconstrained solutions agree for the most part to only six significant digits.

Tables A-3 and A-4 of Appendix A present comparisons between the constrained and unconstrained computer solutions for an integration step size of 0.80. The tables were generated in the same manner as Tables A-1 and A-2. From this data, a choice of the constrained solutions over the unconstrained solutions becomes much more evident. The maximum error in time between the exact and constrained solutions at corresponding values of u occurs at u = 5.8593379 radians and has the value $\hat{\epsilon}_t = 3.04\text{x}10^{-4}$. The maximum error for the unconstrained solutions occurs at a value of u = 5.0462231 and has the value of $\hat{\epsilon}_t = 2.372\text{x}10^{-2}$. In terms of dimensional time these errors are approximately 0.243 and 19.2 seconds respectively. Fig. 4-1 shows the trends of the error in time versus u for a period of slightly less than one and one-half orbits. The curves were obtained by computing the difference between exact time and computer output time at corresponding values of path angle u. The error in time between the unconstrained solution and the exact solution appears to increase rapidly at a point corresponding to approximately two radians after each perigee while the error between the exact solution

solutions occurs at a value of u = 2.4281613 and has a value of $\hat{\epsilon}_t$ = $2\text{x}10^{-6}$, while the maximum error in time for the unconstrained solutions occurs at u = 4.0816408 and has a value of $\hat{\epsilon}_t = 66\text{x}10^{-6}$. For all points, the error between u and time is less for the constrained solutions than for the unconstrained solutions. In addition, a comparison between the exact values of $\hat{r}$, $\hat{v}_r$, and $\hat{v}_n$ and the computer solutions at corresponding values of u shows that the constrained solutions agree with the exact values to at least seven significant digits and in many cases eight significant digits, while the unconstrained solutions agree for the most part to only six significant digits.

Tables A-3 and A-4 of Appendix A present comparisons between the constrained and unconstrained computer solutions for an integration step size of 0.80. The tables were generated in the same manner as Tables A-1 and A-2. From this data, a choice of the constrained solutions over the unconstrained solutions becomes much more evident. The maximum error in time between the exact and constrained solutions at corresponding values of u occurs at u = 5.8593379 radians and has the value $\hat{\epsilon}_t = 3.04\text{x}10^{-4}$. The maximum error for the unconstrained solutions occurs at a value of u = 5.0462231 and has the value of $\hat{\epsilon}_t = 2.372\text{x}10^{-2}$. In terms of dimensional time these errors are approximately 0.243 and 19.2 seconds respectively. Fig. 4-1 shows the trends of the error in time versus u for a period of slightly less than one and one-half orbits. The curves were obtained by computing the difference between exact time and computer output time at corresponding values of path angle u. The error in time between the unconstrained solution and the exact solution appears to increase rapidly at a point corresponding to approximately two radians after each perigee while the error between the exact solution

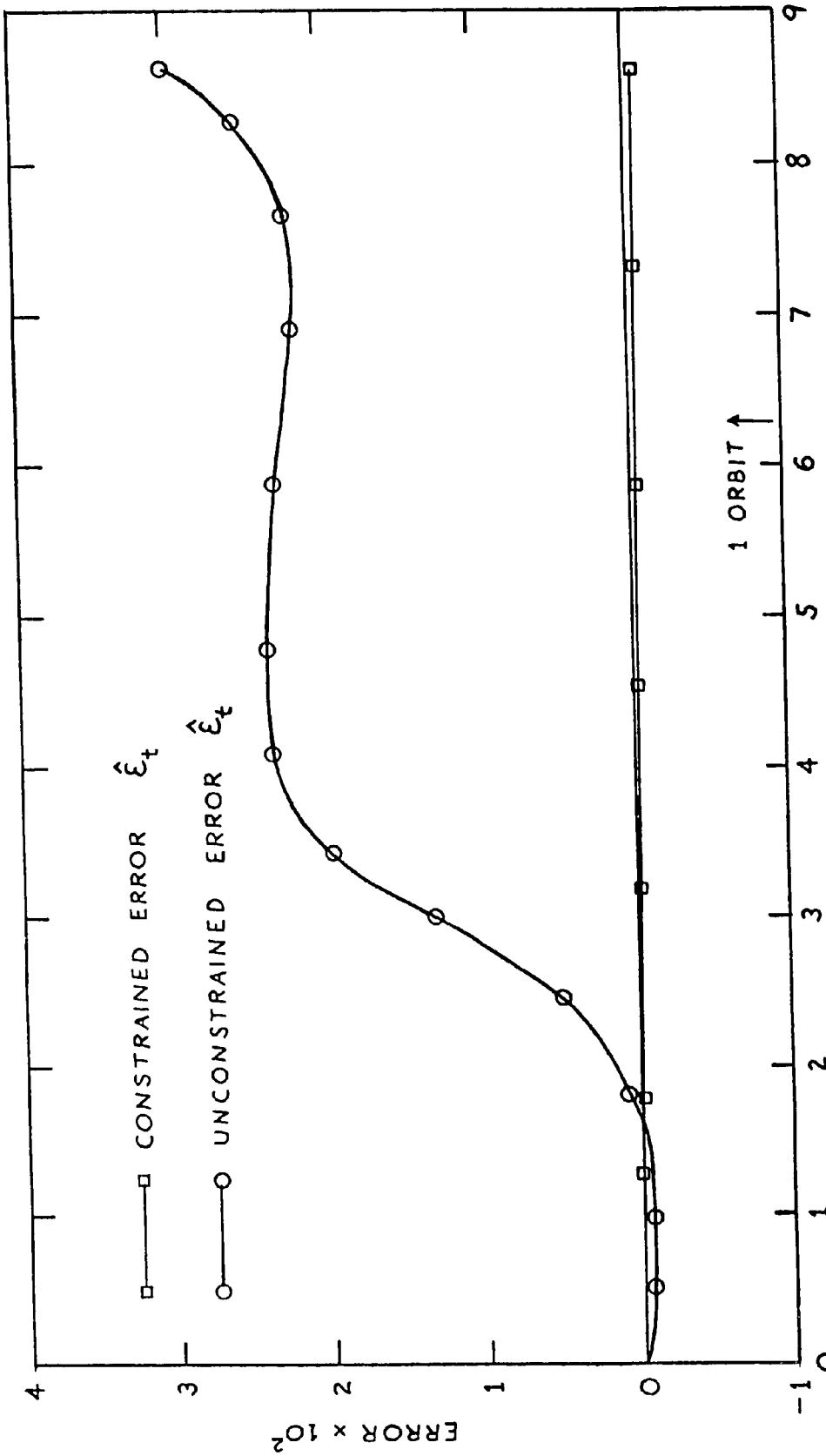

Fig. 4-1: Nondimensional error in time $\hat{\varepsilon}_t$ versus path angle u for 0.8 step size constrained and unconstrained computer solutions for non-perturbed 0.5 eccentricity orbit (computer solutions subtracted from exact solutions).

for time and the constrained solution is slowly increasing over the range of u shown.

Figs. 4-2, 4-3, 4-4 and 4-5 represent trends corresponding to the difference between the 0.8 step size solutions for the constrained and unconstrained equations and the 0.2 step size constrained solutions versus time. From the previous results of Table A-1 we found almost complete agreement between the 0.2 constrained solutions and the exact solutions and therefore, for all practical purposes, these figures represent the error between the 0.8 step size solutions and the exact solution as a function of time. From these figures it can be seen that the errors for the 0.8 step size constrained solutions are considerably less than those resulting from the 0.8 step size unconstrained solutions over the nondimensional time span of 40.0. The relationships between maximum errors are as follows:

$$\epsilon_{u_{uc}} = 62\ \epsilon_{u_c}$$

$$\hat{\epsilon}_{r_{uc}} = 47\ \hat{\epsilon}_{r_c}$$

$$\hat{\epsilon}_{v_{n_{uc}}} = 50\ \hat{\epsilon}_{v_{n_c}}$$

$$\hat{\epsilon}_{v_{r_{uc}}} = 64\ \hat{\epsilon}_{v_{r_c}}$$

where the subscripts uc and c stand for unconstrained and constrained respectively. If these maximum errors are converted to dimensional quantities the errors are

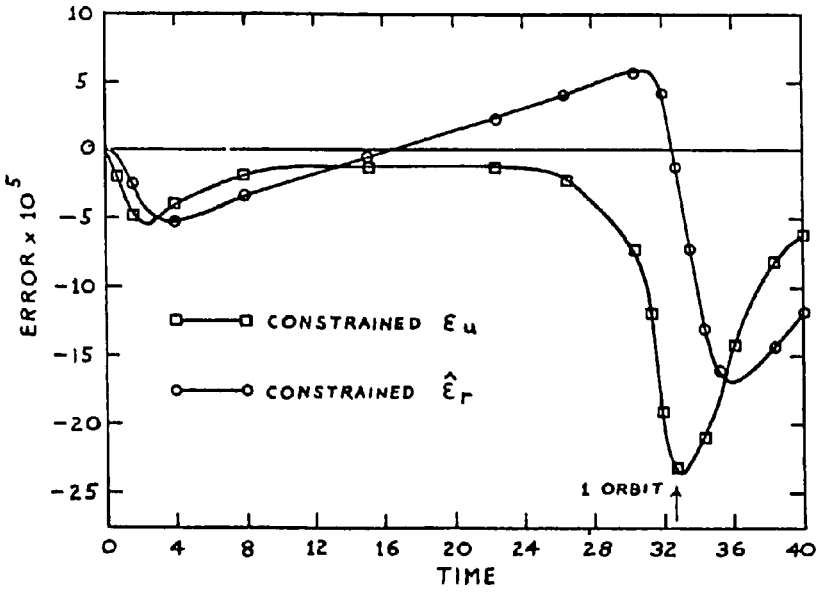

Fig. 4-2: Nondimensional error in radius $\hat{\epsilon}_r$ and path angle ϵ_u versus nondimensional time for 0.8 step size constrained computer solutions for non-perturbed 0.5 eccentricity orbit (0.2 constrained solutions subtracted from 0.8 constrained solutions).

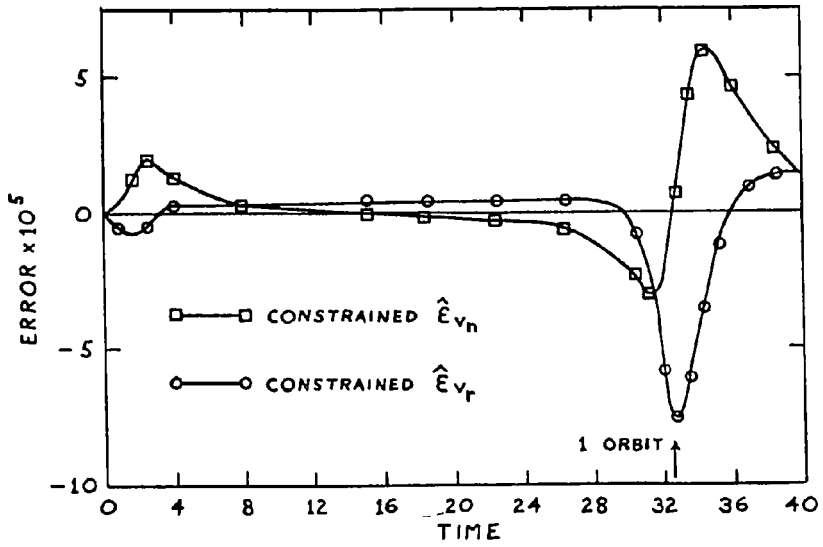

Fig. 4-3: Nondimensional error in radial velocity $\hat{\epsilon}_{v_r}$ and normal velocity $\hat{\epsilon}_{v_n}$ versus nondimensional time for 0.8 step size constrained computer solutions for non-perturbed 0.5 eccentricity orbit (0.2 constrained solutions subtracted from 0.8 constrained solutions).

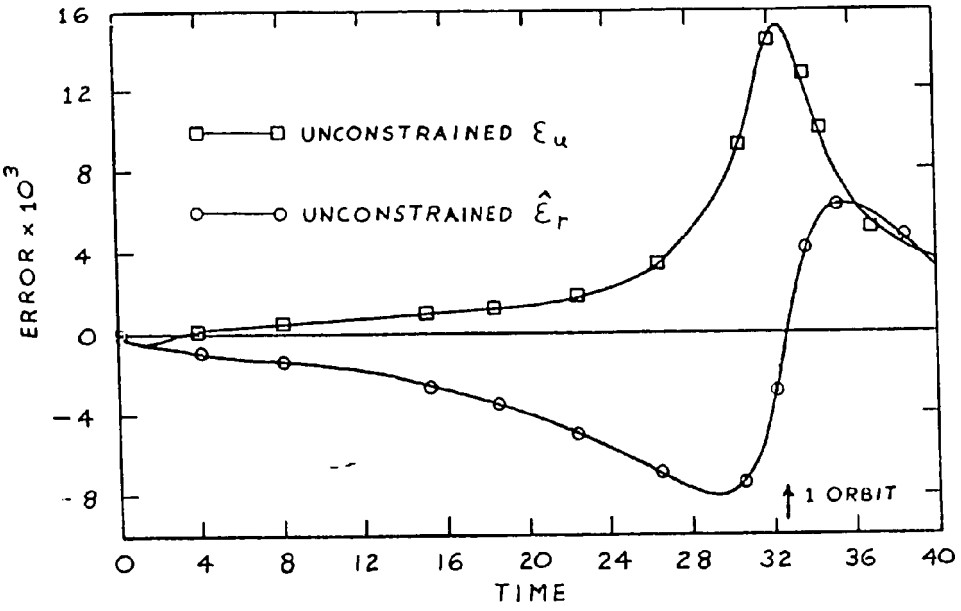

Fig. 4-4: Nondimensional error in radius $\hat{\epsilon}_r$ and path angle ϵ_u versus nondimensional time for 0.8 step size unconstrained computer solutions for non-perturbed 0.5 eccentricity orbit (0.2 constrained solutions subtracted from 0.8 unconstrained solutions).

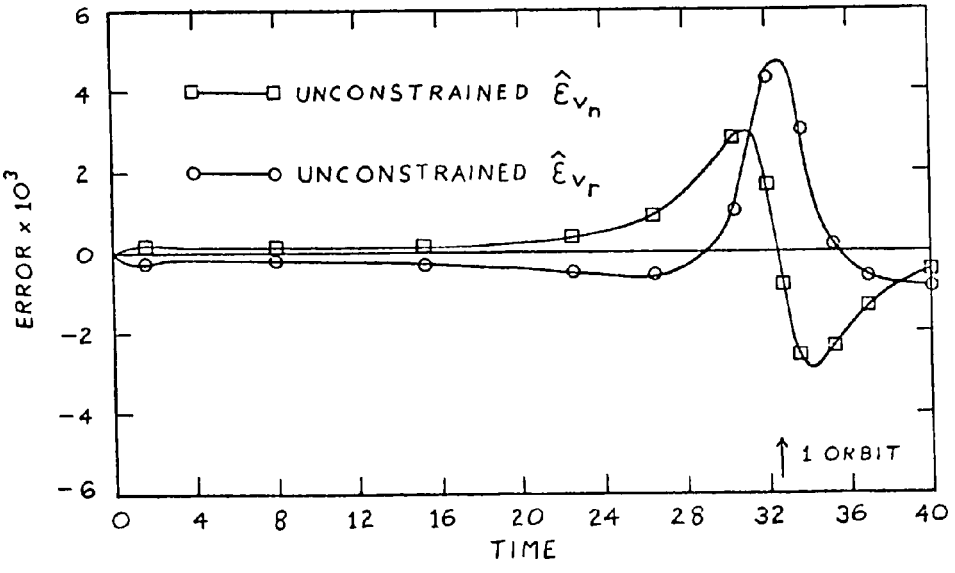

Fig. 4-5: Nondimensional error in radial velocity $\hat{\epsilon}_{v_r}$ and normal velocity $\hat{\epsilon}_{v_n}$ versus nondimensional time for 0.8 step size unconstrained computer solutions for non-perturbed 0.5 eccentricity orbit (0.2 constrained solutions subtracted from 0.8 unconstrained solutions).

Constrained Solution Maximum Error (time treated as independent variable)

ϵ_u = 0.00024 radians

ϵ_r = 0.00017 earth radii = 3570 feet

ϵ_{v_n} = 1.554 feet/second

ϵ_{v_r} = 1.9425 feet/second

Unconstrained Solution Maximum Error (time treated as independent variable)

ϵ_u = 0.015 radians

ϵ_r = 0.008 earth radii = 168,000 feet

ϵ_{v_n} = 77.7 feet/second

ϵ_{v_r} = 124.3 feet/second

An even more interesting result occurs if the two 0.8 step size solutions are compared to the exact solution treating path angle u as the independent variable. In effect, we are comparing the exact solution for the variables $\hat{r}$, $\hat{v}_r$, and $\hat{v}_n$ at each value of u to the constrained and unconstrained solutions for $\hat{r}$, $\hat{v}_r$, and $\hat{v}_n$ at the same value of u as we did in Tables A-3 and A-4. Fig. 4-6 presents the errors between the exact solutions and the 0.8 step size unconstrained solutions as a function of u. In this case, the maximum dimensional errors in the variables $\hat{r}$, $\hat{v}_r$, and $\hat{v}_n$ for the unconstrained solutions over one orbit are as follows:

Unconstrained Maximum Error (u treated as independent variable)

ϵ_r = 63,000 feet

ϵ_{v_n} = 6.475 feet/second

ϵ_{v_r} = 5.18 feet/second

The above errors, and in particular the velocity errors, are considerably improved over the maximum values of error for the unconstrained solutions given before when time was used as the independent variable.

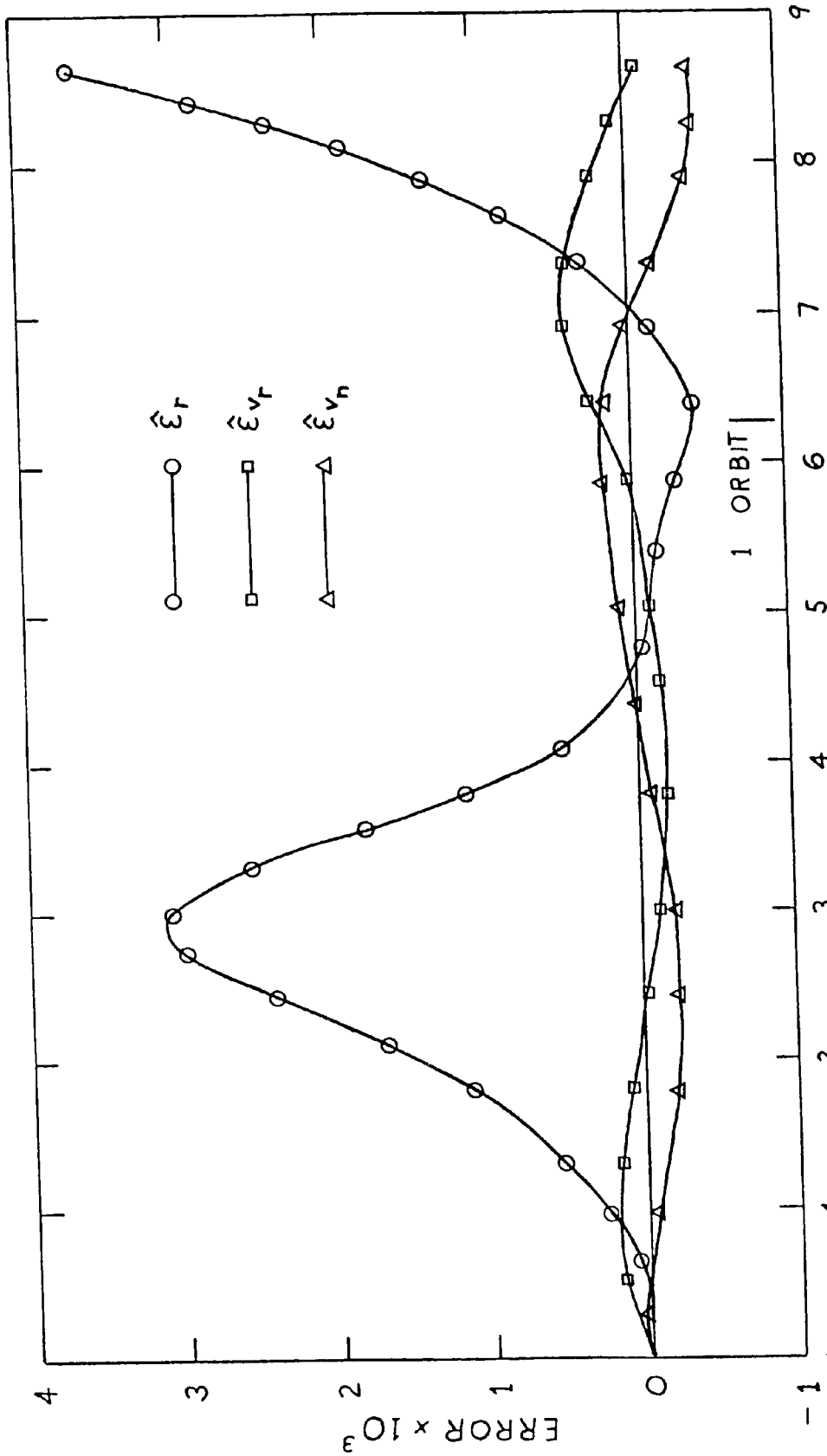

Fig. 4-6: Nondimensional error in radius $\hat{\varepsilon}_r$, radial velocity $\hat{\varepsilon}_{v_r}$, and normal velocity $\hat{\varepsilon}_{v_n}$ versus path angle u for 0.8 step size unconstrained computer solutions for non-perturbed 0.5 eccentricity orbit (0.8 unconstrained solutions subtracted from exact solutions).

However, when this same method of comparison is applied to obtain errors between the exact and constrained solutions, the values of r, v_r, and v_n at corresponding values of path angle are seen from Table A-3 to agree to at least seven significant digits and in many cases to all eight significant digits. Therefore, using this method of comparison between the exact and constrained solutions would result in the following values of dimensional error:

Constrained Maximum Error (u treated as independent variable)

$$\epsilon_r = 2.1 \text{ feet}$$

$$\epsilon_{v_n} = 0.000777 \text{ feet/second}$$

$$\epsilon_{v_r} = 0.00026 \text{ feet/second}$$

Admittedly, the correlation between the exact solution and the constrained solution when compared at the same values of u is not particularly surprising since the variables I, Ω, $\hat{H}$, $\hat{\alpha}$, and $\hat{\gamma}$ are constants of the motion which implies that $\hat{r}$, $\hat{v}_r$, and $\hat{v}_n$ are only functions of the variable u in the constrained solutions. Since the exact solutions for these same variables are also only functions of the variable u, the correspondence between the two solutions is to be expected. However, herein lies a major advantage of the constrained equations. When small perturbing forces are present, the variables I, Ω, $\hat{H}$, $\hat{\alpha}$ and $\hat{\gamma}$ will change very slowly and as a result their values can be determined accurately through numerical integration. In addition, since these variables are changing slowly, they will remain essentially constant for small variations in u and therefore the values $\hat{r}$, $\hat{v}_r$, and $\hat{v}_n$ are again primarily only functions of u over these small variations. The accuracy of u with time and hence the variables $\hat{r}$, $\hat{v}_r$, and $\hat{v}_n$ does of course depend upon the accuracy with which we obtain u. However, the above results indicate that the

deviation of u with time may be less when the constrained equations are used, which suggests that somewhat larger integration step sizes may be used for the constrained equations than for the unconstrained equations. In addition, if one is primarily interested in the values of $\hat{r}$, $\hat{v}_r$, and $\hat{v}_n$ which correspond to a given value of u, even larger integration step sizes may be employed.

4.2 Estimate of Time Difference $\Delta\hat{t}$, and Correction Technique for Path Angle Difference, Δu, Between Computer Solutions at Two Different Integration Step Sizes

The preceding discussion implies that over small variations in the angle u, we would expect any changes of the values $\hat{r}$, $\hat{v}_r$, and $\hat{v}_n$ resulting from the constrained solutions to be predominately only functions of the variation in u. This suggests a technique for estimating the error in time between constrained soltuions obtained for two different integration step sizes and a method for verifying that the constrained solution values of $\hat{r}$, $\hat{v}_r$, and $\hat{v}_n$, when perturbing forces are present, are correct with u even though u is in error with time. Although this method is not important for the case of non-perturbed orbits since exact solutions can be obtained, it will prove valuable when perturbing forces are present since it will provide an estimate of the time error between a solution which is considered correct and one resulting from taking larger step sizes. In addition, it will provide a method of showing the correspondence between path angle u and the variables $\hat{r}$, $\hat{v}_r$, and $\hat{v}_n$ when the constrained equations are used to consider perturbed orbits.

If we were given computer solutions obtained for two different integration step sizes, we would expect some difference in the results at corresponding output times. As an example, the 0.2 and 0.8

constrained solutions at a computer output time of 32.0 are found from Tables A-1 and A-3 to be

0.2 Step Size

u	$\hat{r}$	$\hat{v}_r$	$\hat{v}_n$
5.8595285	1.5455463	-0.13703223	0.97053060

0.8 Step Size

u	$\hat{r}$	$\hat{v}_r$	$\hat{v}_n$
5.8593379	1.5455879	-0.13709014	0.97050446

The value of Δu between these two solutions is $\Delta u = u_{.2} - u_{.8} = 0.0001906$ and if we assume that u varies linearly with time over the small variation in u then we can write

$$\Delta \hat{t} = t_{.2} - t_{.8} \simeq \frac{\Delta u}{\dot{\hat{u}}} \qquad (4\text{-}1)$$

Using the relationship $\dot{\hat{u}} = \frac{\hat{v}_n}{\hat{r}}$ and computing this value from the 0.8 step size solution for $\hat{v}_n$ and $\hat{r}$ yields $\dot{\hat{u}} = 0.62791929$. Therefore the difference in time between the two solutions is estimated to be

$\Delta \hat{t} \simeq 0.0003035\text{4}$.

From the above estimate we see that the difference in the angle u between the 0.2 step size solution and the 0.8 step size solution should represent an approximate difference in time of $\Delta \hat{t} = 0.0003035\text{4}$. From Table A-1 we find that the value of u given by the 0.2 step size solution corresponds to an exact value of time of 31.999999. From Table A-3 we see that the value of u given by the 0.8 step size solution corresponds to an exact value of time of 31.999696. The actual difference in time is therefore $\Delta \hat{t} = 0.000303$ which is in good agreement with the approximate value computed above.

The correspondence between the constrained solutions of r, v_r, and v_n with u has already been demonstrated for the non-perturbed case by comparing the exact solutions for r, v_r, and v_n with the constrained solutions at identical values of u. When perturbed orbits are considered, exact solutions may not be available and therefore it would be of interest to determine whether or not this correspondence is still in effect. To answer this question, the following technique is proposed.

Suppose we have two computer solutions obtained with two different step sizes and that we consider one of these solutions to be essentially correct. If the error in the other solution is primarily only an error between u and time, and if the values of $\hat{r}$, $\hat{v}_r$, and $\hat{v}_n$ are correct with the output value of u, then the difference between the two solutions for $\hat{r}$, $\hat{v}_r$, and $\hat{v}_n$ should be only a function of the difference between the two computer solutions for u. From above, the variation in $\Delta\hat{t}$ was

$$\Delta\hat{t} \simeq \frac{\Delta\hat{u}}{u} \simeq \frac{(\Delta u)(\hat{r})}{\hat{v}_n} \tag{4-2}$$

Therefore we can write

$$\Delta\hat{r} = \hat{r}_{.2} - \hat{r}_{.8} \simeq \dot{\hat{v}}_r\Delta\hat{t} \simeq \frac{\hat{v}_r\hat{r}\Delta u}{\hat{v}_n} \tag{4-3}$$

$$\Delta\hat{v}_n = \hat{v}_{n_{.2}} - \hat{v}_{n_{.8}} \simeq \dot{\hat{v}}_n\Delta\hat{t} \simeq -\left(\frac{\hat{v}_r\hat{v}_n}{\hat{r}}\right)\Delta\hat{t} = -\hat{v}_r\Delta u \tag{4-4}$$

and

$$\Delta\hat{v}_r = \hat{v}_{r_{.2}} - \hat{v}_{r_{.8}} \simeq \dot{\hat{v}}_r\Delta\hat{t} \simeq \left(\frac{\hat{v}_n^2}{\hat{r}} - \frac{1}{\hat{r}^2}\right)\Delta\hat{t} = \left(\hat{v}_n - \frac{1}{\hat{r}\hat{v}_n}\right)\Delta u \tag{4-5}$$

As an example of the use of these equations we can again make use of the 0.2 and 0.8 step size computer solutions for the constrained equations at the computer output time of 32.0 used in the preceding example. As before, the value of Δu is defined by $\Delta u = u_{.2} - u_{.8} = 0.0001906$. Substituting the values resulting from the 0.8 step size solution into Eqs. (4-3), (4-4), and (4-5) we obtain

$$\Delta\hat{r} = -0.0000416$$

$$\Delta\hat{v}_n = 0.00002613$$

$$\Delta\hat{v}_r = 0.00005791$$

The actual values obtained from the 0.2 and 0.8 step size constrained solutions are

$$\Delta\hat{r} = \hat{r}_{.2} - \hat{r}_{.8} = -0.0000416$$

$$\Delta\hat{v}_n = \hat{v}_{n.2} - \hat{v}_{n.8} = 0.00002614$$

$$\Delta\hat{v}_r = \hat{v}_{r.2} - \hat{v}_{r.8} = 0.00005791$$

The accuracy of this technique depends of course on the validity of using the linear approximations; however, if the deviations between the values of u for two different step sizes are not large, the method does yield an approximate technique for evaluating the correspondence between u and the variables $\hat{r}$, $\hat{v}_r$, and $\hat{v}_n$ even when small perturbing forces are present and no exact solutions exist. It should be noted that this method is not valid if the values of the variables substituted into Eqs. (4-3), (4-4), or (4-5) correspond to points in the orbit for which $\hat{v}_r$ or $\hat{v}_r$ are equal to zero, or if the angle Δu is equally distributed on either side of perigee, apogee, or the semilatus rectum of the orbit.

4.3 Orbit Eccentricity, 0.05

The 0.05 eccentricity trajectory considered had the following orbit parameters:

$\hat{r}_p$ = radius at perigee = 1.05 earth radii

$\hat{r}_a$ = radius at apogee = 1.1605263 earth radii

$\hat{v}_{np}$ = nondimensional normal velocity at perigee = 1.0

$\hat{v}_{na}$ = nondimensional normal velocity at apogee = .90476190

$\hat{\tau}$ = nondimensional orbital period = 7.3009336 which corresponds to a dimensional time of 1.6427 hours.

Initial conditions were as follows:

$\hat{r} = 1.05$

$\hat{v}_n = 1.0$

$\hat{v}_r = 0.0$

u = 0.0, u corresponds to true anomaly for this case

I = 0.78539816

$\Omega = 0.0$

The nondimensional computer integration step sizes used were again 0.2 and 0.8 which correspond as before to dimensional increments of time of 2.7 minutes and 10.8 minutes respectively. These step sizes correspond to approximately 37 and 9 integration steps per orbit.

Tables A-5 and A-6 in Appendix A present comparisons between the constrained and unconstrained 0.2 step size computer solutions and those obtained using exact two body Keplerian equations for selected points over approximately three complete orbits. These tables were generated in the same manner as those of the 0.5 eccentricity case discussed previously. For the solutions tabulated in Tables A-5 and A-6, the error between u and time can again be computed by comparing the exact solutions with the 0.2 step size constrained and unconstrained solutions at corresponding values of u. From Table A-5 the maximum error in time for the

constrained solution occurs at a value of u = 14.551008 radians and has the value $\hat{\epsilon}_t = 2\text{x}10^{-6}$. From Table A-6 the maximum error in time for the unconstrained solution occurs at a value of u = 18.561518 radians and has the value $\hat{\epsilon}_t = 3.6\text{x}10^{-5}$. A comparison of the variables $\hat{r}$, $\hat{v}_r$, and $\hat{v}_n$ obtained from the computer solutions with those obtained by the exact solutions at corresponding values of u indicates the constrained solutions are correct to at least seven significant digits in all of the variables. The same comparison shows that the unconstrained solutions are correct with u to approximately six significant digits in $\hat{r}$, four significant digits in $\hat{v}_r$, and five significant digits in $\hat{v}_n$. The above indicates that the maximum dimensional errors between the unconstrained and exact solutions amount to approximately 100 feet in radius and 0.1 feet/second in velocity while the constrained solutions are essentially identical to the exact solutions over the three orbits considered.

Both of these methods provide results which are of sufficient accuracy for a single-precision computation routine. However, as before, the constrained solutions have slightly less error in time than the unconstrained solutions and the variables $\hat{r}$, $\hat{v}_r$, and $\hat{v}_n$ are in much better agreement with u for the constrained solutions than for the unconstrained solutions.

Tables A-7 and A-8 in Appendix A present a comparison between the exact solutions and the computer solutions when the integration step size is increased to a nondimensional increment of 0.8. It should be noted that this represents a very large step size for this orbit since only nine integration steps are being taken per orbit. From these tables it can be seen that the constrained solutions for $\hat{r}$, $\hat{v}_r$, and $\hat{v}_n$ are still in agreement with the exact solutions to seven significant digits and in

some cases to all eight significant digits. The agreement between the exact and unconstrained solutions for the variables $\hat{r}$, $\hat{v}_r$, and $\hat{v}_n$ is now only good to between three to four significant digits in $\hat{r}$, one to two significant digits in $\hat{v}_r$, and two to three significant digits in $\hat{v}_n$. Fig. 4-7 shows the trends in the error in time with path angle u for the constrained and unconstrained computer solutions over a period of three complete orbits. The maximum error in nondimensional time for the unconstrained solutions is approximately $4.2\text{x}10^{-3}$ while that for the constrained solutions is approximately $5.3\text{x}10^{-5}$. These nondimensional time errors correspond to dimensional errors in time of 3.4 seconds and 0.043 seconds respectively.

Fig. 4-8 shows the trends of the error in the variables $\hat{r}$, $\hat{v}_r$, and $\hat{v}_n$ between the exact and unconstrained solutions when u is used as the independent variable. The maximum nondimensional errors over three orbits are seen to be $\hat{\epsilon}_r = 1.8\text{x}10^{-3}$, $\hat{\epsilon}_{v_r} = 1.5\text{x}10^{-3}$, and $\hat{\epsilon}_{v_n} = 1.6\text{x}10^{-3}$. These values correspond to the following dimensional errors:

Unconstrained Maximum Error (u treated as independent variable)

$$\epsilon_r = 37{,}800 \text{ feet}$$

$$\epsilon_{v_r} = 38.85 \text{ feet/second}$$

$$\epsilon_{v_n} = 41.44 \text{ feet/second}$$

The constrained solutions are almost identical to the exact solutions and by this method of comparison would have approximately the following dimensional errors:

Constrained Maximum Error (u treated as independent variable)

$$\epsilon_r = 4.2 \text{ feet}$$

$$\epsilon_{v_r} = 0.000468 \text{ feet/second}$$

$$\epsilon_{v_n} = 0.00234 \text{ feet/second}$$

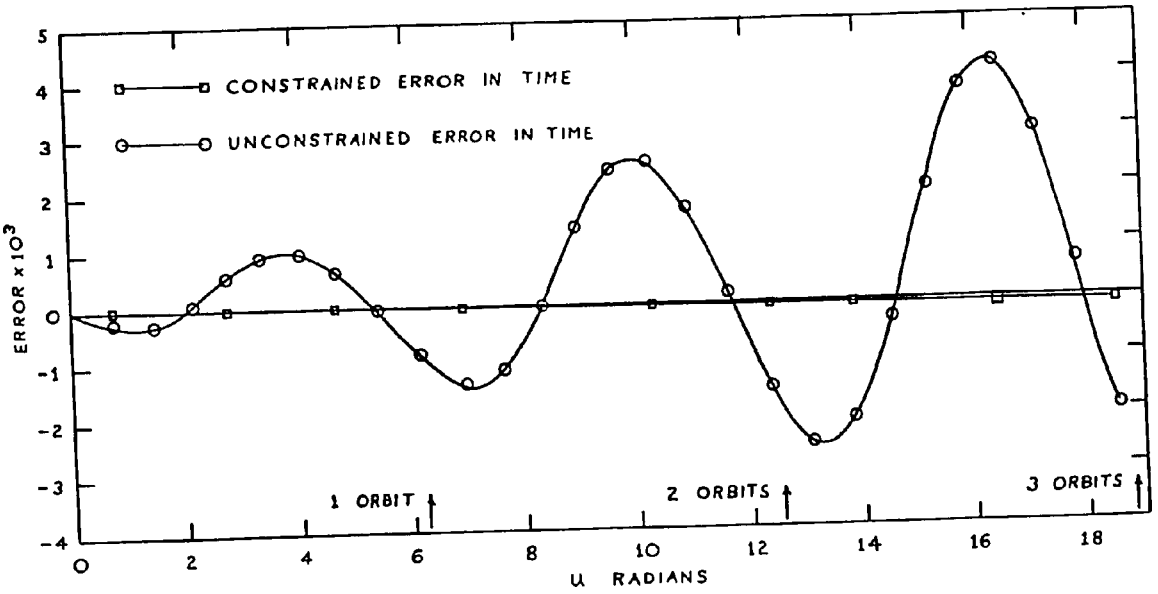

Fig. 4-7: Nondimensional error in time $\hat{\epsilon}_t$ versus path angle u for 0.8 step size constrained and unconstrained computer solutions for non-perturbed 0.05 eccentricity orbit (computer solutions subtracted from exact solutions).

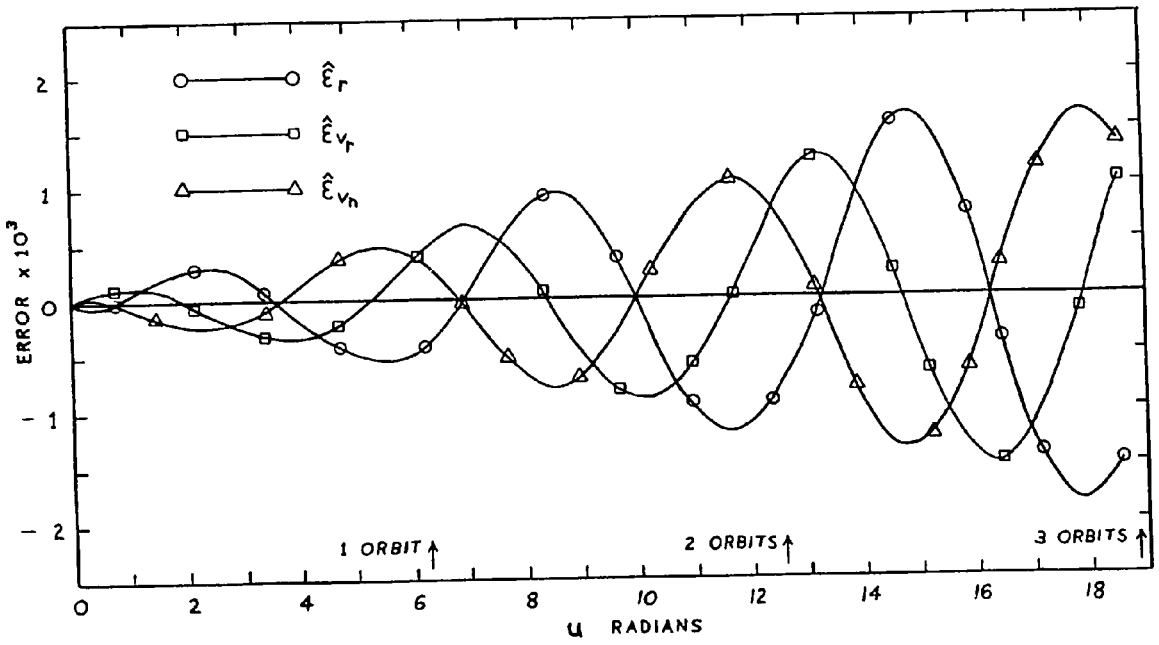

Fig. 4-8: Nondimensional error in radius $\hat{\epsilon}_r$, radial velocity $\hat{\epsilon}_{v_r}$, and normal velocity $\hat{\epsilon}_{v_n}$ versus path angle u for 0.8 step size unconstrained computer solutions for non-perturbed 0.05 eccentricity orbit (0.8 unconstrained solutions subtracted from exact solutions).

Figs. 4-9 and 4-10 present the trends of the differences between the 0.8 and 0.2 constrained solutions when time is used as the independent variable. From Table A-5 we found the 0.2 step size constrained solution to be in good agreement with the exact solutions and therefore these figures essentially represent the error between the 0.8 step size solutions for u, $\hat{r}$, $\hat{v}_r$, and $\hat{v}_n$ and the exact solutions as a function of time. In terms of dimensional quantities the maximum errors over three orbits for the 0.8 step size constrained solutions are as follows:

Constrained Solution Maximum Error (time treated as independent variable)

$\epsilon_r = 52.5$ feet

$\epsilon_{v_r} = 0.062$ feet/second

$\epsilon_{v_n} = 0.057$ feet/second

$\epsilon_u = 0.000051$ radians

Figs. 4-11 and 4-12 present the trends of the differences between the 0.8 step size unconstrained solutions and the 0.2 step size constrained solution over the same period of three orbits. If these values are converted to dimensional quantities the resulting maximum errors are found to be:

Unconstrained Solution Maximum Error (time treated as independent variable)

$\epsilon_r = 37{,}800$ feet

$\epsilon_{v_r} = 38.85$ feet/second

$\epsilon_{v_n} = 41.44$ feet/second

$\epsilon_u = 0.0034$ radians

In the previous 0.5 eccentricity case the 0.8 step size unconstrained maximum errors differed depending upon whether u or time was used as the independent variable. For the 0.05 eccentricity case the

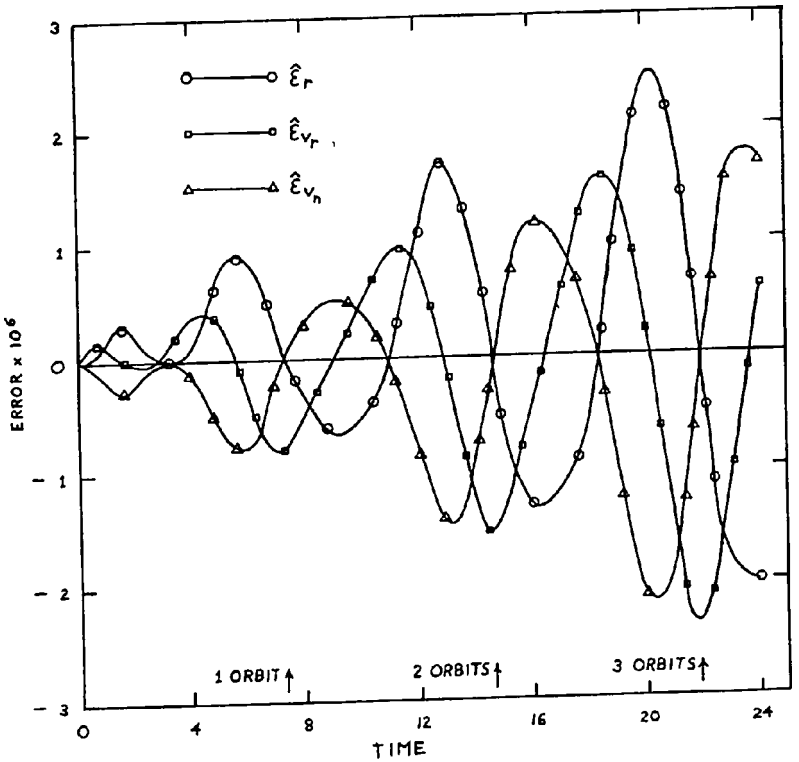

Fig. 4-9: Nondimensional error in radius $\hat{\varepsilon}_r$, radial velocity $\hat{\varepsilon}_{v_r}$, and normal velocity $\hat{\varepsilon}_{v_n}$ versus nondimensional time for 0.8 step size constrained computer solutions for non-perturbed 0.05 eccentricity orbit (0.2 constrained solutions subtracted from 0.8 constrained solutions).

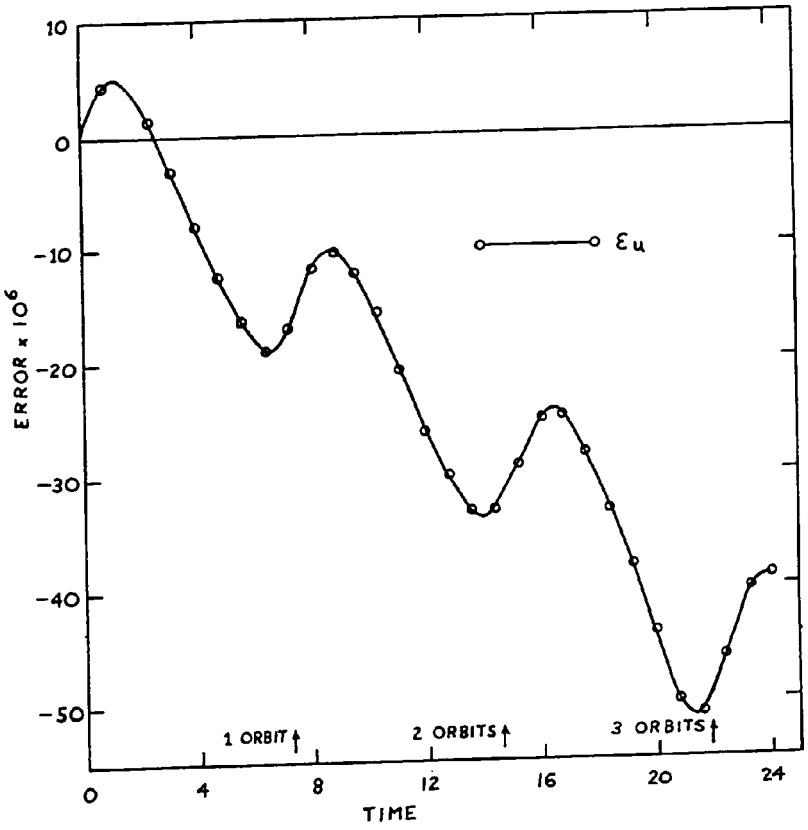

Fig. 4-10: Error in path angle ε_u (in radians) versus nondimensional time for 0.8 step size constrained computer solutions for non-perturbed 0.05 eccentricity orbit (0.2 constrained solutions subtracted from 0.8 constrained solutions).

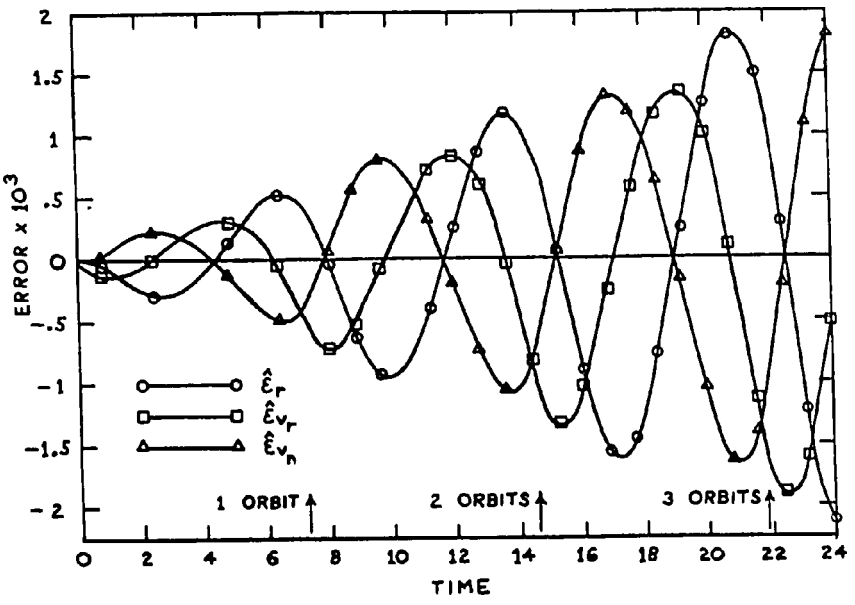

Fig. 4-11: Nondimensional error in radius $\hat{\epsilon}_r$, radial velocity $\hat{\epsilon}_{v_r}$, and normal velocity $\hat{\epsilon}_{v_n}$ versus nondimensional time for 0.8 step size unconstrained computer solutions for non-perturbed 0.05 eccentricity orbit (0.2 constrained solutions subtracted from 0.8 unconstrained solutions).

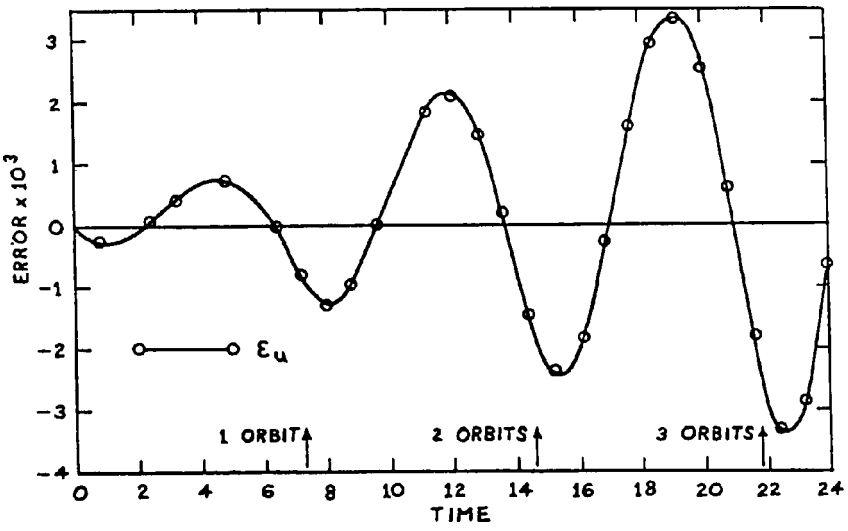

Fig. 4-12: Error in path angle ϵ_u (in radians) versus nondimensional time for 0.8 step size unconstrained computer solutions for non-perturbed 0.05 eccentricity orbit (0.2 constrained solutions subtracted from 0.8 unconstrained solutions.

errors are the same regardless of which method is used in computing errors.

4.4 Orbit Eccentricity, 1.0 (Parabolic Trajectory)

The parabolic trajectory considered had the following orbit parameters:

$\hat{r}_p$ = radius at perigee = 1.0368 earth radii

$\hat{v}_{np}$ = nondimensional normal velocity at perigee = 1.3888889

Initial conditions were as follows:

$\hat{r} = 1.0368$

$\hat{v}_n = 1.3888889$

$\hat{v}_r = 0.0$

u = 0.0, u corresponds to true anomaly for this case

I = 0.78539816

$\Omega = 0.0$

The nondimensional computer integration step sizes used were 0.2 and 0.8. Solutions were obtained up to a nondimensional time of $\hat{t} = 14.40$ at which time the radius had increased to a value of $\hat{r} = 8.8527916$ and the path angle to a value of u = 2.4430322 radians.

Tables A-9 and A-10 in Appendix A present comparisons between the constrained and unconstrained 0.2 step size computer solutions and those obtained using exact two body Keplerian equations. From Table A-9 the maximum error in time for the constrained solution occurs early in the trajectory at a value of u = 1.6913719 radians and has a magnitude of $\hat{\epsilon}_t = 1.52 \times 10^{-5}$. From table A-10 the maximum error in time for the unconstrained solutions occurs at the last computed point when u = 2.4430959 radians and has a magnitude of $\hat{\epsilon}_t = 3.461 \times 10^{-3}$. As in the previous cases, a comparison of the variables $\hat{r}$, $\hat{v}_r$, and $\hat{v}_n$ obtained from the computer

solutions with those obtained from the exact solutions at corresponding values of u indicates the constrained solutions are correct to at least seven significant digits and in many cases to all eight digits. The same comparison shows that the unconstrained solutions are correct with u to between three to five significant digits in $\hat{r}$, four to five significant digits in $\hat{v}_r$, and four significant digits in $\hat{v}_n$. It should be noted that for the unconstrained solution the error in radius is continuously increasing.

Tables A-11 and A-12 in Appendix A present a comparison between the exact solutions and the computer solutions when the integration step size is increased to a nondimensional increment of 0.8. This represents a very large step size for the parabolic case when computing points in the vicinity of perigee since the time rate of change of the path angle is large. During the first integration step the angle u increases to a value of approximately 52 degrees. For this reason the errors in u with time are considerably larger than in the previous cases.

Fig. 4-13 presents the trends of the error in time with path angle for the constrained and unconstrained 0.8 step size computer solutions. The maximum error in time for the constrained solutions is a value of $\hat{\epsilon}_t = 30 \times 10^{-4}$. This error was reached at a value of u = 2.0611923 radians and remains essentially constant for the remainder of the solutions. The error in time for the unconstrained solutions remains essentially constant to a value of u = 1.7 radians at which point it begins to increase rapidly and at the last computed point has the value $\hat{\epsilon}_t = 62.5 \times 10^{-2}$. These nondimensional time errors correspond to dimensional errors of 2.43 seconds and 506 seconds respectively.

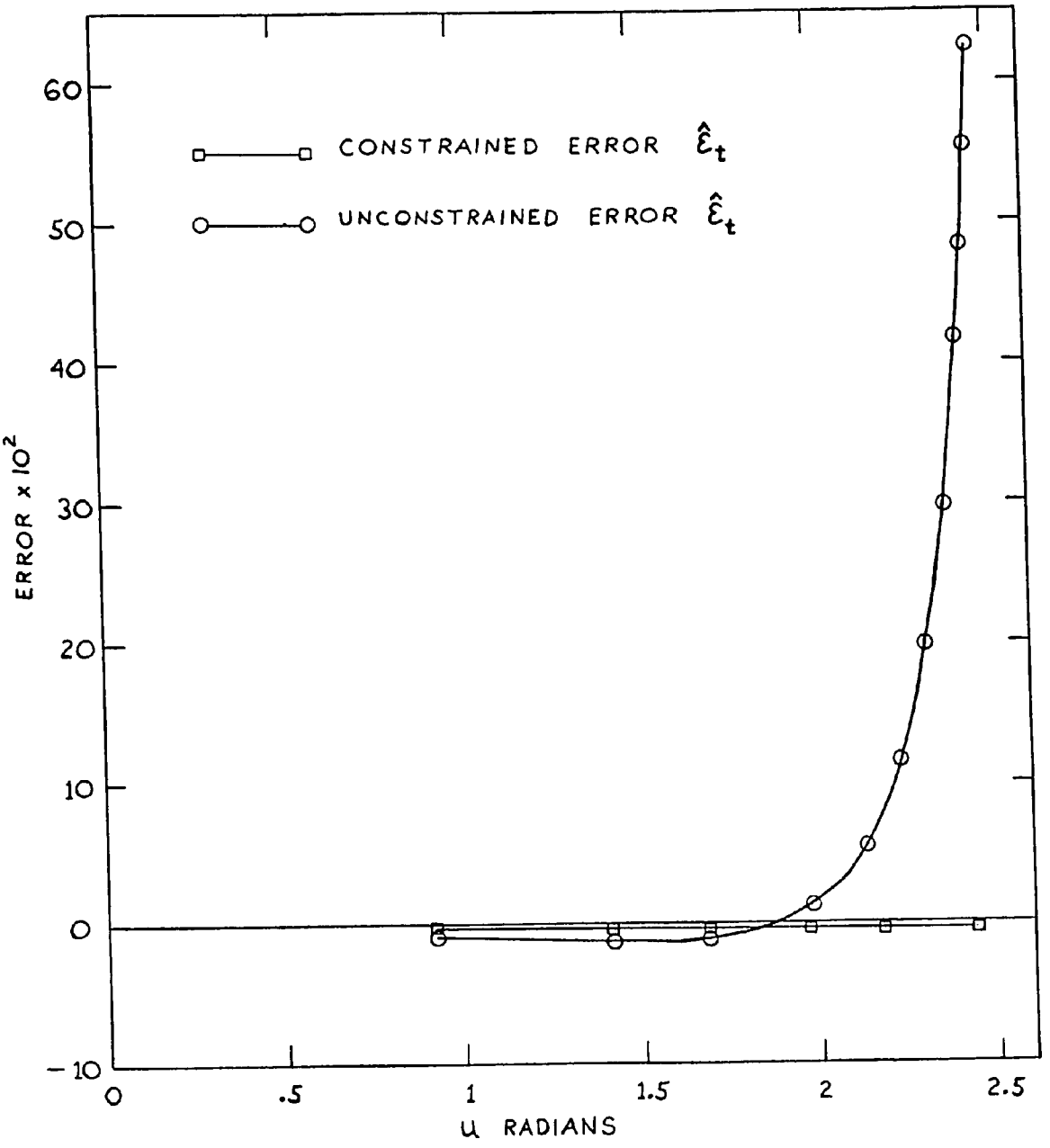

Fig. 4-13: Nondimensional error in time $\hat{\epsilon}_t$ versus path angle u for 0.8 step size constrained and unconstrained computer solutions for non-perturbed parabolic trajectory (computer solutions subtracted from exact solutions).

Figs. 4-14, 4-15, 4-16 and 4-17 present the trends of the differences between the 0.8 step size constrained and unconstrained solutions and the 0.2 step size constrained solutions Since the 0.2 step size constrained solutions were in good agreement with the exact solutions these figures essentially represent the errors of the 0.8 step size solutions as a function of time. The maximum errors in terms of dimensional quantities are as follows:

Constrained Solutions Maximum Error (time treated as independent variable)

ϵ_u = 0.0013 radians

ϵ_r = 42,000 feet

ϵ_{v_r} = 14.3 feet/second

ϵ_{v_n} = 24.7 feet/second

Unconstrained Solution Maximum Error (time treated as independent variable)

ϵ_u = 0.0111 radian

ϵ_r = 3,150,000 feet

ϵ_{v_r} = 345.8 feet/second

ϵ_{v_n} = 55.9 feet/second

From the standpoint of precision trajectory computations the errors in velocity of both methods are unacceptable when the large 0.8 step size is used. However it is interesting to note the effects of the constraints as time increases. In all cases the maximum errors in the constrained solutions occurred early in the trajectory where the time rate of change of u was large. As time increases the errors decrease and at the last computed point the dimensional constrained errors when time is used as the independent variable are as follows:

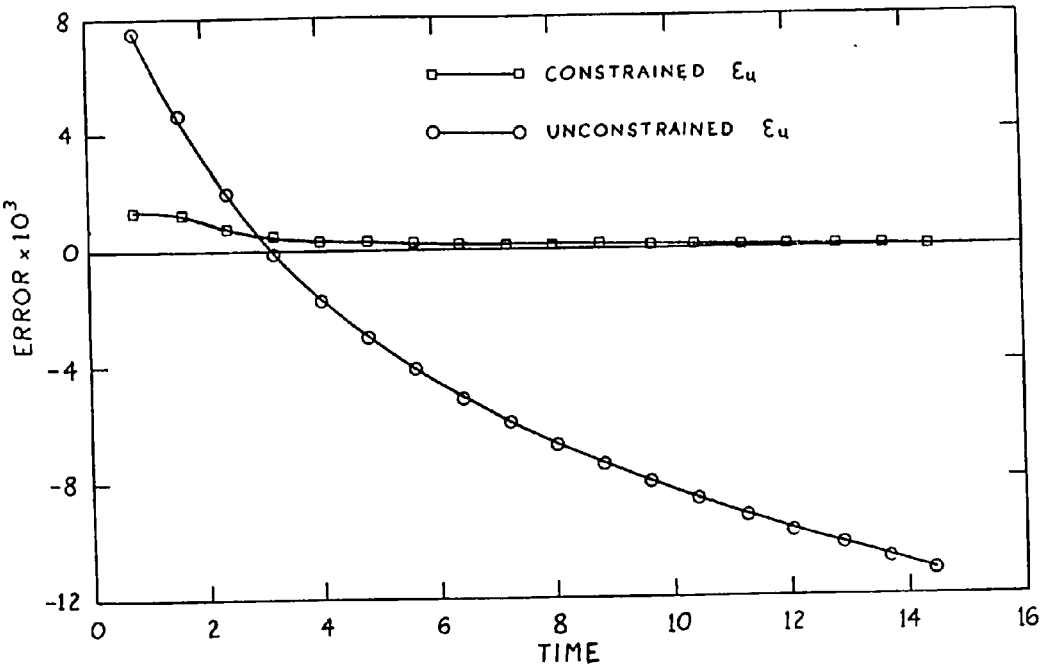

Fig. 4-14: Error in path angle ϵ_u (in radians) versus nondimensional time for 0.8 step size constrained and unconstrained computer solutions for non-perturbed parabolic trajectory (0.8 solutions subtracted from 0.2 constrained solutions).

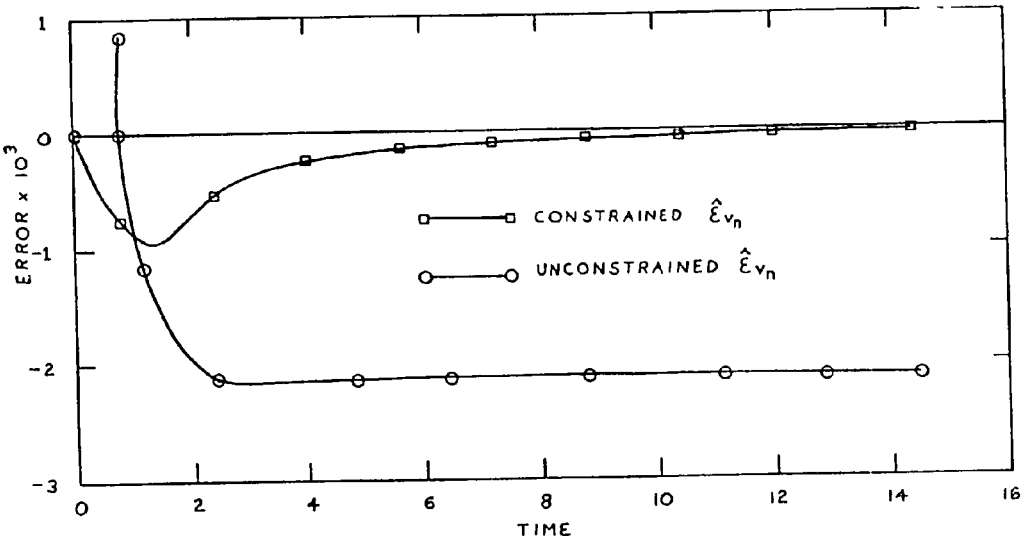

Fig. 4-15: Nondimensional error in normal velocity $\hat{\epsilon}_{v_n}$ versus nondimensional time for 0.8 step size constrained and unconstrained computer solutions for non-perturbed parabolic trajectory (0.8 solutions subtracted from 0.2 constrained solutions).

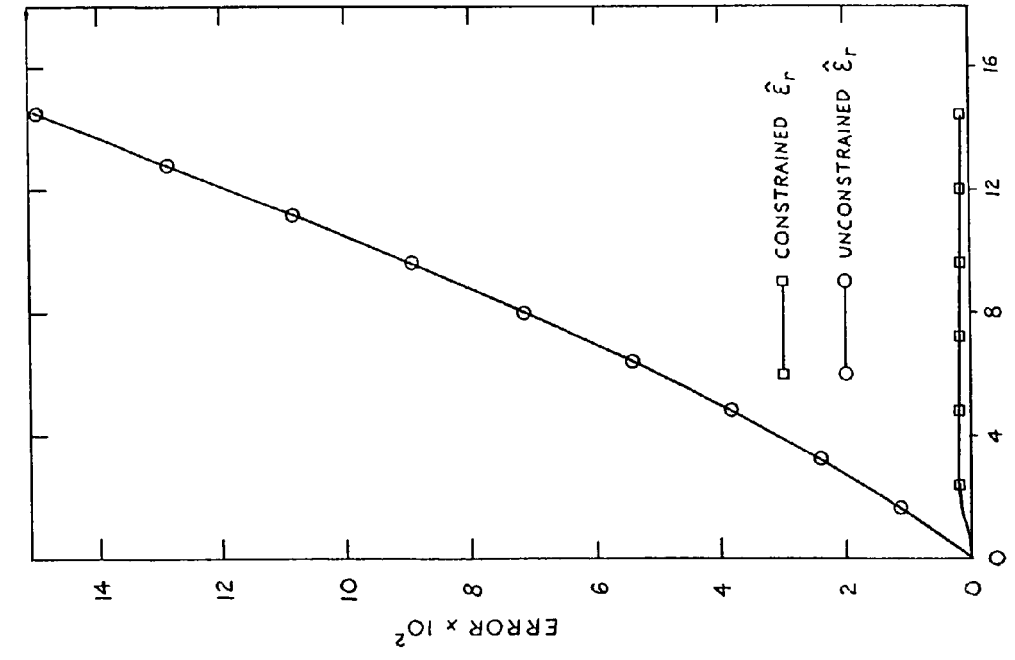

Fig. 4-16: Nondimensional error in radius $\hat{\varepsilon}_r$ versus nondimensional time for 0.8 step size constrained and unconstrained computer solutions for non-perturbed parabolic trajectory (0.8 solutions subtracted from 0.2 constrained solutions).

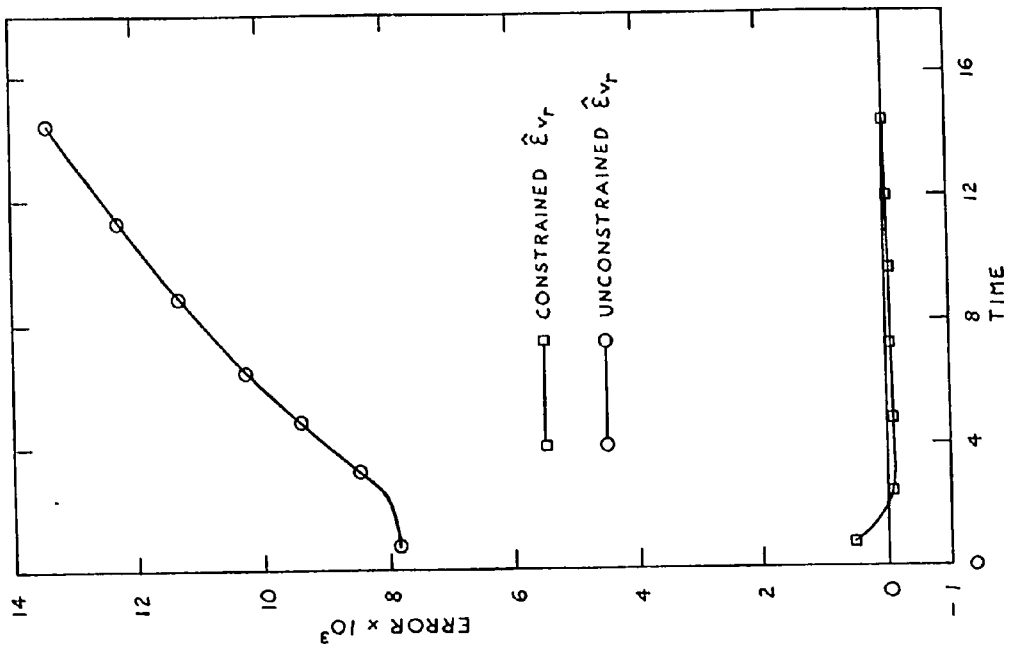

Fig. 4-17: Nondimensional error in radial velocity $\hat{\varepsilon}_{v_r}$ versus nondimensional time for 0.8 step size constrained and unconstrained computer solutions for non-perturbed parabolic trajectory (0.8 solutions subtracted from 0.2 constrained solutions).

Constrained Error at $\hat{t}$ = 14.40

ϵ_u = 0.0000551 radians

ϵ_r = 28,161 feet

ϵ_{v_r} = 0.754 feet/second

ϵ_{v_n} = 0.6396 feet/second

On the other hand, the unconstrained solution errors for u, $\hat{r}$, and $\hat{v}_r$ reach their maximum at the last point computed and are increasing. The unconstrained error for $\hat{v}_n$ reaches its maximum value early in the trajectory and then remains essentially constant although the last few computed values indicate the error to be slowly increasing.

Figs. 4-18 and 4-19 present the trends of the errors for the unconstrained solutions of $\hat{r}$, $\hat{v}_r$, and $\hat{v}_n$ when the path angle u is taken as the independent variable. By this method of comparison the maximum dimensional errors are as follows:

Unconstrained Maximum Error (u treated as independent variable)

ϵ_r = 8,925,000 feet

ϵ_{v_r} = 221 feet/second

ϵ_{v_n} = 182 feet/second

From Table A-11, the same method of comparison for the constrained solutions would yield virtually no error between the constrained 0.8 step size solutions and the exact solutions.

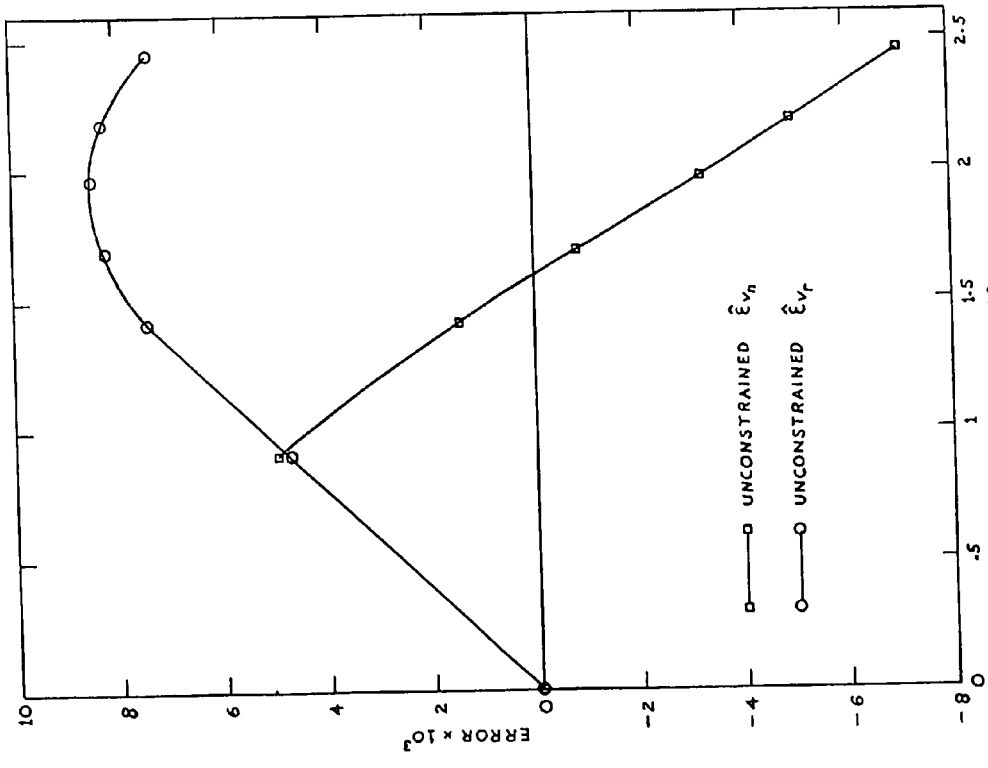

Fig. 4-19: Nondimensional error in radial velocity $\hat{\epsilon}_{v_r}$ and normal velocity $\hat{\epsilon}_{v_n}$ versus path angle u for 0.8 step size unconstrained computer solutions for non-perturbed parabolic trajectory (0.8 unconstrained solutions subtracted from exact solutions).

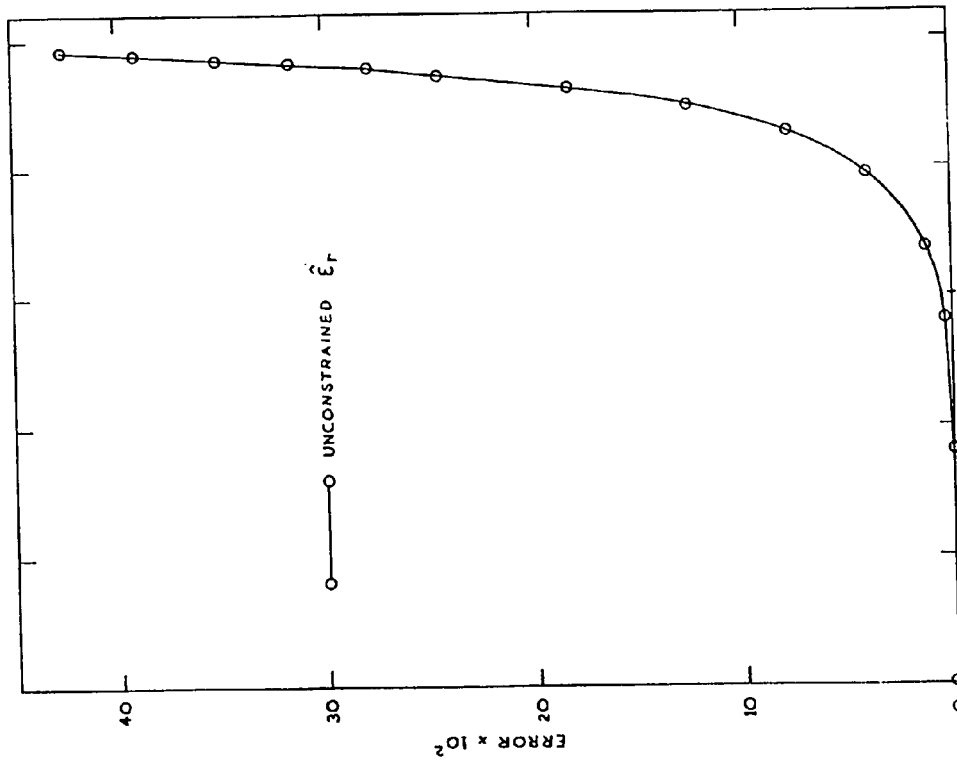

Fig. 4-18: Nondimensional error in radius $\hat{\epsilon}_r$ versus path angle u for 0.8 step size unconstrained computer solutions for non-perturbed parabolic trajectory (0.8 unconstrained solutions subtracted from exact solutions).

CHAPTER 5

RADIAL PERTURBING FORCE

In the previous chapter both the conventional equations of motion and the constrained equations were numerically integrated to obtain solutions for the case of non-perturbed Keplerian orbits. The solutions obtained from both sets of equations were compared with the exact solutions and in all of the cases considered the constrained equations were found to yield more accurate results, particularly when path angle u was treated as the independent variable. For all of these cases, however, the five variables $\hat{H}$, $\hat{\alpha}$, $\hat{\gamma}$, I and Ω were constants. Therefore, it is of interest to seek an example for which the orbit is perturbed, and for which an exact solution exists to provide a standard of comparison.

5.1 Development of Equations

In order to find such an example we can start with the conventional equation for radial acceleration:

$$\ddot{\hat{r}} = \frac{\hat{v}_n^2}{\hat{r}} - \frac{1}{\hat{r}^2} + \hat{F}_r \tag{5-1}$$

If we make a change of variable such that

$$\hat{r} = \frac{1}{Z} \tag{5-2}$$

we can write

$$\dot{\hat{r}} = -\frac{1}{Z^2}\cdot\frac{dZ}{du}\frac{du}{d\hat{t}} \tag{5-3}$$

Next, we set the two perturbing forces $\hat{F}_n$ and $\hat{F}_h$ equal to zero and therefore we have

$$\frac{du}{d\hat{t}} = \frac{\hat{v}_n}{\hat{r}} = \hat{H}Z^2 \tag{5-4}$$

Substituting Eq. (5-4) into Eq. (5-3) yields

$$\dot{\hat{r}} = - \hat{H} \frac{dZ}{du} \tag{5-5}$$

Differentiating Eq. (5-5) with respect to nondimensional time yields

$$\ddot{\hat{r}} = - \hat{H} \frac{d^2Z}{du^2} \frac{du}{d\hat{t}} = - Z^2\hat{H}^2 \frac{d^2Z}{du^2} \tag{5-6}$$

Finally, if we substitute Eq. (5-6) into Eq. (5-1), we obtain the differential equation

$$\frac{d^2Z}{du^2} = \frac{1}{\hat{H}^2} - Z - \hat{F}_r \frac{1}{\hat{H}^2Z^2} \tag{5-7}$$

If we choose the radial perturbing force $\hat{F}_r$ to be of the form

$$\hat{F}_r = K_1\hat{H}^2Z^2 \frac{dZ}{du} \tag{5-8}$$

where K_1 is an arbitrary constant, and substitute this expression into Eq. (5-7) we have

$$\frac{d^2Z}{du^2} = - K_1 \frac{dZ}{du} - Z + \frac{1}{\hat{H}^2} \tag{5-9}$$

For $K_1 < 2$ the general solution for Eq. (5-9) can be written as

$$Z = \left[C_1 \cos\left(\sqrt{\frac{4 - K_1^2}{2}}\, u\right) + C_2 \sin\left(\sqrt{\frac{4 - K_1^2}{2}}\, u\right)\right] e^{\frac{-K_1 u}{2}} + \frac{1}{\hat{H}^2} \tag{5-10}$$

In order to evaluate the constants of integration, C_1 and C_2, we can assume the following initial conditions:

$$\begin{aligned} \hat{r}_i &= \hat{R}_o \\ \hat{v}_{r_i} &= 0.0 \\ \hat{v}_{n_i} &= \hat{V}_o \\ u_i &= 0.0 \end{aligned} \tag{5-11}$$

With the above initial conditions the exact solutions for $\hat{r}$, $\hat{v}_r$, and $\hat{v}_n$ become

$$\frac{1}{\hat{r}} = \left[\frac{1}{\hat{R}_o} - \frac{1}{\hat{H}^2}\right]\left[\cos\left(\frac{\sqrt{4 - K_1^2}}{2}\, u\right) + \frac{K_1}{\sqrt{4 - K_1^2}} \sin\left(\frac{\sqrt{4 - K_1^2}}{2}\, u\right)\right] e^{\frac{-K_1 u}{2}}$$

$$+ \frac{1}{\hat{H}^2} \tag{5-12}$$

$$\hat{v}_r = \frac{2\hat{H}}{\sqrt{4 - K_1^2}}\left[\frac{1}{\hat{R}_o} - \frac{1}{\hat{H}^2}\right] e^{\frac{-K_1 u}{2}} \sin\left(\frac{\sqrt{4 - K_1^2}}{2}\, u\right) \tag{5-13}$$

$$\hat{v}_n = \frac{\hat{H}}{\hat{r}} \tag{5-14}$$

The final form of the perturbing force can be written as

$$\hat{F}_r = \frac{-2\hat{H}^2 K_1}{\sqrt{4 - K_1^2}}\left[\frac{1}{\hat{R}_o} - \frac{1}{\hat{H}^2}\right]\left(\frac{1}{\hat{r}}\right)^2 e^{\frac{-K_1 u}{2}} \sin\left(\frac{\sqrt{4 - K_1^2}}{2}\, u\right) \tag{5-15}$$

From the form of the above equations it can be seen that the effect of the radial perturbing force is to cause the orbit to become circular. If the initial conditions correspond to a circular orbit, the perturbing force is zero ($\frac{1}{\hat{R}_o} = \frac{1}{\hat{H}^2}$) and the orbit is non-perturbed. If the initial conditions correspond to an elliptic orbit the force is such as to cause the orbit to approach a circular orbit of radius $\hat{r} = \hat{H}^2$ and velocity

$\hat{v} = \frac{1}{\hat{H}}$ as the angle u becomes infinite.

Since we have required the perturbing forces $\hat{F}_n$ and $\hat{F}_h$ to be zero in order to obtain an exact solution, the variables $\hat{H}$, I, and Ω will remain constant. The variables $\hat{\alpha}$ and $\hat{\gamma}$ will, however, be influenced by the radial perturbing force and as a result these variables are not constants of the motion. The magnitude of the perturbing force $\hat{F}_r$ can be varied by varying the magnitude of the constant K_1 within the limitation that $K_1 < 2$.

5.2 Computer Solutions for Radial Perturbing Force

The constrained equations given by Eqs. (3-31) through (3-39) in Chapter 3 and the unconstrained equations given in their nondimensional form by Eqs. (3-40) through (3-45) in Chapter 3 were programed on an IBM 7094 digital computer. A fixed-step fourth-order single-precision Runge-Kutta integration scheme was used for all numerical integrations. The perturbing forces $\hat{F}_n$ and $\hat{F}_h$ were set equal to zero and the radial perturbing force $\hat{F}_r$ was programed in the form given by Eq. (5-15). Computer solutions were obtained for various integration step sizes and two different values of the constant K_1 contained in Eq. (5-15). For all of the cases considered, the initial conditions corresponded to the 0.5 eccentricity orbit of the previous chapter. These initial conditions were as follows:

$\hat{r} = 1.5$

$\hat{v}_r = 0.0$

$\hat{v}_n = 1.0$

$I = 0.78539816$ radians

$\Omega = 0.0$ radians

$u = 0.0$ radians

To provide a standard of comparison, the exact equations given by Eqs. (5-12) through (5-14) were also programed and the corresponding constants contained in these equations were as follows:

$\hat{R}_o = 1.5$

$\hat{H} = 1.5$

K_1 = value corresponding to that used in Eq. (5-15) for constrained and unconstrained computer solutions.

The values of path angle u resulting from the computer solutions of the constrained and unconstrained equations were used to obtain the exact values of $\hat{r}$, $\hat{v}_r$, and $\hat{v}_n$ given by Eqs. (5-12) through (5-14).

5.2.1 0.5 Nondimensional Step Size, $K_1 = 5 \times 10^{-4}$

Tables 5-1 and 5-2 present a comparison of the solutions resulting from the constrained and unconstrained equations and the exact solutions for a period corresponding to slightly more than three complete orbits. The value of $K_1 = 5 \times 10^{-4}$ represents a very small radial perturbing force. This is reflected by the fact that the orbit eccentricity has changed from its initial value of 0.5 to a value of approximately 0.497 at the completion of the third orbit. A comparison of the constrained solutions with the exact solutions indicates agreement between the variables $\hat{r}$, $\hat{v}_r$, and $\hat{v}_n$ to at least six significant digits and in some cases to seven significant digits. A similar comparison between the unconstrained solutions and the exact solutions at corresponding values of u indicates agreement between the variables $\hat{r}$, $\hat{v}_r$, and $\hat{v}_n$ to be good on the average to only four significant digits.

5.2.2 1.0 Nondimensional Step Size, $K_1 = 5 \times 10^{-4}$

For this case the magnitude of the radial perturbing force was the same as in the previous case; however, the integration step size was

TABLE 5-1

0.5 Step Size Constrained Solutions Compared to Exact Solutions for Radial Perturbing Force, $K_1 = 5 \times 10^{-4}$

	u	$\hat{r}$	$\hat{v}_r$	$\hat{v}_n$
e*	2.6351208	3.9956112	.16159189	.37541190
c**	"	3.9956110	.16159186	.37541191
e	3.4224932	4.3271468	-.092327909	.34664874
c	"	4.3271458	-.092327943	.34664881
e	4.8970526	2.0612460	-.32726514	.72771519
c	"	2.0612459	-.32726505	.72771520
e	8.6376448	3.4727026	.23560163	.43194024
c	"	3.4727024	.23560151	.42194026
e	9.5063157	4.4746373	-.027084529	.33522263
c	"	4.4746365	-.027084631	.33522276
e	10.536432	2.8887586	-.29802478	.51925401
c	"	2.8887576	-.29802478	.51925436
e	14.523682	2.7698529	.30762394	.54154500
c	"	2.7698544	.30762362	.54154468
e	15.599039	4.4562269	.036095628	.33660756
c	"	4.4562258	.036095291	.33660772
e	16.454066	3.5474810	-.22533161	.42283520
c	"	3.5474797	-.22533171	.42283539
e	21.686475	4.2804640	.099453587	.35042930
c	"	4.2804612	.099453393	.35042952

*e corresponds to exact solution
**c corresponds to constrained solution

TABLE 5-2

0.5 Step Size Unconstrained Solutions Compared to Exact Solutions for Radial Perturbing Force, $K_1 = 5 \times 10^{-4}$

	u	$\hat{r}$	$\hat{v}_r$	$\hat{v}_n$
e*	2.6352378	3.9958125	.16155781	.37539299
uc**	"	3.9953853	.16156879	.37542669
e	3.4227332	4.3268701	-.092404698	.34667091
uc	"	4.3265529	-.092381379	.34669030
e	4.8983089	2.0600822	-.32718798	.72812628
uc	"	2.0600794	-.32717574	.72811393
e	8.6382429	3.4738355	.23546113	.43179938
uc	"	3.4732588	.23548140	.43186667
e	9.5068905	4.4744297	-.027275031	.33523826
uc	"	4.4739769	-.027216238	.33526865
e	10.537881	2.8863583	-.29823785	.51968600
uc	"	2.8864973	-.29818797	.51965544
e	14.525291	2.7723860	.30742196	.54105020
uc	"	2.7718429	.30741765	.54115434
e	15.599981	4.4566761	.035784678	.33657371
uc	"	4.4559391	.035872088	.33662812
e	16.455677	3.5444374	-.22572395	.42319833
uc	"	3.5446654	-.22562813	.42316946
e	21.687876	4.2821628	.099010374	.35029028
uc	"	4.2810808	.099114837	.35037987

*e corresponds to exact solution
**uc corresponds to unconstrained solution

doubled to a nondimensional value of 1.0. It should be noted that this represents a very large integration step size for this orbit since only 32 integration steps are performed per orbit. Tables 5-3 and 5-4 present a comparison of the constrained and unconstrained solutions with the exact solutions during the third orbit. A comparison of the constrained solutions with the exact solutions again indicates agreement between the variables $\hat{r}$, $\hat{v}_r$, and $\hat{v}_n$ to six significant digits. A similar comparison between the unconstrained solutions and the exact solutions indicates agreement to only two to three significant digits over the same orbital period. If these differences are converted to dimensional quantities the maximum errors for the constrained and unconstrained solutions during the third orbit are as follows:

Constrained Solution Maximum Error

$$\epsilon_r \simeq 31.5 \text{ feet}$$

$$\epsilon_{v_r} \simeq 0.0196 \text{ feet/second}$$

$$\epsilon_{v_n} \simeq 0.0078 \text{ feet/second}$$

Unconstrained Solution Maximum Error

$$\epsilon_r \simeq 318{,}045 \text{ feet}$$

$$\epsilon_{v_r} \simeq 42.9 \text{ feet/second}$$

$$\epsilon_{v_n} \simeq 49.4 \text{ feet/second}$$

Although no exact solutions for time were obtained, it is possible to estimate the error in time by the method outlined in Chapter 4. Computer solutions for the case of a radial perturbing force were obtained using an integration step size of 0.125. These solutions were in good agreement with the exact solutions and based on previous studies for the case of 0.5 eccentricity, non-perturbed orbits, the 0.125 step size solutions exhibited good agreement with the exact values of time.

TABLE 5-3

1.0 Step Size Constrained Solutions Compared to Exact Solutions for Radial Perturbing Force, $K_1 = 5 \times 10^{-4}$

	u	$\hat{r}$	$\hat{v}_r$	$\hat{v}_n$
e*	13.085137	1.5702864	.16472969	.95523974
c**	"	1.5702865	.16472995	.95523964
e	14.302575	2.4507407	.32761030	.61205985
c	"	2.4507419	.32761032	.61205955
e	14.846611	3.3303951	.25197130	.45039701
c	"	3.3303966	.25197122	.45039680
e	15.276343	4.1085471	.13891643	.36509256
c	"	4.1085480	.13891640	.36509247
e	15.598896	4.4561598	.036142828	.33661271
c	"	4.4561609	.036142441	.33661261
e	15.823801	4.4528247	-.038373845	.33686483
c	"	4.4528250	-.038374092	.33686479
e	16.060960	4.2240324	-.11477502	.35511092
c	"	4.2240310	-.11477545	.35511102
e	16.453841	3.5479083	-.22527677	.42278432
c	"	3.5479072	-.22527699	.42278444
e	17.135695	2.4222393	-.32851750	.61926168
c	"	2.4222390	-.32851756	.61926176
e	18.383770	1.5574924	-.14902220	.96308657
c	"	1.5574920	-.14902187	.96308677

*e corresponds to exact solution
**c corresponds to constrained solution

TABLE 5-4

1.0 Step Size Unconstrained Solutions Compared to Exact Solutions for Radial Perturbing Force, $K_1 = 5 \times 10^{-4}$

	u	$\hat{r}$	$\hat{v}_r$	$\hat{v}_n$
e*	13.161303	1.5925787	.18620364	.94186869
uc**	"	1.5940495	.18458889	.94132900
e	14.334761	2.4935767	.32567809	.60154557
uc	"	2.4889911	.32474557	.60277317
e	14.866338	3.3672393	.24765373	.44546879
uc	"	3.3565181	.24755082	.44698223
e	15.291947	4.1326672	.13419288	.36296172
uc	"	4.1175218	.13477957	.36437026
e	15.614398	4.4630622	.031021935	.33609212
uc	"	4.4488304	.032067161	.33723515
e	15.840714	4.4436416	-.043945680	.33756098
uc	"	4.4330329	-.042640609	.33843692
e	16.080841	4.1963421	-.12094480	.35745417
uc	"	4.1908964	-.11943689	.35799075
e	16.482801	3.4931681	-.23224084	.42940962
uc	"	3.4947404	-.23059089	.42930322
e	17.196310	2.3465023	-.33077587	.63924933
uc	"	2.3513784	-.32949883	.63805161
e	18.520740	1.5295859	-.10714394	.98065757
uc	"	1.5331744	-.10776437	.97875208

*e corresponds to exact solution
**uc corresponds to unconstrained solution

Therefore, using the 0.125 integration step size solutions as a basis of comparison and computing the values of $\Delta u = u_{.125} - u_{1.0}$ and $\hat{\dot{u}} = \left(\frac{\hat{v}_n}{\hat{r}}\right)_{1.0}$ at corresponding computer output times yields the following estimated maximum errors in time for the constrained and unconstrained 1.0 step size solutions during the third orbit:

Constrained Maximum Error in Time

$$\hat{\epsilon}_t \simeq 0.00223, \quad \epsilon_t \simeq 1.8 \text{ seconds}$$

Unconstrained Maximum Error in Time

$$\hat{\epsilon}_t \simeq 0.212, \quad \epsilon_t \simeq 171 \text{ seconds}$$

5.2.3 1.0 Nondimensional Step Size, $K_1 = 5\text{x}10^{-2}$

For this case the initial magnitude of the radial perturbing force was increased by a factor of 100 over the previous cases by increasing the constant K_1 to a value of $5\text{x}10^{-2}$ while the large integration step size of 1.0 was retained. The larger radial perturbing force causes the orbit eccentricity to decrease from its initial value of 0.5 to a value of approximately 0.288 at the end of the third orbit. Tables 5-5 and 5-6 present a comparison of the constrained and unconstrained solutions with the exact solutions during the third orbit. A comparison of the constrained solutions with the exact solutions indicates agreement in the variables $\hat{r}$, $\hat{v}_r$, and $\hat{v}_n$ to five significant digits. A similar comparison between the unconstrained solutions and the exact solutions shows agreement on the average to only three significant digits. If the differences between the exact solutions and the constrained and unconstrained solutions are converted to dimensional quantities, the maximum errors during the third orbit are as follows:

TABLE 5-5

1.0 Step Size Constrained Solutions Compared to Exact Solutions for Radial Perturbing Force, $K_1 = 5 \times 10^{-2}$

	u	$\hat{r}$	$\hat{v}_r$	$\hat{v}_n$
e*	12.698126	1.6517489	.030934869	.90812835
c**	"	1.6517341	.030936081	.90813646
e	14.036668	2.1518553	.23346406	.69707288
c	"	2.1518548	.23347249	.69707305
e	14.775053	2.8038891	.18577365	.53497122
c	"	2.8039191	.18578071	.53496550
e	15.404134	3.3162883	.068913948	.45231291
c	"	3.3163530	.068916076	.45230407
e	15.930799	3.3563012	-.048392510	.44692056
c	"	3.3563667	-.048395009	.44691183
e	16.360074	3.0823346	-.13352294	.48664412
c	"	3.0823792	-.13352866	.48663707
e	16.710304	2.7628182	-.18442403	.54292389
c	"	2.7628403	-.18443204	.54291953
e	17.466270	2.1417365	-.21190436	.70036626
c	"	2.1417294	-.21191373	.70036855
e	18.755443	1.7168936	-.020823187	.87367092
c	"	1.7168765	-.020823882	.87367961
e	20.115680	2.0459713	.19198473	.73314810
c	"	2.0459638	.19199330	.73315079

*e corresponds to exact solution
**c corresponds to constrained solution

TABLE 5-6

1.0 Step Size Unconstrained Solutions Compared to Exact Solutions for Radial Perturbing Force, $K_1 = 5 \times 10^{-2}$

	u	$\hat{r}$	$\hat{v}_r$	$\hat{v}_n$
e*	12.748314	1.6551275	.042916821	.90627450
uc**	"	1.6559714	.042073494	.90582287
e	14.066543	2.1736272	.23391908	.69009074
uc	"	2.1708781	.23318958	.69091032
e	14.794730	2.8230339	.18296508	.53134325
uc	"	2.8169426	.18295450	.53245469
e	15.420669	3.3244443	.065304835	.45120323
uc	"	3.3174825	.065922195	.45211820
e	15.948795	3.3495111	-.052293632	.44782655
uc	"	3.3456467	-.051323211	.44831213
e	16.382114	3.0635454	-.13730864	.48962879
uc	"	3.0630928	-.13624446	.48966659
e	16.737653	2.7371764	-.18748467	.54800999
uc	"	2.7386427	-.18649030	.54757783
e	17.510059	2.1138673	-.20976451	.70959986
uc	"	2.1164811	-.20930270	.70867010
e	18.819110	1.7151193	-.0075654296	.87457472
uc	"	1.7165262	-.0084366714	.87385714
e	20.159990	2.0701411	.19431325	.72458829
uc	"	2.0678167	.19333613	.72536819

*e corresponds to exact solution
**uc corresponds to unconstrained solution

Constrained Solution Maximum Error

$$\epsilon_r \simeq 1375 \text{ feet}$$

$$\epsilon_{v_r} \simeq 0.2436 \text{ feet/second}$$

$$\epsilon_{v_n} \simeq 0.2288 \text{ feet/second}$$

Unconstrained Solution Maximum Error

$$\epsilon_r \simeq 146{,}181 \text{ feet}$$

$$\epsilon_{v_r} \simeq 27.56 \text{ feet/second}$$

$$\epsilon_{v_n} \simeq 28.6 \text{ feet/second}$$

The fact that the unconstrained errors are somewhat smaller for the case of the larger radial perturbing force than for the previous case is to be expected. The more nearly circular the orbit, the smaller the time rates of change of the unconstrained variables $\hat{r}$, $\hat{v}_r$, and $\hat{v}_n$. Since the larger radial perturbing force causes the orbit eccentricity to decrease more rapidly, the smaller time rates of change of the variables $\hat{r}$, $\hat{v}_r$, and $\hat{v}_n$ are reflected in smaller numerical integration errors. On the other hand, the error in the constrained solutions is larger than in the previous case. This is also to be expected since the time rates of change of the vairables $\hat{\alpha}$ and $\hat{\gamma}$ are directly proportional to the magnitude of the perturbing force and as a result, the larger the perturbing force, for a given integration step size, the larger the error in the values $\hat{r}$, $\hat{v}_r$, and $\hat{v}_n$. In all of the cases considered, however, the solutions obtained using the constrained equations are considerably more accurate than those obtained using the conventional equations of motion.

CHAPTER 6

OBLATE EARTH PERTURBING FORCES

In the previous chapter we considered the case of a radial perturbing force for which exact solutions could be obtained to yield a basis of comparison between the constrained and unconstrained computer solutions. In order to obtain an exact solution, the perturbing forces $\hat{F}_n$ and $\hat{F}_h$ were set equal to zero which resulted in the variables $\hat{H}$, I and Ω being constants of the motion. In this chapter constrained and unconstrained computer solutions are compared for the case of an oblate earth. For this case all three of the perturbing forces are present,and as a result none of the variables $\hat{H}$, $\hat{\alpha}$, $\hat{\gamma}$, I or Ω are constants of motion.

6.1 Oblate Earth Perturbations

If the earth were a homogeneous sphere, the potential field would be a pure inverse-square central-force field such as the type previously considered for non-perturbed orbits. Since the earth does not have this configuration, the potential associated with it will not be exactly that of a central inverse-square force field. There are a variety of assumptions used as to the exact shape and mass distribution of the earth. The complexity of the model used depends upon the accuracy desired. The most obvious departure from the ideal sphere is the so-called "equatorial bulge." The polar radius of the earth is about 13 miles less than the equatorial radius and therefore it is common, as a first approximation, to assume the earth to be a homogeneous oblate spheroid. More accurate models are possible, but this one is sufficient for demonstrating the accuracy of the constrained equations when small perturbing forces are

present. The reader is referred to Kuiper[21] and Jeffries[22] for more detailed information on the earth's potential field.

The potential of the earth, when it is considered as a homogeneous oblate spheroid, is given by MacMillan[23] as

$$V = -3K \sum_{n=0}^{\infty} \frac{(-1)^n}{(2n+1)(2n+3)} \frac{(r_e E_e)^{2n}}{r^{2n+1}} P_{2n}(\sin \theta) \qquad (6\text{-}1)$$

where

K = gravitational constant which would result if all the mass were concentrated at the center

r_e = equatorial radius

E_e = eccentricity of earth

$P_k(x)$ = kth Legendre polynomial

θ = instantaneous latitude

r = distance of satellite from the center of the earth

The instantaneous latitude θ can be expressed in terms of the coordinate variables u and I shown in Fig. 2-1 through the relation

$$\sin \theta = \sin u \sin I \qquad (6\text{-}2)$$

If we expand the series given by Eq. (6-1), and make use of Eq. (6-2) for θ, the first three terms become

$$V = -\frac{K}{r}\left\{1 + \frac{r_e^2 E_e^2}{10 r^2}(1 - 3\sin^2 u \sin^2 I) + \frac{3}{(35)(8)} \frac{r_e^4 E_e^4}{r^4}(3 - 30\sin^2 u \sin^2 I + 35 \sin^4 u \sin^4 I) + \cdots\right\} \qquad (6\text{-}3)$$

From the above expression it can be seen that this function contains the potential function for a spherically symmetric earth and a series of correction terms referred to as zonal harmonics. As the eccentricity of the earth is very small, the above series is rapidly convergent.

If we define quantities $J_2 = \frac{3}{10} E_e^2$ and $J_3 = \frac{(3)(30)}{(35)(8)} E_e^4$ the first three terms of the series can be put in the more conventional form[24]

$$V = -\frac{K}{r}\left\{1 + \frac{J_2}{3}\left(\frac{r_e}{r}\right)^2 (1 - 3 \sin^2 u \sin^2 I) + \frac{J_3}{30}\left(\frac{r_e}{r}\right)^4 (3 - 30 \sin^2 u \sin^2 I + 35 \sin^4 u \sin^4 I)\right\}$$

From satellite measurements[24], the terms J_2 and J_3 are found to be $J_2 \simeq 1620 \times 10^{-6}$ and $J_3 \simeq 8.8 \times 10^{-6}$.

For the purposes of this study only the J_2 term is retained and therefore we have

$$V = -\frac{K}{r} + \frac{J_2 K}{3r}\left(\frac{r_e}{r}\right)^2 (3 \sin^2 u \sin^2 I - 1) \qquad (6\text{-}5)$$

The first term in the above equation represents the potential of the conventional spherical earth and has already been included in the constrained and unconstrained equations. Therefore, the perturbation potential is given by

$$V_p = \frac{J_2 K r_e^2}{3r^3} (3 \sin^2 u \sin^2 I - 1) \qquad (6\text{-}6)$$

The perturbing forces can be obtained from this potential function as

$$\frac{F_r}{m} = -\frac{\partial V_p}{\partial r} \qquad (6\text{-}7)$$

$$\frac{F_n}{m} = -\frac{1}{r}\frac{\partial V_p}{\partial u} \tag{6-8}$$

$$\frac{F_h}{m} = -\frac{1}{r \sin u}\frac{\partial V_p}{\partial I} \tag{6-9}$$

If the above equations are put in their nondimensional form using the characteristic values given in Chapter 4 we have

$$\hat{F}_r = \frac{J_2}{\hat{r}^4}(3 \sin^2 u \sin^2 I - 1) \tag{6-10}$$

$$\hat{F}_n = -\frac{2J_2}{\hat{r}^4} \sin u \cos u \sin^2 I \tag{6-11}$$

$$\hat{F}_h = -\frac{2J_2}{\hat{r}^4} \sin I \cos I \sin u \tag{6-12}$$

6.2 Computer Solutions

The constrained equations given by Eqs. (3-31) through (3-39) and the unconstrained equations given by Eqs. (3-40) through (3-45) in Chapter 3 were programed on the digital computer using a fixed-step single-precision fourth-order Runge-Kutta integration scheme for all numerical integrations. The perturbing forces $\hat{F}_r$, $\hat{F}_n$, and $\hat{F}_h$ were programed in the form given by Eqs. (6-10) through (6-12) above. Solutions were obtained for the 0.5 and 0.05 eccentricity orbits previously considered.

Although no exact solutions were available, computer solutions were obtained with small integration step sizes which yielded very good agreement with the exact solutions for these same orbits when no perturbing forces were present. These small step size solutions were then used

to provide a basis of comparison for solutions obtained using larger integration step sizes.

6.2.1 0.5 Eccentricity Orbit

The initial conditions used for the 0.5 eccentricity orbit were as follows:

$$\hat{r} = 1.5$$

$$\hat{v}_r = 0.0$$

$$\hat{v}_n = 1.0$$

$$I = 0.78539816$$

$$\Omega = 0.0$$

$$u = 0.0$$

The initial condition for inclination angle I was selected on the basis of two considerations. It can be shown[14] that the secular changes in the nodal angle Ω are greatest for equatorial orbits ($I = 0^o$) and vanish for polar orbits ($I = 90^o$). On the other hand, the periodic variations of the inclination angle I vanish for both equatorial and polar orbits and are greatest for $I = 45^o$. Since the purpose of considering the oblate earth case was to provide perturbing forces which cause variations in all of the variables used in the constrained equations, the value $I = 45^o$ was selected as a reasonable compromise.

From Table A-1 in Appendix A it was found that the 0.2 integration step size constrained solutions were in very good agreement with the exact solutions regardless of whether u or time was used as the independent variable. In view of this agreement, a 0.2 step size constrained solution was used to provide a standard of comparison for the constrained and unconstrained solutions obtained with larger integration step sizes.

Figs. 6-1 through 6-4 present the differences between the constrained and unconstrained computer solutions obtained with a 0.8 integration step size and the 0.2 step size constrained solution standard. As before, these nondimensional step sizes represent approximately 41 and 163 integration steps per orbit. These figures were obtained by computing the difference between the 0.8 step size solutions and the 0.2 step size solutions at corresponding values of computer output time. It should be noted that these trends are very similar to those presented in Figs. 4-2 through 4-5 for the non-perturbed case. If these differences are converted to dimensional quantities, the maximum errors in the constrained and unconstrained solutions over a period of two orbits are as follows:

Constrained Solution Maximum Error (time treated as independent variable)

ϵ_r = 4515 feet

ϵ_{v_r} = 2.65 feet/second

ϵ_{v_n} = 2.08 feet/second

ϵ_u = 0.00032 radians

Unconstrained Solution Maximum Error (time treated as independent variable)

ϵ_r = 352,800 feet

ϵ_{v_r} = 273 feet/second

ϵ_{v_n} = 169 feet/second

ϵ_u = 0.0334 radians

As in the non-perturbed case, the nondimensional integration step size of 0.8 is a very large one for this orbit, particularly in the region of perigee where $\hat{u}$ is large. In view of this, it might be expected that a large percentage of the differences between the 0.2 and 0.8 step size solutions for $\hat{r}$, $\hat{v}_r$, and $\hat{v}_n$ are the result of variations

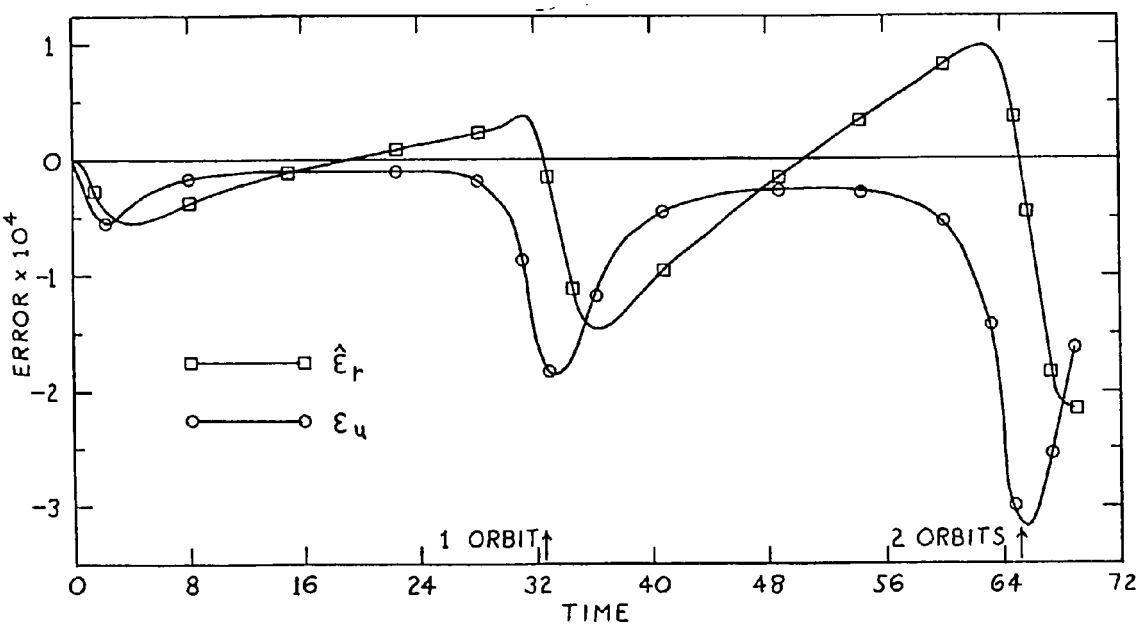

Fig. 6-1: Nondimensional error in radius $\hat{\varepsilon}_r$ and path angle ε_u versus nondimensional time for 0.8 step size constrained computer solutions for oblate earth perturbed 0.5 eccentricity orbit (0.2 constrained solutions subtracted from 0.8 constrained solutions).

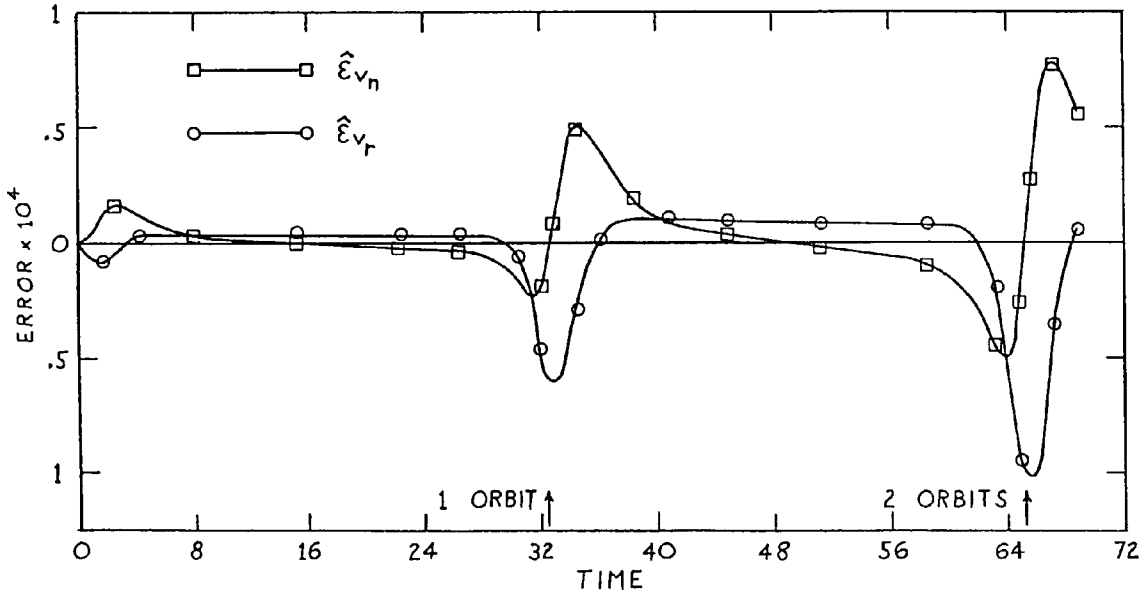

Fig. 6-2: Nondimensional error in radial velocity $\hat{\varepsilon}_{v_r}$ and normal velocity $\hat{\varepsilon}_{v_n}$ versus nondimensional time for 0.8 step size constrained computer solutions for oblate earth perturbed 0.5 eccentricity orbit (0.2 constrained solutions subtracted from 0.8 constrained solutions).

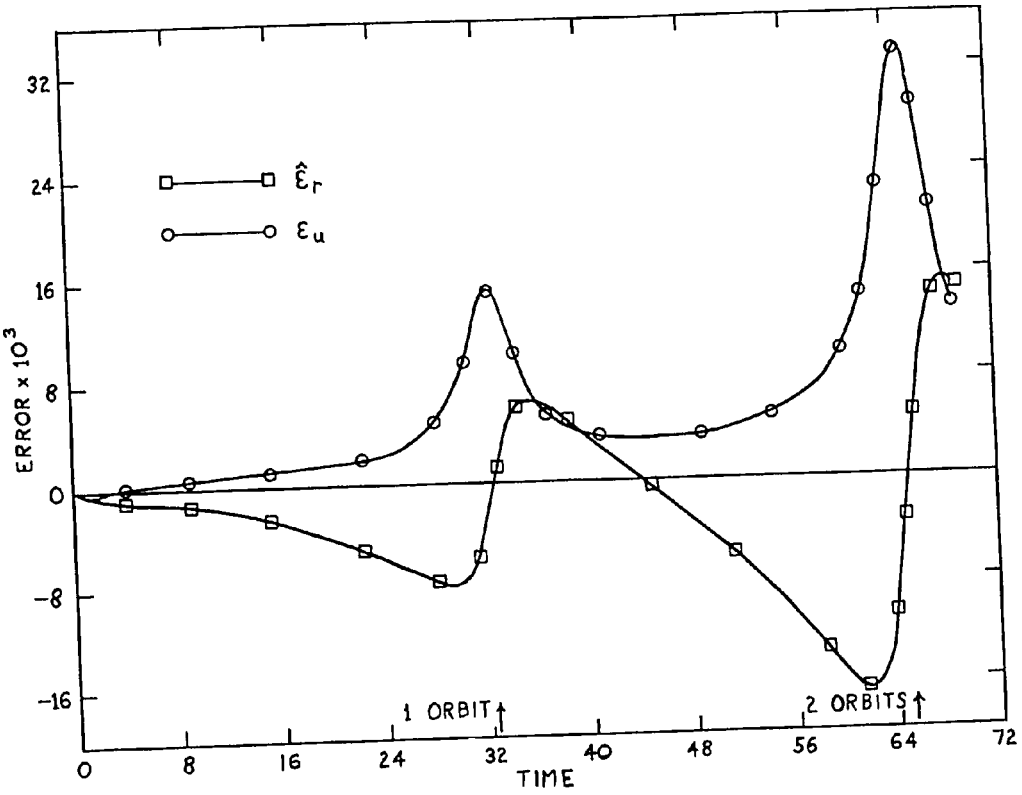

Fig. 6-3: Nondimensional error in radius $\hat{\epsilon}_r$ and path angle ϵ_u versus nondimensional time for 0.8 step size unconstrained computer solutions for oblate earth perturbed 0.5 eccentricity orbit (0.2 constrained solutions subtracted from 0.8 unconstrained solutions).

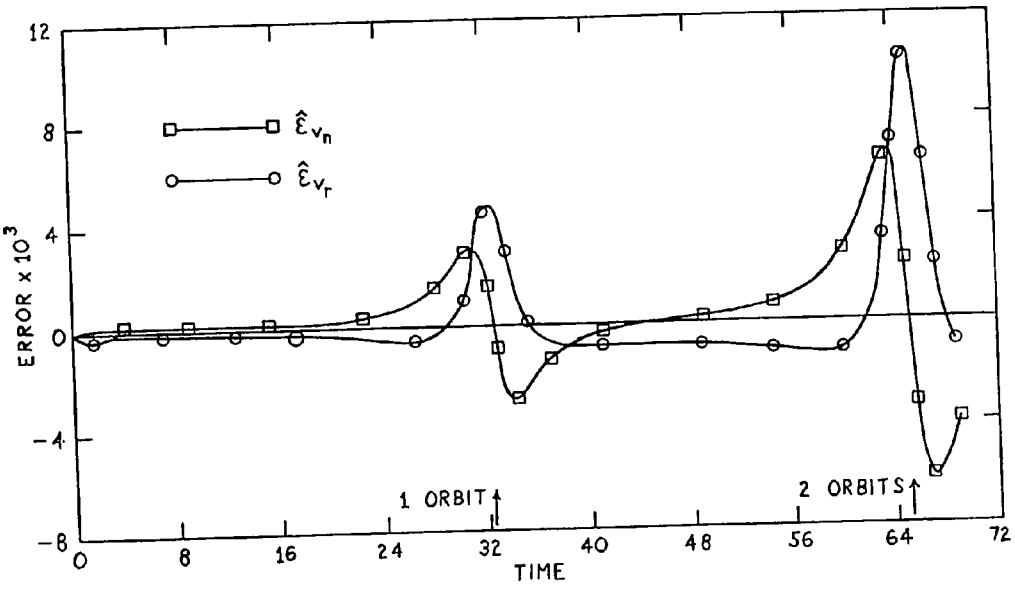

Fig. 6-4: Nondimensional error in radial velocity $\hat{\epsilon}_{v_r}$ and normal velocity $\hat{\epsilon}_{v_n}$ versus nondimensional time for 0.8 step size unconstrained computer solutions for oblate earth perturbed 0.5 eccentricity orbit (0.2 constrained solutions subtracted from 0.8 unconstrained solutions).

in the solutions for path angle u at corresponding values of computer output time. These variations in the solutions for u are due to the large integration step size which causes the 0.8 solutions for u to be in error with time. In order to evaluate the 0.8 step size solution errors when u is treated as the independent variable we can make use of the approximate correction method outlined in Section 4.2 of Chapter 4.

First, we compute the values of $\Delta\hat{r}$, $\Delta\hat{v}_n$, and $\Delta\hat{v}_r$ from the following expressions:

$$\Delta\hat{r} \simeq \frac{\hat{v}_r \hat{r} \Delta u}{\hat{v}_n} \tag{6-13}$$

$$\Delta\hat{v}_n \simeq - \hat{v}_r \Delta u \tag{6-14}$$

$$\Delta\hat{v}_r \simeq (\hat{v}_n - \frac{1}{\hat{r}\hat{v}_n})\Delta u \tag{6-15}$$

where $\Delta u = u_{.2} - u_{.8}$. These terms account for the differences in the variables $\hat{r}$, $\hat{v}_r$, and $\hat{v}_n$ due to small variations in u (within the accuracy of the linear assumptions used in obtaining $\Delta\hat{r}$, $\Delta\hat{v}_r$, and $\Delta\hat{v}_n$).

Next, we add the expressions for $\Delta\hat{r}$, $\Delta\hat{v}_r$, and $\Delta\hat{v}_n$ to the respective 0.8 step size computer solutions to obtain "corrected" values for the variables $\hat{r}$, $\hat{v}_r$, and $\hat{v}_n$. These variables are corrected in the sense that they now represent 0.8 step size solutions at the same value of u as that obtained from the 0.2 step size solution standard. These corrected values are defined as

$$\hat{r} = \hat{r}_{.8} + \Delta\hat{r}$$

$$\hat{v}_n = \hat{v}_{n_{.8}} + \Delta\hat{v}_n$$

$$\hat{v}_r = \hat{v}_{r_{.8}} + \Delta\hat{v}_r$$

Any differences between these corrected variables and the 0.2 step size solutions for $\hat{r}$, $\hat{v}_r$, and $\hat{v}_n$ now represent the errors in the 0.8 step size solutions when u is treated as the independent variable. In essence, this method of computing error is analogous to that used to obtain Fig. 4-6 in Chapter 4 (i.e. it represents the difference between the 0.8 step size solutions for $\hat{r}$, $\hat{v}_r$, and $\hat{v}_n$ and the 0.2 step size solutions at the same value of u).

As an example, suppose we consider the 0.2 and 0.8 computer solutions at a computer output time of $\hat{t} = 8.8$. At this time the solutions for $\hat{r}$, $\hat{v}_r$, and $\hat{v}_n$, and u are as follows:

0.2 Step Size Constrained Solution Standard

$\hat{r}$	$\hat{v}_r$	$\hat{v}_n$	u
3.7806783	0.19491319	0.39670016	2.5172103

0.8 Step Size Constrained Solution

$\hat{r}$	$\hat{v}_r$	$\hat{v}_n$	u
3.7806445	0.19491716	0.39670360	2.5171956

0.8 Step Size Unconstrained Solution

$\hat{r}$	$\hat{v}_r$	$\hat{v}_n$	u
3.7792538	0.19477430	0.39681209	2.5178452

Applying the correction scheme to the 0.8 step size unconstrained solution yields

$$\Delta u = u_{.2} - u_{.8} = - 0.0006349$$

If we use the 0.2 step size solution to evaluate the terms in parentheses in Eqs. (6-13) through (6-15) we obtain

$$\Delta\hat{r} = - 0.00117938$$

$$\Delta\hat{v}_n = + 0.00012375$$

$$\Delta\hat{v}_r = + 0.00017146$$

If the above quantities are added to the 0.8 step size unconstrained solutions the corrected variables $\hat{r}$, $\hat{v}_r$, and $\hat{v}_n$ become

$$\hat{r}_{corr.} = 3.7780744$$

$$\hat{v}_{r_{corr.}} = 0.19494576$$

$$\hat{v}_{n_{corr.}} = 0.39693584$$

The differences between the above corrected values and the 0.2 step size solutions represents the error in the 0.8 step size unconstrained solution when u is treated as the independent variable. These errors are as follows:

$$\hat{\epsilon}_r = \hat{r}_{.2} - \hat{r}_{corr.} = 2.6039\text{x}10^{-3}$$

$$\hat{\epsilon}_{v_r} = \hat{v}_{r_{.2}} - \hat{v}_{r_{corr.}} = -.03257\text{x}10^{-3}$$

$$\hat{\epsilon}_{v_n} = \hat{v}_{n_{.2}} - \hat{v}_{n_{corr.}} = -.23568\text{x}10^{-3}$$

We can also obtain an estimate of the error between the 0.8 unconstrained solution for u and time by a method similar to that used above. A comparison of the computer solution for the 0.2 step size standard and the 0.8 unconstrained solution indicates that the value of u obtained from the 0.8 unconstrained solution is greater than that obtained with the 0.2 step size solution. If we consider the 0.2 step size solution for u to be correct with the computer output time of 8.8 then the u obtained from the 0.8 step size unconstrained solution must correspond to a time which is greater than $\hat{t} = 8.8$. Therefore, we can estimate this difference by

$$\Delta\hat{t} = \frac{\Delta u}{\hat{u}_{.2}} = \frac{u_{.8} - u_{.2}}{\left(\frac{\hat{v}_n}{\hat{r}}\right)_{.2}}$$

which yields

$$\Delta\hat{t} = \hat{\epsilon}_t = \frac{0.0006349}{0.10492830} = .60508\text{x}10^{-2}$$

As a check on the validity of the above correction technique we can make use of Figs. 4-1 and 4-6 of Chapter 4 which were obtained for this same orbit when no perturbing forces were present and for which exact solutions exist. For the perturbed case presently under consideration we found that the value of u for a computer output time of 8.8 was approximately 2.517 radians. If we enter Fig. 4-1 at this same value of u for the non-perturbed orbit we find the error in time as a function of u for the 0.8 step size unconstrained solution to be approximately $.58\text{x}10^{-2}$ which is in good agreement with the nondimensional time error just computed for the perturbed orbit. If we enter Fig. 4-6 at this same value of u we find the non-perturbed 0.8 step size solutions for $\hat{r}$, $\hat{v}_r$, and $\hat{v}_n$ to be in error with u by the amounts $2.58\text{x}10^{-3}$, $-.03\text{x}10^{-3}$, and $-.235\text{x}10^{-3}$ respectively. Again, these errors are in good agreement with those found for the perturbed case by the approximate method. Finally, if we convert the perturbed 0.8 step size unconstrained solution errors obtained on the previous pages to dimensional quantities, through the use of the characteristic values given in Chapter 4, they are as follows:

ϵ_r = 54,421 feet

ϵ_{v_r} = 0.8436 feet/second

ϵ_{v_n} = 6.104 feet/second

ϵ_t = (error in time as a function of u) = 4.89 seconds

If we apply this same correction scheme to the 0.8 step size constrained solution at the computer output time of $\hat{t}$ = 8.8 we have from page 80,

$$\Delta u = u_{.2} - u_{.8} = 0.0000147$$

which results in

$$\Delta \hat{r} = 0.00002731$$

$$\Delta \hat{v}_n = - 0.00000286$$

$$\Delta \hat{v}_r = - 0.00000397$$

Adding these quantities to the 0.8 step size constrained solutions yields the following corrected variables:

$$\hat{r}_{corr.} = 3.7806718$$

$$\hat{v}_{r_{corr.}} = 0.19491319$$

$$\hat{v}_{n_{corr.}} = 0.39670074$$

As before, the differences between the above corrected values and the 0.2 step size solutions represent the error in the 0.8 step size constrained solution when u is treated as the independent variable. These nondimensional errors are as follows:

$$\hat{\epsilon}_r = \hat{r}_{.2} - \hat{r}_{corr.} = 6.5 \times 10^{-6}$$

$$\hat{\epsilon}_{v_r} = \hat{v}_{r_{.2}} - \hat{v}_{r_{corr.}} = 0.0$$

$$\hat{\epsilon}_{v_n} = \hat{v}_{n_{.2}} - \hat{v}_{n_{corr.}} = - 0.65 \times 10^{-6}$$

To obtain an estimate of the error between the 0.8 step size constrained solution for u and time we note that the value of u obtained from the 0.8 constrained solution is less than the value obtained with the 0.2 step size solution for the same value of computer output time. If we again consider the 0.2 step size solution for u to be correct with the nondimensional computer output time of 8.8, then the u obtained from the 0.8 step size constrained solution must correspond to a time which is less than $\hat{t} = 8.8$ Therefore, we can estimate this difference by

$$\Delta \hat{t} = \frac{\Delta u}{\hat{u}_{.2}} = \frac{u_{.8} - u_{.2}}{\left(\frac{\hat{v}_n}{\hat{r}}\right)_{.2}}$$

which yields

$$\Delta\hat{t} = \epsilon_{\hat{t}} = -\frac{0.0000147}{0.10492830} = -1.401\text{x}10^{-4}$$

The difference in time with u between the exact solution and a 0.8 step size constrained solution for this same orbit when no perturbing forces were present represented a nondimensional error in time, at a value of $u \simeq 2.517$ radians, of $-1.57\text{x}10^{-4}$.

If we convert the above 0.8 step size constrained solution errors to dimensional quantities they are as follows:

ϵ_r = 135.8 feet

ϵ_{v_r} = 0.0 feet/second

ϵ_{v_n} = 0.01502 feet/second

ϵ_t = (error in time as a function of u) = 0.113 seconds

The above correction scheme for obtaining errors in the variables $\hat{r}$, $\hat{v}_r$, and $\hat{v}_n$, and time was applied to two additional points for the perturbed 0.5 eccentricity orbit. These points corresponded to computer output times of $\hat{t}$ = 44.8 and $\hat{t}$ = 60.8. The computer solutions for these two cases are listed on the following page.

$\hat{t} = 44.8$

0.2 Step Size Constrained Solution Standard

$\hat{r}$	$\hat{v}_r$	$\hat{v}_n$	u
4.2845484	0.10302331	0.35005551	9.1125670

0.8 Step Size Constrained Solution

$\hat{r}$	$\hat{v}_r$	$\hat{v}_n$	u
4.2844960	0.10303318	0.35005949	9.1125368

0.8 Step Size Unconstrained Solution

$\hat{r}$	$\hat{v}_r$	$\hat{v}_n$	u
4.2840712	0.10221505	0.35008693	9.1158794

$\hat{t} = 60.8$

0.2 Step Size Constrained Solution Standard

$\hat{r}$	$\hat{v}_r$	$\hat{v}_n$	u
2.6460620	-0.31771251	0.56676726	10.693045

0.8 Step Size Constrained Solution

$\hat{r}$	$\hat{v}_r$	$\hat{v}_n$	u
2.6461519	-0.31770590	0.56674736	10.692981

0.8 Step Size Unconstrained Solution

$\hat{r}$	$\hat{v}_r$	$\hat{v}_n$	u
2.6297346	-0.31851174	0.57027333	10.704797

After correction for the deviations in u, the errors in the 0.8 step size constrained and unconstrained solutions for the variables $\hat{r}$, $\hat{v}_r$, $\hat{v}_n$, and time (as a function of path angle, u) are found to be as follows:

Computer Output Time = 44.8

0.8 Constrained Solution

$\hat{\epsilon}_r = + 14.3 \times 10^{-6}$, $\epsilon_r = 298.8$ feet

$\hat{\epsilon}_{v_r} = - 0.31 \times 10^{-6}$, $\epsilon_{v_r} = 0.00803$ feet/second

$\hat{\epsilon}_{v_n} = - 0.87 \times 10^{-6}$, $\epsilon_{v_n} = 0.02253$ feet/second

$\hat{\epsilon}_t = - 3.69 \times 10^{-4}$, $\epsilon_t = 0.2997$ seconds

0.8 Unconstrained Solution

$\hat{\epsilon}_r = + 4655.5 \times 10^{-6}$, $\epsilon_r = 97{,}299$ feet

$\hat{\epsilon}_{v_r} = - 240.73 \times 10^{-6}$, $\epsilon_{v_r} = 6.235$ feet/second

$\hat{\epsilon}_{v_n} = - 372.67 \times 10^{-6}$, $\epsilon_{v_n} = 9.652$ feet/second

$\hat{\epsilon}_t = + 405.4 \times 10^{-4}$, $\epsilon_t = 32.8$ seconds

Computer Output Time = 60.8

0.8 Constrained Solution

$\hat{\epsilon}_r = + 5.0 \times 10^{-6}$, $\epsilon_r = 104.5$ feet

$\hat{\epsilon}_{v_r} = - 0.21 \times 10^{-6}$, $\epsilon_{v_r} = 0.00544$ feet/second

$\hat{\epsilon}_{v_n} = - 0.43 \times 10^{-6}$, $\epsilon_{v_n} = 0.01114$ feet/second

$\hat{\epsilon}_t = - 2.988 \times 10^{-4}$, $\epsilon_t = 0.242$ seconds

0.8 Unconstrained Solution

$\hat{\epsilon}_r = - 1104.4 \times 10^{-6}$, $\epsilon_r = 23{,}082$ feet

$\hat{\epsilon}_{v_r} = - 376.35 \times 10^{-6}$, $\epsilon_{v_r} = 9.747$ feet/second

$\hat{\epsilon}_{v_n} = + 227.69 \times 10^{-6}$, $\epsilon_{v_n} = 5.897$ feet/second

$\hat{\epsilon}_t = + 548.66 \times 10^{-4}$, $\epsilon_t = 44.39$ seconds

From the above results it can be seen that the characteristics of the 0.8 step size solutions for the case of oblate earth perturbations are the same as those previously found for the non-perturbed pure Keplerian 0.5 eccentricity orbit. The larger integration step size

solutions of the constrained equations are considerably more accurate than those obtained by integrating the conventional equations of motion regardless of whether time or path angle is treated as the independent variable. The correspondence between the variables $\hat{r}$, $\hat{v}_r$, and $\hat{v}_n$ and the path angle u is maintained for the constrained solutions in the presence of the oblate earth perturbing forces. As before, the error between u and time is less for the constrained solutions than for the unconstrained solutions.

It should be noted at this point that both the constrained and unconstrained large step size solutions predicted the variables Ω and I accurately when compared to the smaller step size solution standard. This was also found to be true for the 0.05 eccentricity orbit considered in the next section.

6.2.2 0.05 Eccentricity Orbit

The initial conditions used for the 0.05 eccentricity orbit were as follows:

$\hat{r} = 1.05$

$\hat{v}_r = 0.0$

$\hat{v}_n = 1.0$

$I = 0.78539816$ radians

$\Omega = 0.0$ radians

$u = 0.0$ radians

Since solutions for the 0.05 eccentricity orbit were to be obtained up to a computer output time of $\hat{t} = 370$ which corresponds to approximately 50.5 complete orbits, the constrained and unconstrained equations were programed on an IBM 7094 digital computer rather than the smaller IBM 1620 computer which was used for the previous case. A 0.125 step

size constrained solution was selected to provide a standard of comparison for the constrained and unconstrained solutions obtained with larger integration step sizes. This selection was based upon a comparison of the exact solutions and the 0.125 step size solutions for this same orbit when no perturbing forces were present. Tables A-13 and A-14 in Appendix A present a comparison of both the constrained and unconstrained 0.125 step size solutions with the exact solutions during the 50th orbit for the non-perturbed case.

Figs. 6-5 through 6-9 present the differences over the first three orbits between the constrained and unconstrained computer solutions obtained with a 0.5 integration step size and the 0.125 step size constrained solution standard when oblate earth perturbing forces are present. These nondimensional step sizes correspond to approximately 15 and 58 integration steps per orbit. If these differences are converted to dimensional quantities, the maximum errors (with time treated as the independent variable) in the constrained and unconstrained 0.5 step size solutions over the first three orbits are as follows:

Constrained Solution Maximum Error (time treated as independent variable)

ϵ_r = 62.7 feet

ϵ_{v_r} = 0.0388 feet/second

ϵ_{v_n} = 0.0518 feet/second

ϵ_u = 0.0000245 radians

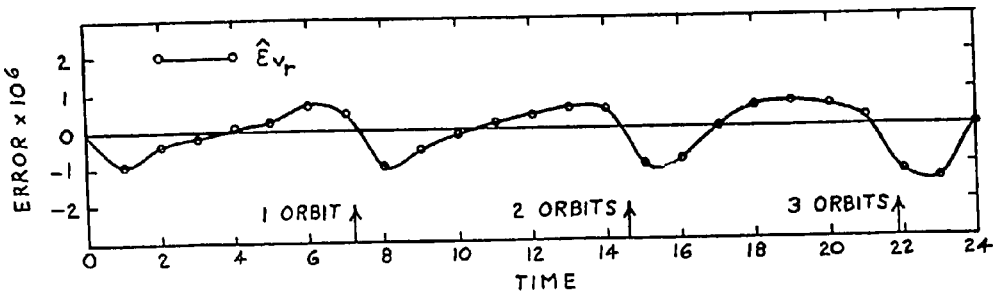

Fig. 6-5: Nondimensional error in radial velocity $\hat{\epsilon}_{v_r}$ versus nondimensional time for 0.5 step size constrained computer solutions for oblate earth perturbed 0.05 eccentricity orbit (0.125 constrained solutions subtracted from 0.5 constrained solutions).

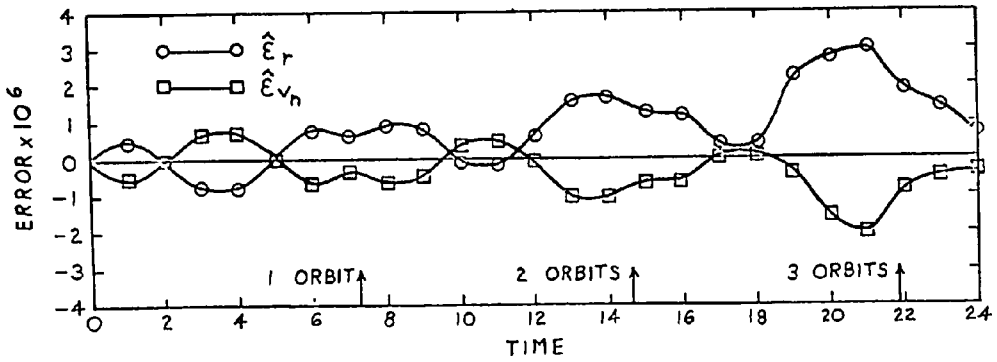

Fig. 6-6: Nondimensional error in radius $\hat{\epsilon}_r$ and normal velocity $\hat{\epsilon}_{v_n}$ versus nondimensional time for 0.5 step size constrained computer solutions for oblate earth perturbed 0.05 eccentricity orbit (0.125 constrained solutions subtracted from 0.5 constrained solutions).

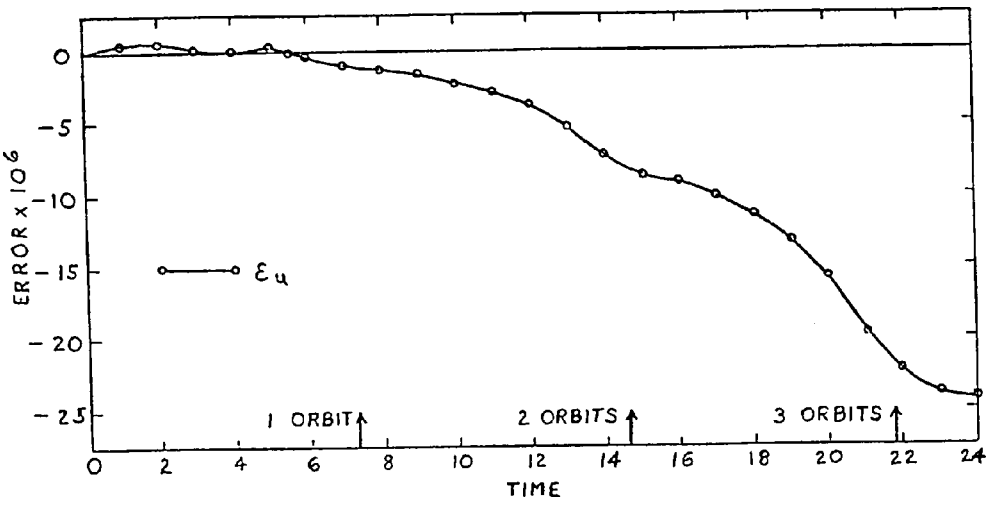

Fig. 6-7: Error in path angle ϵ_u (in radians) versus nondimensional time for 0.5 step size constrained computer solutions for oblate earth perturbed 0.05 eccentricity orbit (0.125 constrained solutions subtracted from 0.5 constrained solutions).

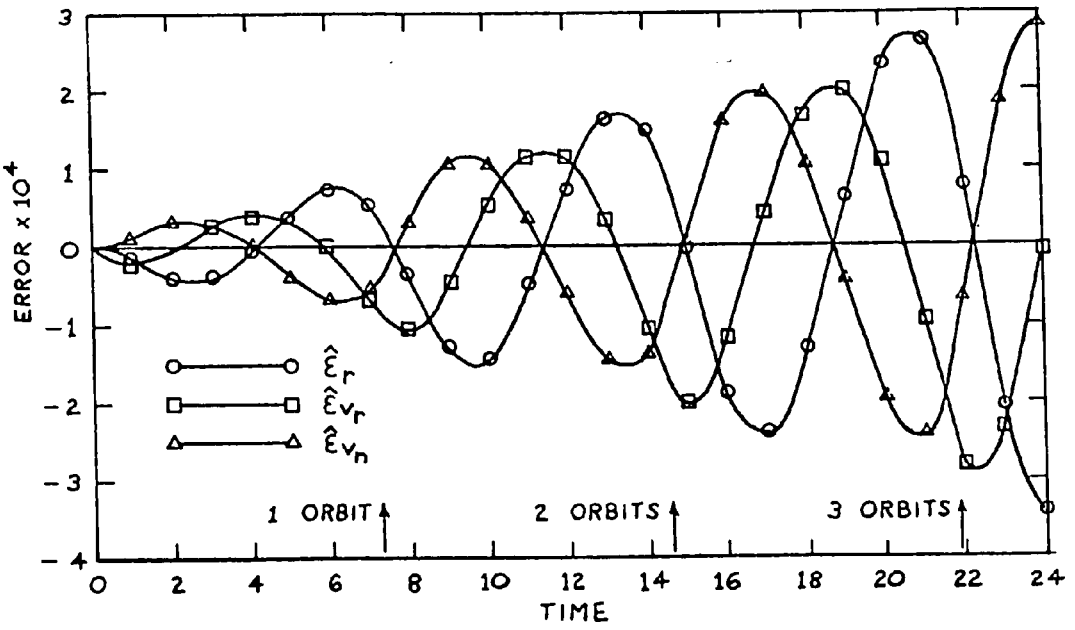

Fig. 6-8: Nondimensional error in radius $\hat{\varepsilon}_r$, radial velocity $\hat{\varepsilon}_{v_r}$, and normal velocity $\hat{\varepsilon}_{v_n}$ versus nondimensional time for 0.5 step size unconstrained computer solutions for oblate earth perturbed 0.05 eccentricity orbit (0.125 constrained solutions subtracted from 0.5 unconstrained solutions).

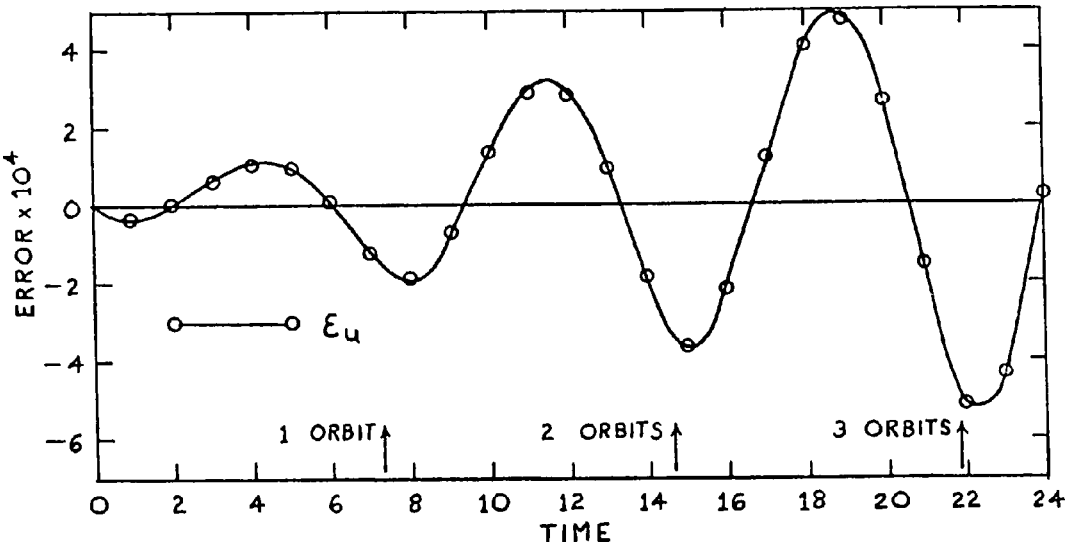

Fig. 6-9: Error in path angle ϵ_u (in radians) versus nondimensional time for 0.5 step size unconstrained computer solutions for oblate earth perturbed 0.05 eccentricity orbit (0.125 constrained solutions subtracted from 0.5 unconstrained solutions).

Unconstrained Solution Maximum Error (time treated as independent variable)

ϵ_r = 7,106 feet

ϵ_{v_r} = 7.25 feet/second

ϵ_{v_n} = 7.38 feet/second

ϵ_u = 0.00051 radians

From the standpoint of precision trajectory computation it can be seen that the 0.5 step size unconstrained solutions would be unacceptable, particularly with respect to the errors in velocity. On the other hand, the constrained solution errors, even with the relatively large nondimentional step size of 0.5, are within acceptable limits for the first several orbits.

Figs. 6-10 through 6-13 present the differences in the 0.5 step size constrained and unconstrained solutions and the 0.125 standard during the 50th orbit. If we convert these differences to dimensional quantities (where time is again treated as the independent variable) the maximum constrained and unconstrained 0.5 step size errors during the 50th orbit are as follows:

Constrained Solution Maximum Error (time treated as independent variable)

ϵ_r = 8,360 feet

ϵ_{v_r} = 9.065 feet/second

ϵ_{v_n} = 9.065 feet/second

ϵ_u = 0.0076 radians

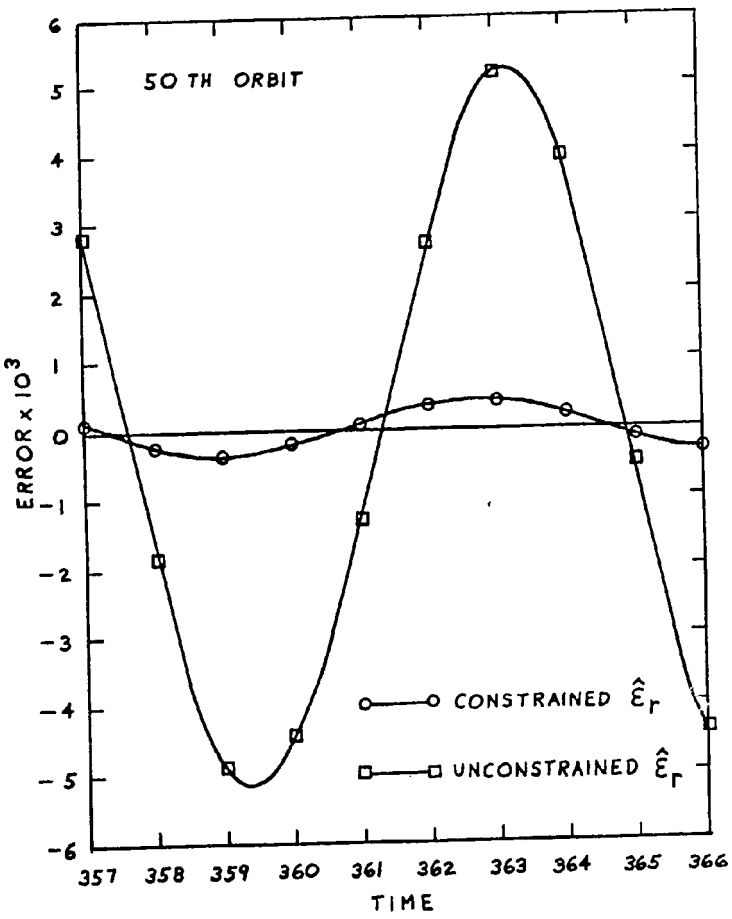

Fig. 6-10: Nondimensional error in radius $\hat{\epsilon}_r$ versus nondimensional time for 0.5 step size constrained and unconstrained computer solutions for 50th orbit of oblate earth perturbed 0.05 eccentricity orbit (0.125 constrained solutions subtracted from 0.5 solutions).

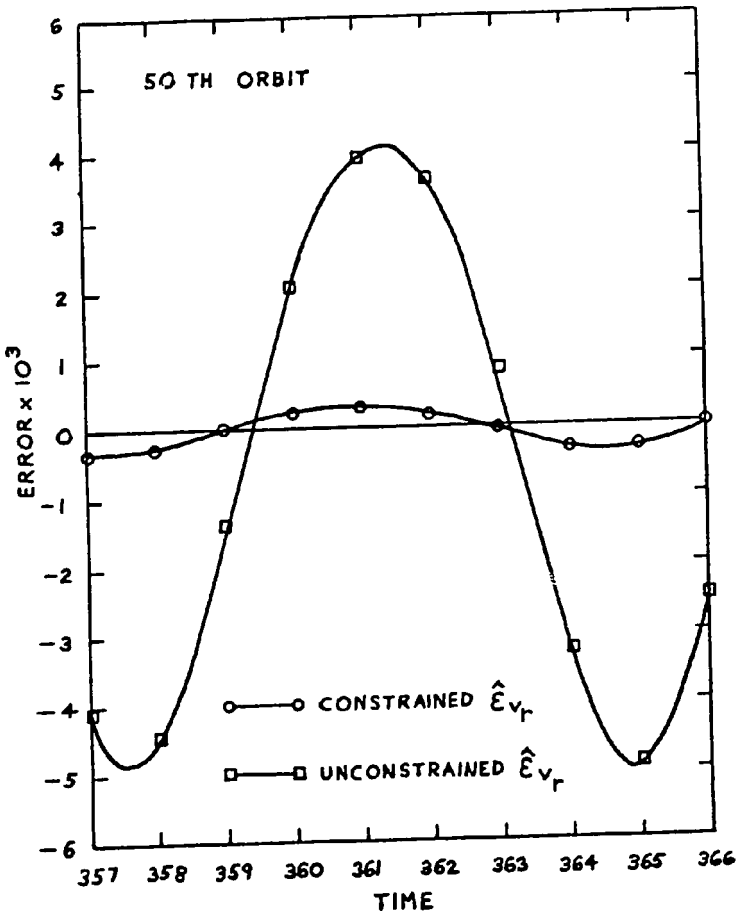

Fig. 6-11: Nondimensional error in radial velocity $\hat{\epsilon}_{v_r}$ versus nondimensional time for 0.5 step size constrained and unconstrained computer solutions for 50th orbit of oblate earth perturbed 0.05 eccentricity orbit (0.125 constrained solutions subtracted from 0.5 solutions).

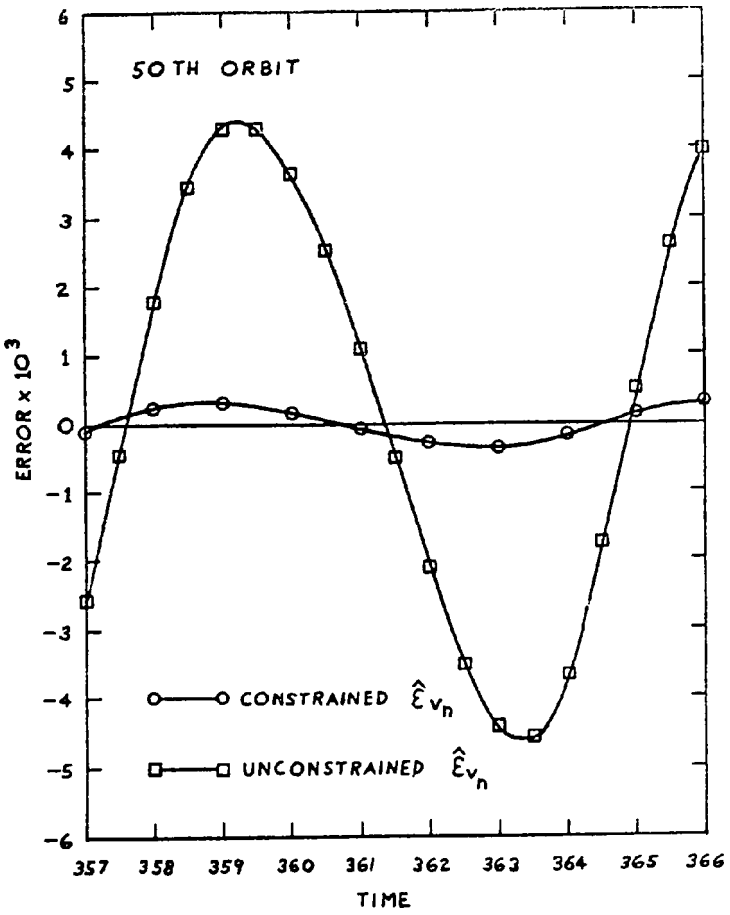

Fig. 6-12: Nondimensional error in normal velocity $\hat{\epsilon}_{v_n}$ versus nondimensional time for 0.5 step size constrained and unconstrained computer solutions for 50th orbit of oblate earth perturbed 0.05 eccentricity orbit (0.125 constrained solutions subtracted from 0.5 solutions).

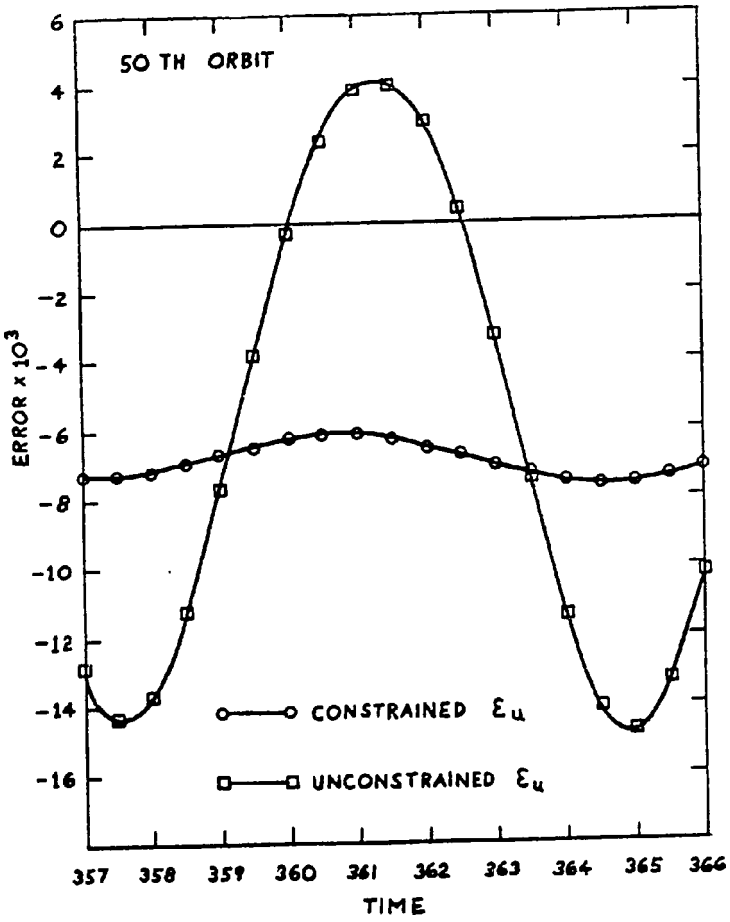

Fig. 6-13: Error in path angle ε_u (in radians) versus nondimensional time for 0.5 step size constrained and unconstrained computer solutions for 50th orbit of oblate earth perturbed 0.05 eccentricity orbit (0.125 constrained solutions subtracted from 0.5 solutions).

Unconstrained Solutions Maximum Error (time treated as independent variable)

ϵ_r = 108,680 feet

ϵ_{v_r} = 129.5 feet/second

ϵ_{v_n} = 119.14 feet/second

ϵ_u = 0.0148 radians

Although the constrained errors, with time treated as the independent variable, are smaller than the unconstrained errors, neither of the large step size solutions appears to be sufficiently accurate for precision trajectory calculations over a large number of orbits. However, as in the previous 0.5 eccentricity case, a large percentage of the above errors may be the result of the error in the path angle u with time. From Fig. 6-13 it can be seen that the 0.5 step size constrained solution for u as a function of time is lagging the 0.125 step size standard solution for this variable. This might be expected since the 0.5 integration step size results in only 15 integration steps per orbit. To investigate this possibility, the approximate correction technique developed in Chapter 4 and used in the previous section was employed at nondimensional computer output times corresponding to $\hat{t}$ = 359, $\hat{t}$ = 360.5, and $\hat{t}$ = 363. The computer solutions for these three cases are listed on the following pages.

$\hat{t} = 359$

0.125 Step Size Constrained Solution Standard

$\hat{r}$	$\hat{v}_r$	$\hat{v}_n$	u
1.1063063	0.046652192	0.94852377	1.9755834

0.5 Step Size Constrained Solution

$\hat{r}$	$\hat{v}_r$	$\hat{v}_n$	u
1.1059755	0.046677341	0.94881811	1.9689079

0.5 Step Size Unconstrained Solution

$\hat{r}$	$\hat{v}_r$	$\hat{v}_n$	u
1.1014132	0.045321730	0.95281721	1.9678826

$\hat{t} = 360.5$

0.125 Step Size Constrained Solution Standard

$\hat{t}$	$\hat{v}_r$	$\hat{v}_n$	u
1.1562542	0.011807927	0.90804597	3.1973607

0.5 Step Size Constrained Solution

$\hat{r}$	$\hat{v}_r$	$\hat{v}_n$	u
1.1561928	0.012087645	0.90810772	3.1912031

0.5 Step Size Unconstrained Solution

$\hat{r}$	$\hat{v}_r$	$\hat{v}_n$	u
1.1531565	0.015050779	0.91056785	3.1997392

$\hat{t} = 363$

0.125 Step Size Constrained Solution Standard

$\hat{r}$	$\hat{v}_r$	$\hat{v}_n$	u
1.0902467	-0.045521125	0.96256801	5.2336593

0.5 Step Size Constrained Solution

$\hat{r}$	$\hat{v}_r$	$\hat{v}_n$	u
1.0906409	-0.045587324	0.96223010	5.2266371

0.5 Step Size Unconstrained Solution

$\hat{r}$	$\hat{v}_r$	$\hat{v}_n$	u
1.0953779	-0.044665739	0.95814309	5.2304207

After correction for the deviations in u, the errors in the 0.5 step size constrained and unconstrained solutions for the variables $\hat{r}$, $\hat{v}_r$, $\hat{v}_n$ and time (as a function of path angle, u) were found to be as follows:

Computer Output Time = 359 (u treated as independent variable)

0.5 Constrained Solution

$\hat{\epsilon}_r = -32.4\times10^{-6}$, $\epsilon_r = 677.2$ feet

$\hat{\epsilon}_{v_r} = +4.49\times10^{-6}$, $\epsilon_{v_r} = 0.1163$ feet/second

$\hat{\epsilon}_{v_n} = +17.09\times10^{-6}$, $\epsilon_{v_n} = 0.4426$ feet/second

$\hat{\epsilon}_t = -77.86\times10^{-4}$, $\epsilon_t = 6.31$ seconds

0.5 Unconstrained Solution

$\hat{\epsilon}_r = +4474.1\times10^{-6}$, $\epsilon_r = 93{,}508$ feet

$\hat{\epsilon}_{v_r} = +1364.65\times10^{-6}$, $\epsilon_{v_r} = 35.344$ feet/second

$\hat{\epsilon}_{v_n} = -3934.18\times10^{-6}$, $\epsilon_{v_n} = 101.89$ feet/second

$\hat{\epsilon}_t = -89.82\times10^{-4}$, $\epsilon_t = 7.27$ seconds

Computer Output Time = 360.5 (u treated as independent variable)

0.5 Constrained Solution

$\hat{\epsilon}_r = -31.2\times10^{-6}$, $\epsilon_r = 652.1$ feet

$\hat{\epsilon}_{v_r} = -6.34\times10^{-6}$, $\epsilon_{v_r} = 0.1642$ feet/second

$\hat{\epsilon}_{v_n} = +10.96\times10^{-6}$, $\epsilon_{v_n} = 0.2839$ feet/second

$\hat{\epsilon}_t = -78.41\times10^{-4}$, $\epsilon_t = 6.351$ seconds

0.5 Unconstrained Solution

$\hat{\epsilon}_r = +3133.5\times10^{-6}$, $\epsilon_r = 65{,}490$ feet

$\hat{\epsilon}_{v_r} = -3348.45\times10^{-6}$, $\epsilon_{v_r} = 86.72$ feet/second

$\hat{\epsilon}_{v_n} = -2549.96\times10^{-6}$, $\epsilon_{v_n} = 66.04$ feet/second

$\hat{\epsilon}_t = +30.28\times10^{-4}$, $\epsilon_t = 2.453$ seconds

Computer Output Time = 363 (u treated as independent variable)

0.5 Constrained Solution

$\hat{\epsilon}_r = -32.1\times10^{-6}$, $\epsilon_r = 670.9$ feet

$\hat{\epsilon}_{v_r} = -1.741\times10^{-6}$, $\epsilon_{v_r} = 0.045$ feet/second

$\hat{\epsilon}_{v_n} = +18.25\times10^{-6}$, $\epsilon_{v_n} = 0.4727$ feet/second

$\hat{\epsilon}_t = -79.54\times10^{-4}$, $\epsilon_t = 6.442$ seconds

0.5 Unconstrained Solution

$\hat{\epsilon}_r = -4964.3\times10^{-6}$, $\epsilon_r = 103{,}753$ feet

$\hat{\epsilon}_{v_r} = -886.73\times10^{-6}$, $\epsilon_{v_r} = 22.966$ feet/second

$\hat{\epsilon}_{v_n} = +4277.5\times10^{-6}$, $\epsilon_{v_n} = 110.78$ feet/second

$\hat{\epsilon}_t = -36.68\times10^{-4}$, $\epsilon_t = 2.97$ seconds

From the above results, the advantages of the constrained equations are clearly evident. Even though only 15 integrations were performed for each complete orbit, the constrained solutions are in error with

position in the orbit by less than 700 feet in radius and 0.5 feet/second in total velocity after 50 orbits. The small error in u with time at the end of the 50th orbit amounts to only 6.5 seconds out of a total dimensional time in orbit of approximately 82.35 hours.

CHAPTER 7

PERTURBING FORCES RESULTING FROM AERODYNAMIC DRAG

In this chapter the constrained and unconstrained equations are used to consider the case in which the perturbations arise from aerodynamic forces acting on a non-lifting body. As a result, the perturbing forces are now functions of vehicle velocity and altitude, which differs from the previous cases in which the perturbing forces were either zero or solely dependent upon position (i.e. dependent upon $\hat{r}$, u, I and Ω). Two problems of particular interest are considered. In the first, the case of a slightly eccentric orbit is considered under the influence of small aerodynamic drag forces. In the second, the constrained and unconstrained equations are applied to a re-entry trajectory. This represents a case for which the perturbing forces are very large and for which the constrained solutions incur large errors.

7.1 Development of Equations

For simplicity in developing the perturbing forces, the rotation of the atmosphere will be neglected and the drag force will therefore be considered to act along the flight path as computed from inertial velocities. In addition, the density will be considered to vary exponentially with altitude above the earth's surface, and the drag coefficient will be assumed to be constant. With the above assumptions, the perturbing force due to drag can be written in the form

$$\vec{F}_P = -\frac{1}{2}\rho v^2 A_r c_d \frac{\vec{v}}{v} \tag{7-1}$$

where

ρ = atmospheric density = $\rho_b e^{-\beta h}$

ρ_b = base density (taken to be density at h = 0 for this study)

h = atitude above earth's surface = $r - r_e$

β = scale height = $\frac{1}{24,000}$ $ft.^{-1}$ for this study

A_r = reference area

c_d = drag coefficient (assumed constant for this study)

$v = \sqrt{v_r^2 + v_n^2}$

If we nondimensionalize the perturbing force by selecting characteristic values such that

r_o = reference radius = radius of spherical earth, r_e

g_o = reference acceleration at reference radius r_o

m = mass of vehicle

then Eq. (7-1) becomes

$$\frac{\vec{F}_P}{mg_o} = -\frac{1}{2}\rho_b e^{-\beta h} v^2 \frac{A_r c_d}{mg_o}\frac{\vec{v}}{v} \tag{7-2}$$

If we define the quantities

$\mathbb{D} = \frac{A_r c_d}{mg_o}$ = drag-weight parameter

$\hat{\mathbb{D}}$ = nondimensional drag-weight parameter = $g_o \rho_b r_o \mathbb{D}$

$\hat{\beta}$ = nondimensional scale factor = βr_o

$\hat{h} = \frac{r - r_e}{r_o} = \hat{r} - 1$ = nondimensional altitude

$\hat{v} = \frac{v}{g_o r_o}$ = nondimensional velocity

then Eq. (7-2) becomes

$$\hat{\vec{F}}_P = -\frac{1}{2}\hat{v}^2 \hat{\mathbb{D}} e^{-\hat{\beta}\hat{h}} \frac{\hat{\vec{v}}}{\hat{v}} \tag{7-3}$$

Finally, if we define a flight path angle Ψ measured from the vector $\vec{e}_n$ in the $\vec{e}_r$, $\vec{e}_n$ plane to the vector $\frac{\hat{\vec{V}}}{\hat{V}}$, we can write

$$\frac{\hat{\vec{V}}}{\hat{V}} = \cos \Psi \, \vec{e}_n + \sin \Psi \, \vec{e}_r = \frac{\hat{V}_n}{\hat{V}} \vec{e}_n + \frac{\hat{V}_r}{\hat{V}} \vec{e}_r \tag{7-4}$$

Substituting Eq. (7-4) into Eq. (7-3) yields the final expression for the perturbing force

$$\hat{\vec{F}}_P = -\frac{1}{2}\hat{\rho}\hat{D}e^{-\hat{\beta}\hat{h}}\hat{V}_r\hat{V}\vec{e}_r - \frac{1}{2}\hat{\rho}\hat{D}e^{-\hat{\beta}\hat{h}}\hat{V}_n\hat{V}\vec{e}_n \tag{7-5}$$

or in terms of $\vec{e}_r$, $\vec{e}_n$, $\vec{e}_h$ components

$$\hat{F}_r = -\frac{1}{2}\hat{\rho}\hat{D}e^{-\hat{\beta}\hat{h}}\hat{V}_r\hat{V} \tag{7-6}$$

$$\hat{F}_n = -\frac{1}{2}\hat{\rho}\hat{D}e^{-\hat{\beta}\hat{h}}\hat{V}_n\hat{V} \tag{7-7}$$

and

$$\hat{F}_h = 0 \tag{7-8}$$

7.2 Computer Solutions for Small Eccentricity Orbit

The constrained equations given by Eqs. (3-31) through (3-39) and the unconstrained equations given in their nondimensional form by Eqs. (3-40) through (3-45) in Chapter 3, were programed on the digital computer using a fixed-step single-precision fourth-order Runge-Kutta integration scheme for all numerical integrations. The perturbing forces $\hat{F}_r$, $\hat{F}_n$, and $\hat{F}_h$ were programed in the form given by Eqs. (7-6) through (7-8) above. The small eccentricity orbit selected for this investigation corresponded to a non-perturbed orbit with the following characteristics:

$\hat{r}_p$ = radius at perigee = 1.02 earth radii

$\hat{r}_a$ = radius at apogee = 1.2 earth radii

$\hat{v}_{np}$ = nondimensional normal velocity at perigee = 1.0295063

$\hat{v}_{na}$ = nondimensional normal velocity at apogee = 0.8750804

E = eccentricity = 0.081081

$\hat{\tau}$ = nondimensional orbital period = 7.347951 which corresponds to a dimensional time of 1.6533 hours.

The factors used to represent the atmospheric density variation corresponded to a base density of ρ_b = 0.00238 slug/ft.^{3} and a scale height of $\beta = \frac{1}{24{,}000}$ ft.$^{-1}$. For simplicity, these values were assumed constant throughout the altitude range of the trajectory. The dimensional drag-weight parameter $\mathbb{D}$ was taken to be 0.01 ft^2/lb.

The initial conditions used for this study were as follows:

$\hat{r}$ = 1.02

$\hat{v}_r$ = 0.0

$\hat{v}_n$ = 1.0295063

I = 0.78539816

Ω = 0.0

u = 0.0

Solutions were obtained up to a nondimensional time of $\hat{t}$ = 78 which corresponds to approximately 10.5 orbits. At the end of this time the angular momentum had decreased from its original nondimensional value of 1.0500964 to a value of 1.0493298, indicating the very small perturbations resulting from the drag forces. Solutions were obtained for nondimensional step sizes of 0.8, 0.5, 0.2 and 0.125. These step

sizes correspond to approximately 9, 15, 37, and 59 integration steps per orbit. The 0.125 step size constrained solution was selected as the standard against which the larger step size constrained and unconstrained solutions were compared. This standard was selected, as in the previous cases, on the basis of the good agreement between a 0.125 step size constrained solution and the exact solution for this same orbit in the absence of perturbing forces.

Figs. 7-1 through 7-4 present the differences between the constrained and unconstrained computer solutions obtained with a 0.5 nondimensional step size and the 0.125 step size constrained solution standard during the 10th orbit. If these differences are converted to dimensional quantities, the maximum errors in the 0.5 step size constrained and unconstrained solutions during the 10th orbit are as follows:

Constrained Solution Maximum Error (.5 step size)

ϵ_r = 729 feet

ϵ_{v_r} = .754 feet/second

ϵ_{v_n} = .669 feet/second

ϵ_u = .0187 degrees

Unconstrained Solution Maximum Error (.5 step size)

ϵ_r = 218,237 feet

ϵ_{v_r} = 222 feet/second

ϵ_{v_n} = 209 feet/second

ϵ_u = 7.44 degrees

A representative example of the results obtained with the other integration step sizes is shown on the following page for a nondimensional computer output time of $\hat{t}$ = 68, where the values of u have been reduced to correspond to values between 0 and 2π.

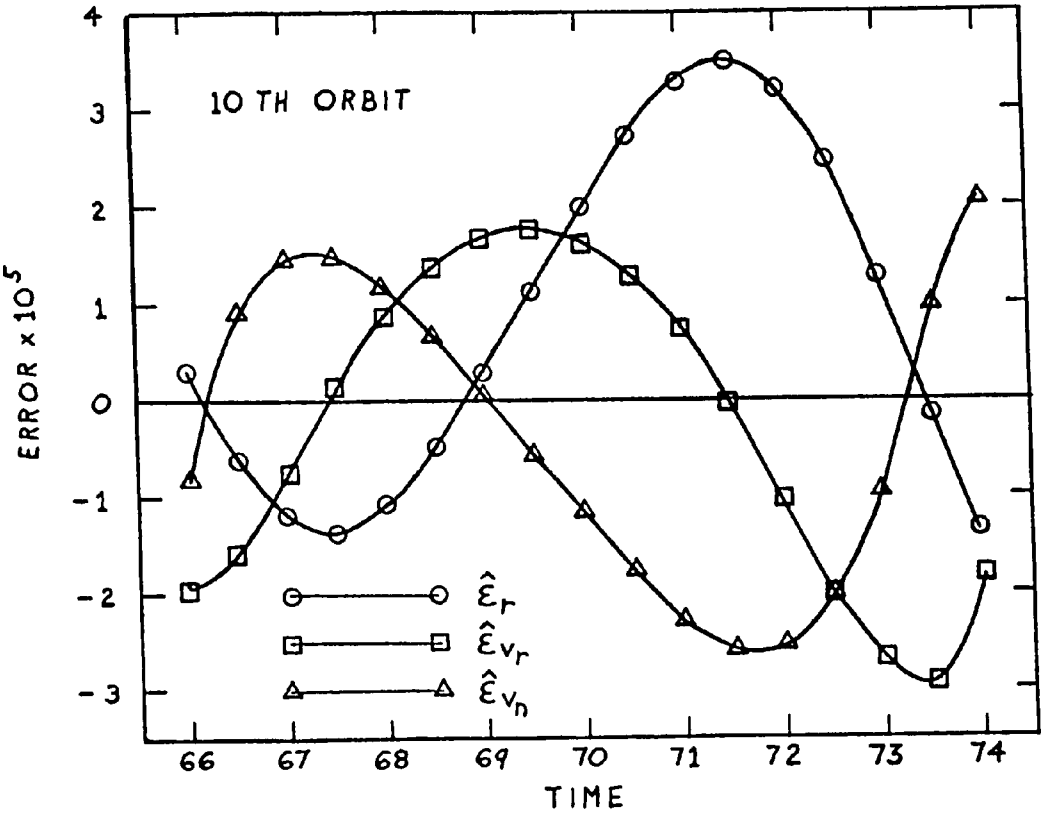

Fig. 7-1: Nondimensional error in radius $\hat{\varepsilon}_r$, radial velocity $\hat{\varepsilon}_{v_r}$, and normal velocity $\hat{\varepsilon}_{v_n}$ versus nondimensional time for 0.5 step size constrained computer solutions for 10th orbit of drag perturbed small eccentricity orbit (0.125 constrained solutions subtracted from 0.5 constrained solutions).

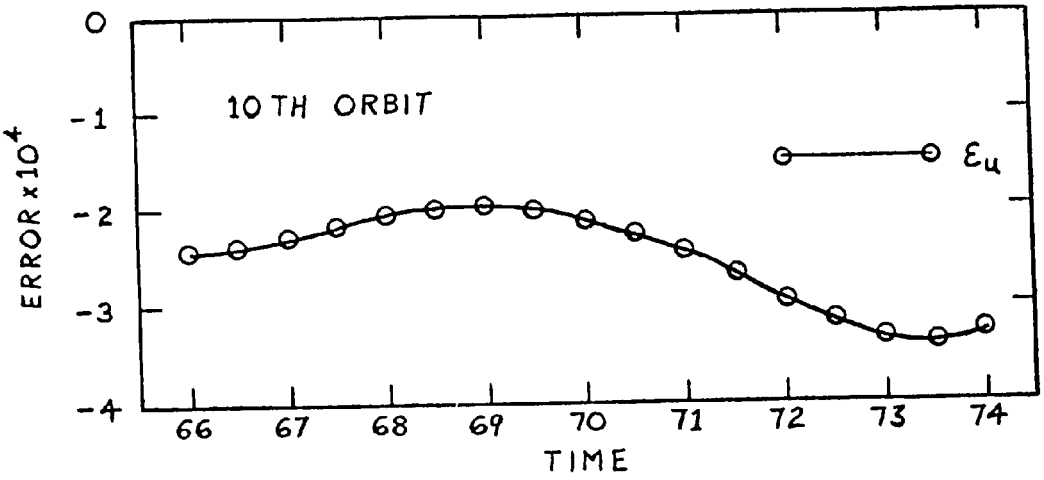

Fig. 7-2: Error in path angle ε_u (in radians) versus nondimensional time for 0.5 step size constrained computer solutions for 10th orbit of drag perturbed small eccentricity orbit (0.125 constrained solutions subtracted from 0.5 constrained solutions).

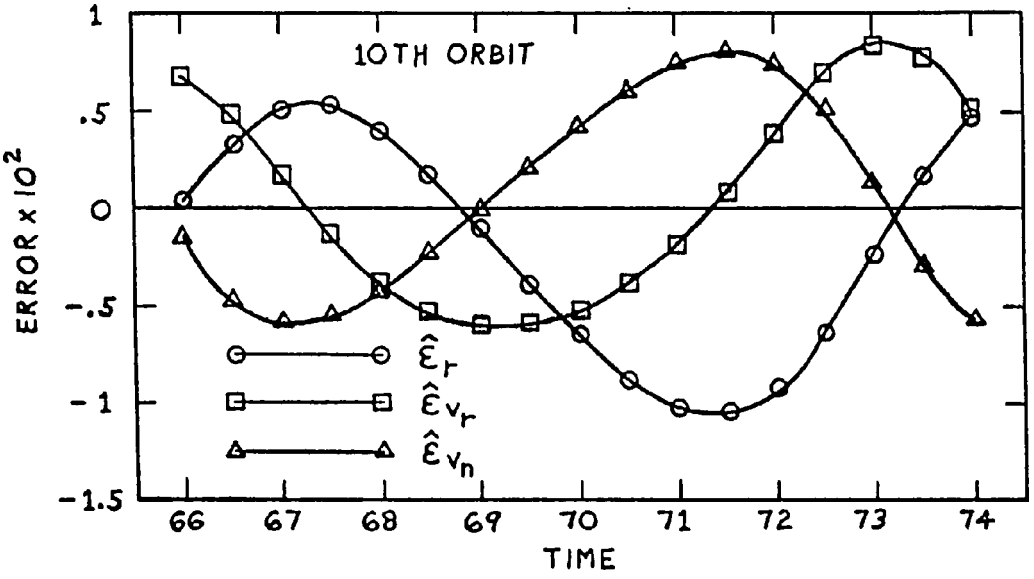

Fig. 7-3: Nondimensional error in radius $\hat{\epsilon}_r$, radial velocity $\hat{\epsilon}_{v_r}$, and normal velocity $\hat{\epsilon}_{v_n}$ versus nondimensional time for 0.5 step size unconstrained computer solutions for 10th orbit of drag perturbed small eccentricity orbit (0.125 constrained solutions subtracted from 0.5 unconstrained solutions).

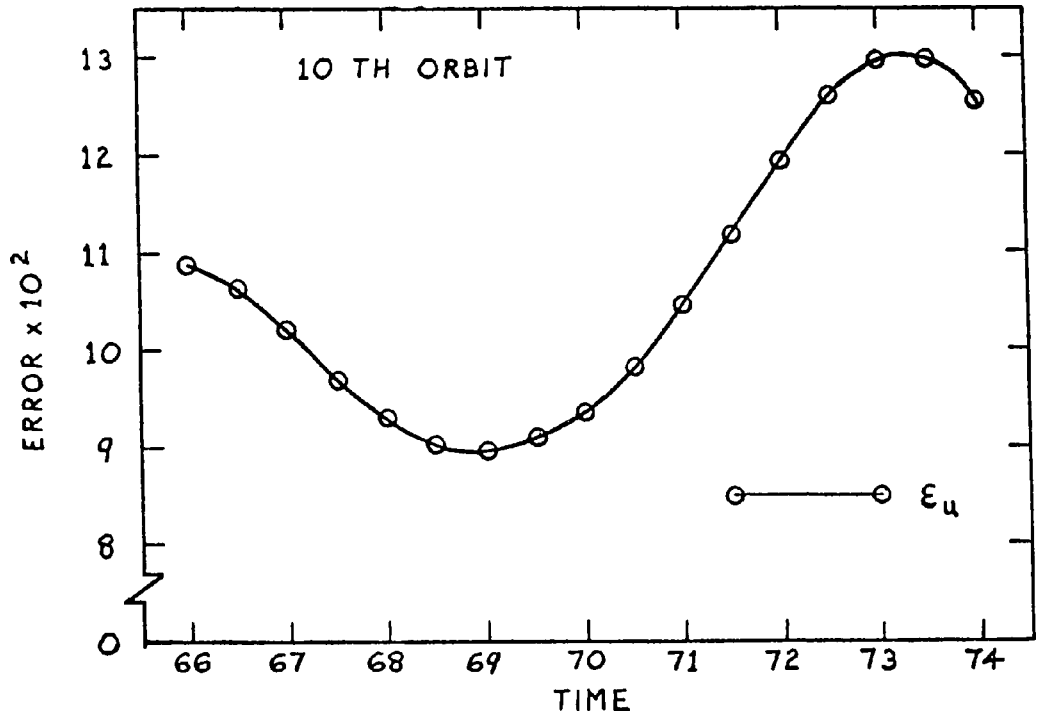

Fig. 7-4: Error in path angle ϵ_u (in radians) versus nondimensional time for 0.5 step size unconstrained computer solutions for 10th orbit of drag perturbed small eccentricity orbit (0.125 constrained solutions subtracted from 0.5 unconstrained solutions).

Constrained Solutions at $\hat{t} = 68$

step size	$\hat{r}$	$\hat{v}_r$	$\hat{v}_n$	u
.8	1.1231397	.073515923	.93431441	1.8190920
.5	1.1233479	.073572726	.93417826	1.8201511
.2	1.1233554	.073565217	.93416943	1.8203000
.125	1.1233585	.073563675	.93416619	1.8203566

Unconstrained Solutions at $\hat{t} = 68$

step size	$\hat{r}$	$\hat{v}_r$	$\hat{v}_n$	u
.8	1.1470989	.024760499	.90816399	2.7850681
.5	1.1274038	.069956441	.93006966	1.9133711
.2	1.1234588	.073477905	.93405884	1.8227738
.125	1.1234041	.073535234	.93411785	1.8212656

From the above results, the sensitivity of the unconstrained solutions to the choice of step size is evident. If the 0.125 step size constrained solution is used as a standard, the dimensional errors of the above solutions as a function of step size are as follows:

Constrained Solution Error at $\hat{t} = 68$

step size	ϵ_r	ϵ_{v_r}	ϵ_{v_n}	ϵ_u
.8	.866 miles	1.24 fps	3.85 fps	0.072 deg
.5	.042 miles	0.234 fps	0.313 fps	0.0118 deg
.2	.012 miles	0.04 fps	0.084 fps	0.0032 deg

Unconstrained Solution Error at $\hat{t} = 68$

step size	ϵ_r	ϵ_{v_r}	ϵ_{v_n}	ϵ_u
.8	93.9 miles	1263 fps	673 fps	55 deg
.5	16 miles	93 fps	106 fps	5.33 deg
.2	.397 miles	2.2 fps	2.78 fps	0.138 deg
.125	.18 miles	0.737 fps	1.25 fps	0.052 deg

As in all of the previous cases, the constrained equations provide superior accuracy over that of the unconstrained equations and, in addition, allow the use of larger integration step sizes.

7.3 Computer Solutions for Terminal Re-entry

In the discussion of singularities in Chapter 3 it was noted that a singularity could occur in the constrained equations for a case where angular momentum approaches zero. This situation could occur for the idealized case of a non-lifting re-entry through the atmosphere of a non-rotating planet. For this case, the aerodynamic drag forces become very large during the period of maximum deceleration. As a result, the time rates of change of the angular momentum and the components of the eccentricity vector become large. In the analysis which follows, this factor was found to be of greater significance in causing inaccuracies in the constrained solutions for terminal re-entry than was that of the singularity as $\hat{H}$ approaches zero.

In order to investigate the behavior of the constrained equations during terminal re-entry, a zero-lift re-entry through a non-rotating atmosphere was analyzed with solutions being obtained for both the constrained and unconstrained equations. The initial conditions for this trajectory corresponded to those at the apogee of a non-perturbed

elliptical orbit whose perigee would be tangent to the surface of a spherical earth. These initial conditions were as follows:

$\hat{r}$ = 1.06 earth radii

$\hat{v}_n$ = 0.95703640

$\hat{v}_r$ = 0.0

u = 0.0

I = 0.78539816

Ω = 0.0

E = non-perturbed eccentricity = 0.02912621

$\frac{\hat{\tau}}{2}$ = non-perturbed half-period = 3.284022

The drag forces were programed in the form given by Eqs. (7-6) through (7-8) and the values for base density, scale height and drag-weight parameter were the same as those used in the previous section.

Since some of the time rates of change of the variables in both the constrained and unconstrained equations become large during the maximum deceleration phase of the re-entry, it was not possible to use the same fixed integration step throughout all phases of the re-entry. To account for this factor the following method was used. First, solutions were obtained using a fixed nondimensional step size of 6.25×10^{-2}. Next, the constrained and unconstrained solutions resulting from this integration step size were compared and a point was selected which corresponded to a time prior to that at which the solutions of both methods began to disagree. For the 6.25×10^{-2} step size this point in the trajectory was taken at a time of $\hat{t}$ = 2.3125. The solutions corresponding to this time were then used as the initial conditions for a smaller step size solution, the nondimensional value of this step being 1.9531250×10^{-3}. The initial conditions for this smaller step size were as follows:

$\hat{t} = 2.3125$

$\hat{r} = 1.0126069$

$\hat{v}_r = - .024209692$

$v_n = 0.99547826$

$u = 2.1642294$ radians

I and Ω unchanged from original values

Solutions for this smaller step size and the above initial conditions were obtained for the remainder of re-entry. The constrained and unconstrained solutions resulting from this smaller step size were again compared to find a time prior to the point at which the solutions began to disagree. This point corresponded to a nondimensional time of $\hat{t} = 2.4355467$. As before, the solutions corresponding to this point were taken as initial conditions and the step size was reduced to a nondimensional value of 4.8828125×10^{-4}. The initial conditions for this smaller step size were as follows:

$\hat{t} = 2.4355467$

$\hat{r} = 1.0095561$

$\hat{v}_r = - 0.027199370$

$v_n = 0.92300759$

$u = 2.2826957$ radians

I and Ω unchanged from original values

Solutions for this smaller step size and the above initial conditions were again obtained for the remainder of the re-entry. Although the constrained and unconstrained solutions obtained with this step size began to disagree in the fourth significant digit of the solutions for $\hat{v}_n$, at a nondimensional time of $\hat{t} = 2.5390624$, no further reduction in step size was undertaken. It should be noted that the unconstrained

solutions for both of the smaller step sizes were in reasonably good agreement over the portion of the trajectory starting from $\hat{t} = 2.4355467$ to the termination of computation which occured at $\hat{t} = 2.75$. On the other hand, the constrained solutions for all three step sizes were completely in error prior to the termination of computation at $\hat{t} = 2.75$. The last computed values for the unconstrained solutions with the two smallest step sizes were as follows:

Step Size, 1.9531250×10^{-3}

$\hat{r}$	$\hat{v}_r$	$\hat{v}_n$	u
1.0001530	-.012353617	$.20322252 \times 10^{-4}$	2.3744959

Step Size, 4.8828125×10^{-4}

$\hat{r}$	$\hat{v}_r$	$\hat{v}_n$	u
1.0001516	-.012345655	$.20208880 \times 10^{-4}$	2.3744638

The constrained solutions exhibited two characteristics after they began to deviate from the unconstrained solutions. First, a reduction in step size caused the constrained solutions to approach the corresponding values of the unconstrained solutions. Second, at some point in the trajectory, after maximum deceleration, the constrained solutions for the variables, $\hat{r}$, $\hat{v}_r$, and $\hat{v}_n$ tended to approach constant values, with these values becoming smaller in magnitude with decreasing step size.

An example of the first characteristic is shown on the following page for a computer output time of $\hat{t} = 2.5625$.

Constrained Solution

step size	$\hat{r}$	$\hat{v}_r$	$\hat{v}_n$	u
6.25×10^{-2}	1.0440127	-.060637475	.75066339	2.3771800
1.9531250×10^{-3}	1.0058071	-.046811128	.30985792	2.3673957
4.8828125×10^{-4}	1.0050038	-.040299059	.25106920	2.3664013

Unconstrained Solution

step size	$\hat{r}$	$\hat{v}_r$	$\hat{v}_n$	u
6.25×10^{-2}	1.0049764	-.040377579	.25609978	2.3665252
1.9531250×10^{-3}	1.0050068	-.040315474	.25139030	2.3664279
4.8828125×10^{-4}	1.0050054	-.040305887	.25118294	2.3664092

From the above solutions it can be seen that the constrained equations require a smaller step size than the unconstrained equations for comparable accuracy. This is to be expected since all three of the constrained variables, $\hat{H}$, $\hat{\alpha}$, and $\hat{\gamma}$ must undergo rapid changes during reentry. For example, $\hat{H}$ must undergo a change from near unity to zero while the eccentricity, from which $\hat{\alpha}$ and $\hat{\gamma}$ are derived, must change from a value near zero to a value near unity. On the other hand, two of the unconstrained variables, $\hat{r}$ and $\hat{v}_r$, undergo much smaller changes over the same time period. Despite this apparent explanation, however, a discrepancy still remains. The unconstrained variable $\hat{v}_n$ must undergo changes on the same order of magnitude as $\hat{H}$ and E, and yet from the above results it is evident that it is being obtained more accurately for a given intetration step size than the corresponding $\hat{v}_n$ obtained with the constrained solutions. Therefore, it must be concluded that some additional factor, other than the large time rates of change of the variables $\hat{H}$, $\hat{\alpha}$, and $\hat{\gamma}$, must be influencing the accuracy of the constrained solutions.

In arriving at a step size for numerical integration one must not only be concerned with the magnitude of the rate at which a variable is changing, but also with the derivative of this rate. If the rate of the variable is smoothly varying i.e. relatively constant over the integration step , the step size can be relatively large. If, however, the rate of change of a variable is itself undergoing rapid changes over the integration step, the step size must be reduced. In view of the fact that the constrained solutions deviated from the unconstrained solutions, even for the two smallest step sizes, the relative behavior of the time rates of change of the constrained variables $\hat{H}$, $\hat{\alpha}$, and $\hat{\gamma}$ and the unconstrained variables $\hat{r}$, $\hat{v}_r$, and $\hat{v}_n$ was investigated.

Before proceding with this discussion it is beneficial to briefly outline the method used in the Runge-Kutta integration scheme for obtaining the rates of change of the variables being integrated. For a more detailed discussion of this method, the reader is referred to any of the standard numerical analysis texts such as those of Ralston[25] or Henrici[26]. For purposes of this discussion, let us consider the numerical integration of a single first-order differential equation where y represents the dependent variable, z represents the independent variable, and f(z, y) indicates the first derivative with respect to z. In general, a discrete variable method for solving a differential equation consists of an algorithm which, corresponding to each point z_n, furnishes a number y_n which is to be regarded as an approximation to the value $y(z_n)$ of the exact solution at the point z_n. The primary requirement for the applicability of most discrete variable methods is the ability to calculate a good approximation to the value of f(z, y) for a given z and y[26]. The Runge-Kutta method of integration is in the class of

methods which are termed one-step methods. Any algorithm for solving a differential equation in which the approximation y_{n+1} to the solution at the point z_{n+1} can be calculated knowing only z_n, y_n, and the step size, s, is termed a one-step method. The functional dependence of y_{n+1} on the quantities z_n, y_n, and s can be expressed as

$$y_{n+1} = y_n + s\Phi(z, y; s) \tag{7-9}$$

where Φ is called the increment function, and the quantity $s\Phi(z, y; s)$ represents the increment of the approximate solution. The simplest form of a one-step method occurs for the case where $\Phi(z, y; s) = f(z_n, y_n)$ in which case y_{n+1} becomes

$$y_{n+1} = y_n + sf(z_n, y_n) \tag{7-10}$$

In the fourth-order Runge-Kutta method, the increment function Φ is a weighted average of four evaluations of the function f, with the arguments in each evaluation depending on the preceding evaluation. The relationships are as follows:

$$\Phi(z, y; s) = \frac{1}{6}\{\delta_1 + 2\delta_2 + 2\delta_3 + \delta_4\} \tag{7-11}$$

where the weighting parameters are defined by

$$\begin{aligned} \delta_1 &= f(z_n, y_n) \\ \delta_2 &= f(z_n + \tfrac{1}{2}s, y_n + \tfrac{1}{2}s\delta_1) \\ \delta_3 &= f(z_n + \tfrac{1}{2}s, y_n + \tfrac{1}{2}s\delta_2) \\ \delta_4 &= f(z_n + s, y_n + s\delta_3) \end{aligned} \tag{7-12}$$

and y_{n+1} is given by

$$y_{n+1} = y_n + \frac{s}{6}\{\delta_1 + 2\delta_2 + 2\delta_3 + \delta_4\} \qquad (7\text{-}13)$$

For simplicity, the above discussion has been given for the case of a single differential equation. The method, however, is directly extensible to cases of systems of first-order differential equations.

With the above definitions for δ_1, δ_2, δ_3, δ_4, and Φ in mind, we can return to the problem at hand. In order to investigate the character of the rates of the variables, $\hat{H}$, $\hat{\alpha}$, $\hat{\gamma}$, and $\hat{r}$, $\hat{v}_r$, $\hat{v}_n$ resulting from the fourth-order Runge-Kutta integration scheme, the values given by Eq. (7-12) were printed out for each integration step of the 1.9531250×10^{-3} step size computer solutions. An example of the values given by Eq. (7-12) and used in computing the increment function Φ for the variables $\hat{H}$, $\hat{\alpha}$, and $\hat{\gamma}$ resulting from the constrained equations and for the variables $\hat{r}$, $\hat{v}_r$ and $\hat{v}_n$ resulting from the unconstrained equations is shown below for the integration step occurring over the time interval $t = 2.5371093$ to $t = 2.5390624$. This time increment corresponds to the region of the trajectory where maximum deceleration is occurring.

Weighting Parameters for Constrained Solution Rates

	$\dot{\hat{H}}$	$\dot{\hat{\alpha}}$	$\dot{\hat{\gamma}}$
δ_1	-7.0784513	5.0032921	-2.9222036
δ_2	-5.8048914	4.0484176	-2.3541232
δ_3	-8.7644631	6.1315566	-3.5661771
δ_4	-4.4562075	3.0428010	-1.7616443

Weighting Parameters for Unconstrained Solution Rates

	$\dot{\hat{r}}$	$\dot{\hat{v}}_r$	$\dot{\hat{v}}_n$
δ_1	-.041724209	-.030402802	-8.0782296
δ_2	-.041753900	-.023199983	-8.0763309
δ_3	-.041746866	-.023307055	-8.0766001
δ_4	-.041769731	-.016099609	-8.0695023

From the above results it can be seen that the discrete variable algorithm which is being solved for the constrained equations involves time rates of change which are both large and which are undergoing large variations within the integration interval. On the other hand, the time rates of change of the unconstrained equations are either small or smoothly varying. In view of the rapid variations of the large rates of the variables $\hat{H}$, $\hat{\alpha}$, and $\hat{\gamma}$ it is not surprising that these variables are not being integrated accurately and hence that the constrained variables $\hat{r}$, $\hat{v}_r$ and $\hat{v}_n$ are in error. Of course, it should be realized that the actual time rates of change of angular momentum and eccentricity, although large, are not fluctuating as rapidly as the discrete-variable algorithm for the solutions of the constrained equations would indicate. This fact is apparent if one notes the smooth variation of the unconstrained rates of change of the variables $\hat{r}$, $\hat{v}_r$, and $\hat{v}_n$, since these variables, along with their rates, can be used directly to compute the time rates of change of angular momentum and eccentricity.

In resolving the apparent large fluctuations of the variables $\hat{H}$, $\hat{\alpha}$, and $\hat{\gamma}$ in the constrained solutions it is necessary to consider the form of the large perturbing force. This force is an exponential function of altitude and is therefore very sensitive to small changes in $\hat{r}$

at low altitudes. For the constrained equations, the increment of the approximate solution obtained at each of the four steps of the Runge-Kutta method represents a significant change in the values of $\hat{H}$, $\hat{\alpha}$, and $\hat{\gamma}$ due to the large time rates of change of these variables. At each of these steps, the values of $\hat{r}$, $\hat{v}_r$, and $\hat{v}_n$ are determined from the preceding approximate evaluations of the variables $\hat{H}$, $\hat{\alpha}$, and $\hat{\gamma}$ through the relations given by Eqs. (3-37) through (3-39). The resulting approximate values of $\hat{r}$, $\hat{v}_r$, and $\hat{v}_n$ are then used to evaluate the sensitive drag force which in turn is fed back to compute the next value of δ given in Eq. (7-12). The success of the constrained equations is totally dependent upon the accuracy with which the variables $\hat{H}$, $\hat{\alpha}$, and $\hat{\gamma}$ are obtained. In all of the previous problems the perturbing forces, and hence the time rates of change of $\hat{H}$, $\hat{\alpha}$, and $\hat{\gamma}$, were very small and as a result the approximate eveluations of these variables and the corresponding values of $\hat{r}$, $\hat{v}_r$, and $\hat{v}_n$ could be determined very accurately over the four steps of the integration cycle. As a result, the weighted average of the four evaluations of the parameters δ in Eq. (7-12) gave an accurate evaluation of the increment functions Φ used in determining the final evaluations of the variables $\hat{H}$, $\hat{\alpha}$, and $\hat{\gamma}$ at the end of the integration cycle. In this problem, any errors in the approximate evaluations of the variables $\hat{H}$, $\hat{\alpha}$, and $\hat{\gamma}$ at each of the four steps during the integration cycle appear to be magnified, through the use of the constraints on these relatively inaccurate approximations, in evaluating the large and sensitive perturbing force which must in turn be used to evaluate the next value of δ in Eq. (7-12). As a result, the weighted average of the four values of δ do not give an accurate evaluation of the increment functions Φ

used in determining the final evaluations of $\hat{H}$, $\hat{\alpha}$, and $\hat{\gamma}$ at the end of the integration cycle.

With the above factors in mind, we can now examine a possible explanation for the second characteristic of the constrained solutions. This characteristic involved the fact that at some point in the trajectory after maximum deceleration, the variables $\hat{r}$, $\hat{v}_r$, and $\hat{v}_n$ appear to be approaching or fluctuating about constant values and that these values decreased in magnitude with decreasing step size.

If we return to the coordinate transformation equations given by Eqs. (3-18) and (3-19) and make use of the fact that the inclination angle I and the nodal angle Ω remain constant at values of 45° and 0° respectively, we can write the transformation variables A, B, D, and L as

$$\begin{aligned} A &= \cos u \\ B &= \frac{\sin u}{\sqrt{2}} \\ D &= -\sin u \\ L &= \frac{\cos u}{\sqrt{2}} \end{aligned} \tag{7-14}$$

With the above substitutions, the nondimensional form of Eqs. (3-23) and (3-24) become

$$\hat{\alpha} = (\hat{H}\hat{v}_n - 1)\cos u + \hat{H}\hat{v}_r \sin u \tag{7-15}$$

$$\hat{\gamma} = (\hat{H}\hat{v}_n - 1)\frac{\sin u}{\sqrt{2}} - \hat{H}\hat{v}_r \frac{\cos u}{\sqrt{2}} \tag{7-16}$$

The expressions relating $\hat{r}$, $\hat{v}_r$ and $\hat{v}_n$ to the values of $\hat{H}$, $\hat{\alpha}$, and $\hat{\gamma}$ are given by Eqs. (3-37), (3-38), and (3-39) as

$$\hat{v}_n = \frac{1}{\hat{H}}\left[1 + \frac{\hat{\alpha}L - \hat{\gamma}D}{\cos I}\right] \tag{7-17}$$

$$\hat{v}_r = \frac{1}{\hat{H}}\left[\frac{\hat{\alpha}B - \hat{\gamma}A}{\cos I}\right] \tag{7-18}$$

$$\hat{r} = \frac{\hat{H}}{\hat{v}_n} \tag{7-19}$$

Before proceding, it should be noted that although the quantities $\hat{\alpha}$ and $\hat{\gamma}$ are defined by Eqs. (7-15) and (7-16), the actual values of these quantities along with that of $\hat{H}$ are obtained through numerical integration.

For the moment, let us assume that all of the quantities being obtained from integration of the constrained equations are determined with complete accuracy. With this in mind, let us consider the final phases of the idealized re-entry after maximum deceleration has taken place. For this case, as zero altitude is approached, we would expect the variables $\hat{r}$, $\hat{v}_r$, $\hat{v}_n$, $\hat{H}$, and u to approach the following values:

$\hat{r} \rightarrow 1.0$

$\hat{v}_r \rightarrow$ a small, near terminal velocity v_{r_T}

$\hat{v}_n \rightarrow 0.0$

$\hat{H} \rightarrow 0.0$

$u \rightarrow$ a constant value, u_T

In addition, we could expect the rates $\dot{\hat{\alpha}}$, $\dot{\hat{\gamma}}$, $\dot{\hat{H}}$, and $\dot{\hat{u}}$ to approach zero. As $\hat{H}$ and $\hat{v}_n$ become small, we see from Eqs. (7-15) and (7-16) that $\hat{\alpha}$ and $\hat{\gamma}$ should approach the following values:

$$\hat{\alpha} \rightarrow -\cos u \rightarrow -\cos u_T$$

$$\hat{\gamma} \rightarrow -\frac{\sin u}{\sqrt{2}} \rightarrow -\frac{\sin u_T}{\sqrt{2}}$$

If the quantities $\hat{\alpha}$, $\hat{\gamma}$, and $\hat{H}$ are accurately determined throughout the entire trajectory, they would approach these theoretical values given above. If this were the case, the solutions for $\hat{v}_n$, $\hat{v}_r$, and $\hat{r}$ obtained by substituting these terminal values for $\hat{\alpha}$, $\hat{\gamma}$, and $\hat{H}$ into Eqs. (7-17) through (7-19) would be

$$\hat{v}_n = \frac{0}{\hat{H}} \rightarrow \text{indeterminacy}$$

$$\hat{v}_r = \frac{0}{\hat{H}} \rightarrow \text{indeterminacy}$$

$$\hat{r} = \frac{\hat{H}}{\hat{v}_n} \rightarrow \text{indeterminacy}$$

If all of the above did indeed occur, we would have the case corresponding to the indeterminacy of the constrained solutions as $\hat{H}$ approaches zero. Of course, for all of this to actually occur, the quantities $\hat{\alpha}$, $\hat{\gamma}$, and $\hat{H}$ would have to be obtained very accurately throughout the entire trajectory. In the actual solutions, the values for $\hat{\alpha}$, $\hat{\gamma}$, and $\hat{H}$ became very inaccurate during the maximum deceleration phase of the trajectory. Therefore, at the end of this phase of the re-entry these variables are in error. After the maximum deceleration phase, the rates of $\hat{H}$, $\hat{\alpha}$, $\hat{\gamma}$, and u do become small, although they are not zero. As a result, the changes in these incorrect variables become smaller and the variables tend to approach values different from the "idealized" case presented above. As a result, the variables $\hat{r}$, $\hat{v}_r$, and $\hat{v}_n$ also appear to be approaching or fluctuating about incorrect terminal values.

Although it is possible that a more elaborate integration scheme of the predictor-corrector type or a Runge-Kutta integration scheme with error control would improve the accuracy of the constrained solutions during re-entry, this procedure does not seem warranted. Either of the

above schemes would require that smaller step sizes be used for the constrained equations than would be required if the unconstrained equations were used. In effect, the unconstrained equations provide a better set of variables from the standpoint of numerical integration than do the constrained equations over the portion of the trajectory corresponding to maximum deceleration. In addition, the unconstrained equations do not pose the problem of a possible singularity during the final phases of the re-entry. On the other hand, the constrained equations do provide more accurate results during the initial phases of orbit decay, when the perturbation forces are small. In view of this, the following procedure is suggested if it is desired to consider a problem which involves both orbit decay and re-entry. First, the constrained equations in their existing form can be used for the portion of the trajectory in which the drag forces are small. In addition, the unconstrained equations given by Eqs. (3-40) through (3-42) can be included in the program. At the end of each complete integration cycle for the constrained equations, the values of $\hat{r}$, $\hat{v}_r$, and $\hat{v}_n$ obtained from the constraints can be used to evaluate the unconstrained variables $\hat{\dot{r}}$, $\hat{\dot{v}}_r$, and $\hat{\dot{v}}_n$ given by Eqs. (3-40) through (3-42). A simple comparison test can be programed to compare the absolute magnitudes of the variables $\hat{\dot{r}}$, $\hat{\dot{v}}_r$, and $\hat{\dot{v}}_n$ and those of the variables $\hat{H}$, $\hat{\alpha}$, and $\hat{\gamma}$. Based upon the results of this comparison, the computer can be programed to automatically "make the decision" to change from integration of the constrained equations given by Eqs. (3-31), (3-34) and (3-35) to integration of the unconstrained equations given by Eqs. (3-40) through (3-42). It should be noted that this scheme would cause no additional integrations to be performed, and little additional

computer time or "memory space" since the variables required to perform the comparison test are already available in the computer program.

CHAPTER 8

CONCLUSIONS

In view of the results obtained for the orbital problems considered in Chapters 4 through 7, the general conclusions regarding the constrained equations developed in this thesis are as follows:

1. From the standpoint of numerical integration, the equations resulting from use of the angular momentum vector, referred to a rotating coordinate system, and two components of the eccentricity vector, referred to an inertial coordinate system, provide an efficient set of variables for the treatment of orbital problems in which the perturbing forces are small. For the problems considered, the large step size constrained solutions are on the order of 10^2 more accurate than solutions obtained for the same step size with the standard equations of motion referred to a rotating coordinate system. If the large step size solutions are compared treating path angle as the independent variable, the accuracy of the constrained solutions, in some cases, is increased by a factor of 10^3 to 10^4 over that of the solutions obtained with the standard equations of motion.

2. From the standpoint of possible singularities, the constrained equations provide a significant improvement over those resulting from the use of the standard elliptical orbital elements. Since the only significant singularity occurring in the constrained equations is for the case when angular momentum approaches zero, the constrained equations can be used without adjustment to consider the full range of circular, elliptic, parabolic, and hyperbolic trajectories, including transitions from one to another.

3. From the standpoint of computer programing, the constrained equations are only slightly more complex than the standard equations of motion referred to a rotating coordinate system. This slight additional complexity is due to the necessity of transforming the components of the perturbing forces from the rotating coordinate system to components in the inertial coordinate system for the purpose of integrating the time rate of change of eccentricity. Although the constrained equations and the equations of motion referred to a rotating coordinate system are both more complex than equations of motion referred to a non-rotating cartesian system, the additional complexity appears warranted in view of the advantages accrued from better computer scaling of the resulting variables.

4. From the standpoint of computer time, the constrained equations compare favorably with the standard equations of motion referred to the rotating reference frame. The definition of computer time is open to some interpretation. If a trajectory with one set of initial conditions is to be computed for only a few orbits, then computer time is most accurately evaluated on the basis of the sum of both the program compilation time and the actual execution time since on high speed computers the compilation time may be the longer of the two. On this basis, the constrained equations required between two to ten percent more computer time than that required by the standard equations of motion. If a trajectory is to be computed for a large number of different initial conditions or for a large number of orbits, then the execution time becomes the predominant factor. On this basis of comparison, the constrained equations required between 20 to 30 per cent more computer time than did the standard equations of motion. One additional factor should be taken into consideration. The above estimates of time are based upon

constrained and unconstrained solutions obtained for the same integration step size. Since the constrained equations (particularly when solutions are desired as a function of path angle rather than time) can be obtained with larger integration steps than the unconstrained equations for comparable accuracy, the constrained equations will require less computer time than the unconstrained equations if accuracy is used as the governing criterion. Also, if the accuracy of the solution for path angle as a function of time is not critical, an integration scheme of lower order can be used for the constrained equations which again will result in a reduction of computer time.

5. The most serious disadvantage of the constrained equations is that they become very inefficient for problems dealing with terminal re-entry due to the large time rates of change of the variables during the portion of the trajectory corresponding to peak deceleration. In addition, for the idealized case of non-lifting re-entry through a non-rotating atmosphere, the possibility of a singularity arises due to the angular momentum approaching zero. However, as discussed in Chapter 7, the difficulty of the large time rates of change can be overcome by including a relatively simple comparison test in the computer program which will automatically switch the integration to the unconstrained equations when the time rates of change of the constrained variables become large. It should be noted that this scheme will also remove the second problem of the singularity due to angular momentum becoming zero, since the change-over in equations would take place well before the singularity could arise.

APPENDIX A

COMPUTER SOLUTIONS COMPARED TO EXACT SOLUTIONS FOR NON-PERTURBED KEPLERIAN TRAJECTORIES

The tables contained in this appendix contain computer solutions for the non-perturbed trajectories referred to in Chapters 4 and 6 and in Appendices B and C. In addition, these tables also contain the corresponding exact solutions for the variables $\hat{r}$, $\hat{v}_r$, $\hat{v}_n$, and $\hat{t}$ as a function of path angle u.

TABLE A-1

0.2 Step Size Constrained Solutions Compared to Exact Solutions for Non-Perturbed 0.5 Eccentricity Case

	u	$\hat{t}$	$\hat{r}$	$\hat{v}_r$	$\hat{v}_n$
e*	.51751281	.79999978	1.5684621	.16490672	.95635081
c**	"	.80	1.5684621	.16490672	.95635080
e	1.7848429	3.9999997	2.5173639	.32572645	.59586141
c	"	4.0	2.5173639	.32572644	.59586140
e	2.4281613	7.9999978	3.6177146	.21814404	.41462640
c	"	8.0	3.6177146	.21814403	.41462640
e	3.0581258	15.199999	4.4843880	.027789991	.33449380
c	"	15.20	4.4843880	.027789990	.33449380
e	3.2965824	18.400001	4.4466983	-.051456650	.33732893
c	"	18.40	4.4466983	-.051456654	.33732893
e	3.6254938	22.400001	4.0365507	-.15507865	.37160440
c	"	22.40	4.0365500	-.15507864	.37160446
e	4.0816313	26.400001	3.1909390	-.26919363	.47008106
c	"	26.40	3.1909390	-.26919362	.47008106
e	5.0367402	30.400000	1.9407476	-.31595257	.77289803
c	"	30.40	1.9407477	-.31595256	.77289800
e	5.4003463	31.200000	1.7078055	-.25751488	.87832015
c	"	31.20	1.7078056	-.25751487	.87832013
e	5.8595285	31.999999	1.5455463	-.13703224	.97053061
c	"	32.0	1.5455463	-.13703223	.97053060

*e corresponds to exact solution
**c corresponds to constrained solution

TABLE A-2

0.2 Step Size Unconstrained Solutions Compared to Exact Solutions for Non-Perturbed 0.5 Eccentricity Case

	u	$\hat{t}$	$\hat{r}$	$\hat{v}_r$	$\hat{v}_n$
e*	.51751201	.79999853	1.5684618	.16490649	.95635099
uc**	"	.80	1.5684614	.16490595	.95635107
e	1.7848441	4.0000044	2.5173656	.32572637	.59586101
uc	"	4.0	2.5173610	.32572632	.59586182
e	2.4281638	8.0000201	3.6177193	.21814341	.41462586
uc	"	8.0	3.6177109	.21814371	.41462664
e	3.0581295	15.200048	4.4843898	.027788762	.33449367
uc	"	15.20	4.4843813	.027789341	.33449422
e	3.2965868	18.400058	4.4466948	-.051458100	.33732920
uc	"	18.40	4.4466885	-.051457459	.33732960
e	3.6254996	22.400064	4.0365405	-.15508036	.37160534
uc	"	22.40	4.0365375	-.15507971	.37160553
e	4.0816408	26.400066	3.1909218	-.26919550	.47008360
uc	"	26.40	3.1909215	-.26919492	.47008356
e	5.0367655	30.400064	1.9407277	-.31594988	.77290595
uc	"	30.40	1.9407286	-.31594960	.77290545
e	5.4003785	31.200062	1.7077893	-.25750806	.87832849
uc	"	31.20	1.7077905	-.25750791	.87832779
e	5.8595668	32.000060	1.5455379	-.13702060	.97053588
uc	"	32.0	1.5455396	-.13702083	.97053508

*e corresponds to exact solution
**uc corresponds to unconstrained solution

TABLE A-3

0.8 Step Size Constrained Solutions Compared to Exact Solutions for Non-Perturbed 0.5 Eccentricity Case

	u	$\hat{t}$	$\hat{r}$	$\hat{v}_r$	$\hat{v}_n$
e*	.51749500	.79997058	1.5684573	.16490156	.95635373
c**	"	.80	1.5684573	.16490155	.95635373
e	1.7848044	3.9998370	2.5173110	.32572918	.59587393
c	"	4.0	2.5173110	.32572917	.59587393
e	2.4281434	7.9998419	3.6176803	.21814856	.41463033
c	"	8.0	3.6176804	.21814855	.41463033
e	3.0581142	15.199843	4.4843836	.027793844	.33449413
c	"	15.20	4.4843836	.027793842	.33449413
e	3.2965706	18.399845	4.4467062	-.051452765	.33732833
c	"	18.40	4.4467062	-.051452764	.33732833
e	3.6254794	22.399845	4.0365746	-.15507440	.37160220
c	"	22.40	4.0365746	-.15507439	.37160220
e	4.0816085	26.399847	3.1909806	-.26918915	.47007493
c	"	26.40	3.1909806	-.26918914	.47007493
e	5.0366671	30.399816	1.9408057	-.31596033	.77287489
c	"	30.40	1.9408058	-.31596032	.77287486
e	5.4002276	31.199769	1.7078649	-.25754000	.87828961
c	"	31.20	1.7078649	-.25753999	.87828960
e	5.8593379	31.999696	1.5455879	-.13709015	.97050449
c	"	32.0	1.5455879	-.13709014	.97050446

*e corresponds to exact solution
**c corresponds to constrained solution

TABLE A-4

0.8 Step Size Unconstrained Solutions Compared to Exact Solutions for Non-Perturbed 0.5 Eccentricity Case

	u	$\hat{t}$	$\hat{r}$	$\hat{v}_r$	$\hat{v}_n$
e*	.51724027	.79955281	1.5683884	.16482777	.95639574
uc**	"	.80	1.5683804	.16467038	.95638120
e	1.7850234	4.0007625	2.5176124	.32571367	.59580259
uc	"	4.0	2.5164803	.32561957	.59601337
e	2.4287382	8.0050334	3.6188126	.21799861	.41450060
uc	"	8.0	3.6163979	.21801586	.41473810
e	3.0592049	15.214467	4.4847876	.027431527	.33446400
uc	"	15.20	4.4817654	.027548149	.33465774
e	3.2979628	18.418193	4.4457573	-.051911220	.33740033
uc	"	18.40	4.4431956	-.051767130	.33756279
e	3.6274958	22.421731	4.0331745	-.15566905	.37191547
uc	"	22.40	4.0315931	-.15550069	.37202606
e	4.0851133	26.423591	3.1845808	-.26987651	.47101961
uc	"	26.40	3.1840679	-.26970447	.47105103
e	5.0462231	30.423720	1.9332655	-.31493099	.77588929
uc	"	30.40	1.9333503	-.31483453	.77577673
e	5.4125281	31.223602	1.7017581	-.25491752	.88144137
uc	"	31.20	1.7019063	-.25485491	.88128005
e	5.8742022	32.023319	1.5424028	-.13255884	.97250860
uc	"	32.0	1.5426920	-.13258981	.97230197

*e corresponds to exact solution
**uc corresponds to unconstrained solution

TABLE A-5

0.2 Step Size Constrained Solutions Compared to Exact Solutions for Non-Perturbed 0.05 Eccentricity Case

	u	$\hat{t}$	$\hat{r}$	$\hat{v}_r$	$\hat{v}_n$
e*	.75518183	.80000005	1.0637709	.032639099	.98705463
c**	"	.80	1.0637710	.032639099	.98705457
e	2.7896446	3.2000000	1.1567942	.016415576	.90768089
c	"	3.20	1.1567943	.016415577	.90768085
e	4.7194316	5.6000001	1.1021119	-.047617867	.95271632
c	"	5.60	1.1021119	-.047617866	.95271628
e	6.1870718	7.2000004	1.0502308	-.0045697902	.99978023
c	"	7.20	1.0502308	-.0045697903	.99978019
e	8.3512211	9.6000000	1.1294371	.041852509	.92966664
c	"	9.60	1.1294371	.041852509	.92966666
e	10.915744	12.800001	1.1069136	-.047467394	.94858352
c	"	12.80	1.1069136	-.047467393	.94858352
e	12.374228	14.400001	1.0509209	-.0090934385	.99912372
c	"	14.40	1.0509209	-.0090934381	.99912371
e	14.551008	16.799998	1.1251221	.043599197	.93323204
c	"	16.80	1.1251221	.043599190	.93323200
e	17.112804	19.999999	1.1116823	-.046964804	.94451445
c	"	20.0	1.1116822	-.046964807	.99451452
e	18.561553	21.600001	1.0520634	-.013525635	.99803871
c	"	21.60	1.0520633	-.013525628	.99803876

*e corresponds to exact solution
**c corresponds to constrained solution

TABLE A-6

0.2 Step Size Unconstrained Solutions Compared to Exact Solutions for Non-Perturbed 0.05 Eccentricity Case

	u	t	$\hat{r}$	$\hat{v}_r$	$\hat{v}_n$
e*	.77418125	.79999942	1.0637708	.032639079	.98705473
uc**	"	.80	1.0637706	.032638767	.98705490
e	2.7896470	3.2000032	1.1567944	.016415469	.90768074
uc	"	3.20	1.1567940	.016416564	.90768118
e	4.7194315	5.6000000	1.1021119	-.047617867	.95271632
uc	"	5.60	1.1021142	-.047617621	.95271447
e	6.1870655	7.1999938	1.0502308	-.0045700889	.99978023
uc	"	7.20	1.0502319	-.0045723600	.99977939
e	8.3512210	9.5999999	1.1294371	.041852511	.92966664
uc	"	9.60	1.1294340	.041853788	.92966945
e	10.915741	12.799997	1.1069137	-.047467382	.94858343
uc	"	12.80	1.1069193	-.047466451	.94857903
e	12.374211	14.399982	1.0509211	-.0090942330	.99912353
uc	"	14.40	1.0509240	-.0090985040	.99912141
e	14.551002	16.799991	1.1251219	.043599312	.93323221
uc	"	16.80	1.1241170	.043600853	.93323690
e	17.112793	19.999986	1.1116828	-.046964718	.94451402
uc	"	20.0	1.1116918	-.046962699	.94450724
e	18.561518	21.599964	1.0520638	-.013527233	.99803833
uc	"	21.60	1.0520691	-.013533336	.99803427

*e corresponds to exact solution
**uc corresponds to unconstrained solution

TABLE A-7

0.8 Step Size Constrained Solutions Compared to Exact Solutions for Non-Perturbed 0.05 Eccentricity Case

	u	$\hat{t}$	$\hat{r}$	$\hat{v}_r$	$\hat{v}_n$
e*	.75518639	.80000498	1.0637710	.032639257	.98705454
c**	"	.80	1.0637711	.032639257	.98705447
e	2.7896418	3.1999965	1.1567942	.016415701	.90768089
c	"	3.20	1.1567943	.016415702	.90768085
e	4.7194154	5.5999815	1.1021128	-.047517872	.95271554
c	"	5.60	1.1021128	-.047517872	.95271552
e	6.1870550	7.1999828	1.0502308	-.0045705866	.99978023
c	"	7.20	1.0502308	-.0045705866	.99978019
e	8.3512089	9.5999851	1.1294365	.041852786	.92966713
c	"	9.60	1.1294365	.041852786	.92966714
e	10.915714	12.799966	1.1069151	-.047467280	.94858223
c	"	12.80	1.1069153	-.047467279	.94858214
e	12.374195	14.399966	1.0509212	-.0090949805	.99912343
c	"	14.40	1.0509212	-.0090949953	.99912342
e	14.550983	16.799968	1.1251209	.043599675	.93323304
c	"	16.80	1.1251209	.043599668	.93323304
e	17.112760	19.999947	1.1116846	-.046964458	.94451249
c	"	20.0	1.1116846	-.046964461	.94451247
e	18.561502	21.599947	1.0520641	-.013527963	.99803804
c	"	21.60	1.0520641	-.013527945	.99803800

*e corresponds to exact solution
**c corresponds to constrained solution

TABLE A-8

0.8 Step Size Unconstrained Solutions Compared to Exact Solutions for Non-Perturbed 0.05 Eccentricity Case

	u	$\hat{t}$	$\hat{r}$	$\hat{v}_r$	$\hat{v}_n$
e*	.75498007	.79978260	1.0637637	.032632102	.98706131
uc**	"	.80	1.0637491	.032525053	.98707390
e	2.7900686	3.2005405	1.1568031	.016396622	.90767391
uc	"	3.20	1.1565321	.016583563	.90788747
e	4.7199685	5.6006213	1.1020823	-.047617680	.95274191
uc	"	5.60	1.1024946	-.047405525	.95238351
e	6.1862689	7.1991571	1.0502346	-.0046078456	.99977662
uc	"	7.20	1.0506456	-.0050385980	.99940068
e	8.3512237	9.6000031	1.1294373	.041852450	.92966648
uc	"	9.60	1.1284946	.041787822	.93045244
e	10.917207	12.801708	1.1068325	-.047472899	.94865302
uc	"	12.80	1.1077761	-.046875354	.94785908
e	12.372797	14.398495	1.0509346	-.0091603180	.99911069
uc	"	14.40	1.0518427	-.0099419920	.99827796
e	14.550753	16.799691	1.1251088	.043604078	.93324307
uc	"	16.80	1.1235563	.043359169	.93455679
e	17.115339	20.002982	1.1115421	-.046984594	.94463358
uc	"	20.0	1.1129403	-.045930126	.94347690
e	18.559688	21.598035	1.0520900	-.013610763	.99801347
uc	"	21.60	1.0535691	-.014653044	.99665639

*e corresponds to exact solution
**uc corresponds to unconstrained solution

TABLE A-9

0.2 Step Size Constrained Solutions Compared to Exact Solutions for Non-Perturbed 1.0 Eccentricity Case

	u	$\hat{t}$	$\hat{r}$	$\hat{v}_r$	$\hat{v}_n$
e*	.91979724	.79999099	1.2911730	.55241580	1.1152649
c**	"	.80	1.2911730	.55241578	1.1152649
e	1.4203076	1.5999859	1.8032536	.68659578	.79855654
c	"	1.60	1.8032538	.68659576	.79855645
e	1.6913719	2.3999848	2.3571233	.68940247	.61091416
c	"	2.40	2.3571233	.68940244	.61091416
e	1.8597083	3.1999851	2.8997728	.66566279	.49659063
c	"	3.20	2.8997728	.66566277	.49659062
e	1.9756900	3.9999851	3.4213362	.63829464	.42088819
c	"	4.0	3.4213362	.63829462	.42088819
e	2.1819146	6.3999860	4.8651354	.56875477	.29598354
c	"	6.40	4.8651354	.56875475	.29598354
e	2.2966772	8.7999885	6.1676564	.51938540	.23347604
c	"	8.80	6.1676564	.51938539	.23347604
e	2.3725598	11.199992	7.3684405	.48294485	.19542805
c	"	11.20	7.3684407	.48294484	.19542805
e	2.4430322	14.400000	8.8527916	.44660832	.16266056
c	"	14.40	8.8527919	.44660831	.16266055

*e corresponds to exact solution
**c corresponds to constrained solution

TABLE A-10

0.2 Step Size Unconstrained Solutions Compared to Exact Solutions for Non-Perturbed 1.0 Eccentricity Case

	u	$\hat{t}$	$\hat{r}$	$\hat{v}_r$	$\hat{v}_n$
e*	.91978586	.79997777	1.2911657	.55241101	1.1152712
uc**	"	.80	1.2911375	.55238561	1.1152771
e	1.4203212	1.6000165	1.8032748	.68659719	.79854717
uc	"	1.60	1.8032004	.68657537	.79856716
e	1.6913976	2.4000839	2.3571916	.68940033	.61089646
uc	"	2.40	2.3570549	.68938218	.61092214
e	1.8597411	3.2001764	2.8999002	.66565631	.49656881
uc	"	3.20	2.8996872	.66564094	.49659736
e	1.9757278	4.0002920	3.4215326	.63828430	.42086403
uc	"	4.0	3.4212328	.63827104	.42089416
e	2.1819619	6.4007614	4.8655772	.56873592	.29595666
uc	"	6.40	4.8649689	.56872676	.29598897
e	2.2967308	8.8014043	6.1683921	.51936070	.23344819
uc	"	8.80	6.1674175	.51935400	.23348139
e	2.3726182	11.202194	7.3695037	.48291570	.19539986
uc	"	11.20	7.3681207	.48291068	.19543344
e	2.4430959	14.403461	8.8543377	.44657445	.16263215
uc	"	14.40	8.8523530	.44657108	.16266607

*e corresponds to exact solution
**uc corresponds to unconstrained solution

TABLE A-11

0.8 Step Size Constrained Solutions Compared to Exact Solutions for Non-Perturbed 1.0 Eccentricity Case

	u	$\hat{t}$	$\hat{r}$	$\hat{v}_r$	$\hat{v}_n$
e*	.91844207	.79842305	1.2903074	.55184501	1.1160131
c**	"	.80	1.2903074	.55184499	1.1160131
e	1.4190472	1.5971427	1.8013018	.68646401	.79942184
c	"	1.60	1.8013019	.68646399	.79942180
e	1.6906019	2.3970164	2.3550769	.68946659	.61144500
c	"	2.40	2.3550769	.68946656	.61144500
e	1.8591968	3.1970001	2.8977856	.66576391	.49693117
c	"	3.20	2.8977856	.66576389	.49693118
e	1.9753223	3.9969977	3.4194292	.63839518	.42112292
c	"	4.0	3.4194293	.63839516	.42112291
e	2.1817326	6.3969956	4.8634340	.56882728	.29608708
c	"	6.40	4.8634341	.56882726	.29608708
e	2.2263108	7.1969959	5.3110292	.55051001	.27113389
c	"	7.20	5.3110294	.55050999	.27113388
e	2.3724804	11.196999	7.3669954	.48298447	.19546639
c	"	11.20	7.3669957	.48298445	.19546638
e	2.4109524	12.796997	8.1237143	.46343513	.17725882
c	"	12.80	8.1237146	.46343511	.17725881
e	2.4429771	14.396995	8.8514501	.44663763	.16268521
c	"	14.40	8.8514505	.44663761	.16268520

*e corresponds to exact solution
**c corresponds to constrained solution

TABLE A-12

0.8 Step Size Unconstrained Solutions Compared to Exact Solutions for Non-Perturbed 1.0 Eccentricity Case

	u	$\hat{t}$	$\hat{r}$	$\hat{v}_r$	$\hat{v}_n$
e*	.91229972	.79134291	1.2864094	.54924520	1.1193948
uc**	"	.80	1.2866718	.54453101	1.1144074
e	1.4156214	1.5894463	1.7960199	.68610035	.80177285
uc	"	1.60	1.7917047	.67862779	.80029900
e	1.6894227	2.3924806	2.3519492	.68956398	.61225812
uc	"	2.40	2.3392716	.68131020	.61303423
e	1.8597889	3.2004557	2.9000859	.66564685	.49653701
uc	"	3.20	2.8753272	.65717566	.49874924
e	1.9773541	4.0135463	3.4299892	.63783853	.41982639
uc	"	4.0	3.3899280	.62935145	.42303727
e	2.1869384	6.4833673	4.9124752	.56674581	.29313125
uc	"	6.40	4.8106703	.55851499	.29810029
e	2.2323420	7.3165987	5.3767177	.54794695	.26782139
uc	"	7.20	5.2498618	.53981960	.27316182
e	2.3817414	11.554186	7.5386777	.47834279	.19101493
uc	"	11.20	7.2596899	.47067268	.19753753
e	2.4212396	13.281436	8.3469154	.45809031	.17251882
uc	"	12.80	7.9962620	.45057018	.17934144
e	2.4541923	15.026494	9.1307070	.44064587	.15770958
uc	"	14.40	8.7029991	.43325983	.16477781

*e corresponds to exact solution
**uc corresponds to unconstrained solution

TABLE A-13

0.125 Step Size Constrained Solutions Compared to Exact Solutions for Non-Perturbed 0.05 Eccentricity Case - 50th Orbit

	u	$\hat{t}$	$\hat{r}$	$\hat{v}_r$	$\hat{v}_n$
e*	5.5783606	356.999930	1.0620504	-.030852396	.98865364
c**	"	357.0	1.0620505	-.030852392	.98865357
e	.24185419	357.999928	1.0514572	.011404917	.99861411
c	"	358.0	1.0514572	.011404917	.99861406
e	1.1700656	358.999928	1.0814075	.043846485	.97095683
c	"	359.0	1.0814076	.043846481	.97095673
e	2.0310286	359.999928	1.1275402	.042664255	.93123065
c	"	360.0	1.1275402	.042664250	.93123065
e	2.8321273	360.999928	1.1576320	.014502354	.90702399
c	"	361.0	1.1576319	.014502349	.90702397
e	3.6140774	361.999928	1.1538727	-.021671438	.90997906
c	"	362.0	1.1538727	-.021671440	.90997904
e	4.4248629	362.999928	1.1183572	-.045664208	.93887713
c	"	363.0	1.1183572	-.045664205	.93887711
e	5.3008964	363.999928	1.0727254	-.039608103	.97881526
c	"	364.0	1.0727254	-.039608099	.97881524
e	6.2386604	364.999928	1.0500496	-.0021195332	.99995276
c	"	365.0	1.0500495	-.0021195304	.99995279
e	.89667984	365.999927	1.0691319	.037202798	.98210520
c	"	366.0	1.0691319	.037202795	.98210511

*e corresponds to exact solution
**c corresponds to constrained solution

TABLE A-14

0.125 Step Size Unconstrained Solutions Compared to Exact Solutions for Non-Perturbed 0.05 Eccentricity Case - 50th Orbit

	u	t	$\hat{r}$	$\hat{v}_r$	$\hat{v}_n$
e*	5.5935355	357.016224	1.0615523	-.030298431	.98911754
uc**	"	357.0	1.0614991	-.030309787	.98913707
e	.25740405	358.016304	1.0516498	.012122428	.99843122
uc	"	358.0	1.0515836	.012108088	.99846376
e	1.1848558	359.016412	1.0821326	.044116419	.97030622
uc	"	359.0	1.0820521	.044110688	.97034888
e	2.0447345	360.016534	1.1282462	.042370373	.93064793
uc	"	360.0	1.1281605	.042376959	.93069019
e	2.8452249	361.016648	1.1578695	.013907059	.90683794
uc	"	361.0	1.1577912	.013921091	.90687146
e	3.6273402	362.016740	1.1535037	-.022231884	.91027016
uc	"	362.0	1.1534399	-.022218889	.91029255
e	4.4390456	363.016810	1.1175847	-.045851130	.93952610
uc	"	363.0	1.1175323	-.045847217	.93954114
e	5.3163673	364.016872	1.0720577	-.039194417	.97942489
uc	"	364.0	1.0720059	-.039202958	.97944197
e	6.2548697	365.016949	1.0500200	-.0013481820	.99998095
uc	"	365.0	1.0499570	-.0013632624	1.0000099
e	.91240031	366.017051	1.0697730	.037665459	.98151663
uc	"	366.0	1.0696945	.037656067	.98155808

*e corresponds to exact solution
**uc corresponds to unconstrained solution

APPENDIX B

PROOF OF CORRESPONDENCE BETWEEN THE CONSTRAINED VARIABLES $\hat{r}$, $\hat{v}_r$, $\hat{v}_n$ AND u FOR 0.5 ECCENTRICITY ORBIT WITH OBLATE EARTH PERTURBING FORCES

In the study of oblate earth perturbations presented in Chapter 6, two assemptions were made concerning the computer solutions. First, the differences between the large 0.8 step size constrained solutions and the 0.2 step size constrained solution standard, as a function of time, were considered to result from the fact that the computer solutions for path angle u were slightly different at corresponding values of computer output time. Second, a technique developed in Chapter 4 and based on linear assumptions was used to correct for this difference in u so that the computer solutions for $\hat{r}$, $\hat{v}_r$, and $\hat{v}_n$ arising from two different integration step sizes could be compared at the same value of u.

Sterne[24] presents an analytical technique which provides approximate closed form solutions for the effects of an oblate earth on the orbital elements defined below.

a = semi-major axis of ellipse

E = eccentricity of ellipse

I = inclination angle of orbit plane with respect to equatorial plane

Ω = nodal angle to intersection of orbit plane with equatorial plane (longitude of ascending node)

ω = argument of perifocus

The approximate closed-form solutions of these variables provide a method to verify that the differences between the 0.8 step size

constrained solutions and the 0.2 step size constrained solution standard, as a function of time, are primarily the result of small differences in u, and also that the linear technique used for correction is valid.

The actual development of Sterne's equations is not presented here as it is long and tedious. The general method, however, will be briefly outlined for the case of the variable Ω. In the standard variation of orbital elements approach for the case of an oblate earth, the time rate of change of the variable Ω can be expressed as a function of the other orbital elements and the perturbed true anomaly σ', where the relationship between the path angle u and the perturbed anomaly is given by $u = \sigma' + \omega$. Therefore, we have

$$\frac{d\Omega}{d\hat{t}} = f(\hat{a},\ E,\ I,\ \omega,\ \sigma') \tag{B-1}$$

In addition, we have the standard Keplerian relationship between time and the undisturbed true anomaly given by

$$\hat{a}_o^{-\frac{3}{2}} d\hat{t} = (1-E_o^2)^{\frac{3}{2}} (1 + E_o \cos \sigma)^{-2} d\sigma \tag{B-2}$$

where the subscript o refers to initial values of the undisturbed pure Keplerian elements and σ refers to the undisturbed true anomaly. If we use Eq. (B-2) to change the variable of integration from $\hat{t}$ to σ in Eq. (B-1) we have

$$d\Omega = f(\hat{a},\ E,\ I,\ \omega,\ \sigma')\hat{a}_o^{\frac{3}{2}} (1 - E_o^2)^{\frac{3}{2}}(1 + E_o \cos \sigma')^{-2} d\sigma \tag{B-3}$$

If we now assume the disturbed elements within the function f to be essentially constant and assume that $\sigma' \simeq \sigma$ we can integrate the above expression to obtain

$$\Omega = C_\Omega + F(\hat{a}_o, E_o, I_o, \omega_o, \sigma) \tag{B-4}$$

which yields the perturbed element Ω as a function of the undisturbed true anomaly. The constant C_Ω is adjusted to provide the correct initial value for Ω_o and σ is the true anomaly in pure elliptical motion in which the elements and mean motion retain their initial osculating values $\hat{a}_o$, E_o, I_o, Ω_o, and ω_o. If the above procedure is applied to each of the orbital elements, the equations given by Sterne and presented here in their nondimensional form become

$$\begin{aligned}
\hat{a} = C_a + \frac{6(J_2/3)}{\hat{a}_o(1 - E_o^2)^3} \Big\{ & E_o(1 + \tfrac{1}{4} E_o^2)(1 - \tfrac{3}{2} \sin^2 I_o)\cos \sigma \\
& + \tfrac{3}{4} E_o(1 + \tfrac{1}{4} E_o^2)\sin^2 I_o \cos (2\omega_o + \sigma) \\
& + \tfrac{1}{16} E_o^3 \sin^2 I_o \cos (2\omega_o - \sigma) \\
& + \tfrac{1}{2} E_o^2(1 - \tfrac{3}{2} \sin^2 I_o)\cos 2\sigma + (\tfrac{1}{2} + \tfrac{3}{4} E_o^2)\sin^2 I_o \cos(2\omega_o + 2\sigma) \\
& + \tfrac{1}{12} E_o^3(1 - \tfrac{3}{2} \sin^2 I_o)\cos 3\sigma \\
& + \tfrac{3}{4} E_o(1 + \tfrac{1}{4} E_o^2)\sin^2 I_o \cos (2\omega_o + 3\sigma) \\
& + \tfrac{3}{8} E_o^2 \sin^2 I_o \cos (2\omega_o + 4\sigma) \\
& + \tfrac{1}{16} E_o^3 \sin^2 I_o \cos (2\omega_o + 5\sigma) \Big\}
\end{aligned} \tag{B-5}$$

$$E = C_E + \frac{3(J_2/3)}{\hat{a}_o^2(1 - E_o^2)^2}\left\{(1 + \tfrac{1}{4}E_o^2)(1 - \tfrac{3}{2}\sin^2 I_o)\cos\sigma\right.$$

$$+ \tfrac{1}{4}(1 + \tfrac{11}{4}E_o^2)\sin^2 I_o \cos(2\omega_o + \sigma) \qquad \text{(B-6)}$$

$$+ \tfrac{1}{16}E_o^2 \sin^2 I_o \cos(2\omega_o - \sigma) + \tfrac{1}{2}E_o(1 - \tfrac{3}{2}\sin^2 I_o)\cos 2\sigma$$

$$+ \tfrac{5}{4}E_o \sin^2 I_o \cos(2\omega_o + 2\sigma) + \tfrac{1}{12}E_o^2(1 - \tfrac{3}{2}\sin^2 I_o)\cos 3\sigma$$

$$+ \tfrac{1}{12}(7 + \tfrac{17}{4}E_o^2)\sin^2 I_o \cos(2\omega_o + 3\sigma)$$

$$+ \tfrac{3}{8}E_o \sin^2 I_o \cos(2\omega_o + 4\sigma)$$

$$\left. + \tfrac{1}{16}E_o^2 \sin^2 I_o \cos(2\omega_o + 5\sigma)\right\}$$

$$I = C_I + \frac{3(J_2/3)\sin 2I_o}{4\hat{a}_o^2(1 - E_o^2)^2}\left[E_o \cos(2\omega_o + \sigma) + \cos(2\omega_o + 2\sigma)\right.$$

$$\left. + \tfrac{1}{3}E_o \cos(2\omega_o + 3\sigma)\right] \qquad \text{(B-7)}$$

$$\Omega = C_\Omega - \frac{3(J_2/3)\cos I_o}{2\hat{a}_o^2(1 - E_o^2)^2}\left[2\sigma + 2E_o \sin\sigma - E_o \sin(2\omega_o + \sigma)\right.$$

$$\left. - \sin(2\omega_o + 2\sigma) - \tfrac{1}{3}E_o \sin(2\omega_o + 3\sigma)\right] \qquad \text{(B-8)}$$

$$\omega = C_\omega + \frac{3(J_2/3)}{2\hat{a}_o^2(1 - E_o^2)^2}\left\{(4 - 5\sin^2 I_o)\sigma + \frac{1}{E_o}\left[(2 - 3\sin^2 I_o)\right.\right.$$

$$+ E_o^2\left(\frac{7}{2} - \frac{17}{4}\sin^2 I_o\right) + \frac{1}{4}E_o^2 \sin^2 I_o \cos 2\omega_o\left.\right]\sin\sigma$$

$$- \frac{1}{E_o}\left[E_o^2 + \left(\frac{1}{2} - \frac{7}{4}E_o^2\right)\sin^2 I_o\right]\sin(2\omega_o + \sigma) \qquad \text{(B-9)}$$

$$+ \left(1 - \tfrac{3}{2}\sin^2 I_o\right)\sin 2\sigma - \left(1 - \tfrac{5}{2}\sin^2 I_o\right)\sin(2\omega_o + 2\sigma)$$

$$+ \frac{1}{6}E_o\left(1 - \frac{3}{2}\sin^2 I_o\right)\sin 3\sigma$$

$$- \frac{1}{3E_o}\left[E_o^2 - \left(\frac{7}{2} + \frac{19}{8}E_o^2\right)\sin^2 I_o\right]\sin(2\omega_o + 3\sigma)$$

$$\left. + \frac{3}{4}\sin^2 I_o \sin(2\omega_o + 4\sigma) + \frac{1}{8}E_o \sin^2 I_o \sin(2\omega_o + 5\sigma)\right\}$$

The above equations were programed on the IBM 1620 computer with initial conditions corresponding to those of the 0.5 eccentricity orbit considered in Chapter 6. These initial conditions corresponded to the following:

$\hat{a} = 3.0$

$E = 0.5$

$I = 0.78539816$

$\Omega = 0.0$

$\omega = 0.0$

$\sigma = 0.0$

Since the actual computer solutions given in Chapter 6 were obtained as a function of path angle u rather than in terms of σ' and ω, an

iterative solution was employed such that the sum of the variables σ and ω in Sterne's equations would correspond to the values u resulting from the numerically integrated computer solutions of Chapter 6. In addition, since the numerically integrated computer solutions were in terms of $\hat{r}$, $\hat{v}_r$, and $\hat{v}_n$, the perturbed elements resulting from Sterne's equations were transformed through the Keplerian relations

$$\hat{r} = \frac{\hat{a}(1 - E^2)}{1 + E \cos \sigma} \tag{B-10}$$

$$\hat{v}_r = \frac{E \sin \sigma}{\sqrt{\hat{a}(1 - E^2)}} \tag{B-11}$$

$$\hat{v}_n = \frac{\sqrt{\hat{a}(1 - E^2)}}{\hat{r}} \tag{B-12}$$

to obtain values for $\hat{r}$, $\hat{v}_r$, and $\hat{v}_n$ from the orbital elements. A representative example of the results obtained with Sterne's equations and the 0.2 step size constrained solution for a value of u = 0.51754407 radians is shown below.

0.2 Step Size Constrained Solution

$\hat{r}$	$\hat{v}_r$	$\hat{v}_n$
1.5683685	0.16469202	0.95635289
I	Ω	u
0.78534067	$-0.28955576 \times 10^{-4}$	0.51754407

Sterne's Solution

$\hat{r}$	$\hat{v}_r$	$\hat{v}_n$	u
1.5683868	0.16471229	0.95634170	0.51754407
I	Ω	ω	σ
0.78534076	$-0.28879217 \times 10^{-4}$	$0.46789866 \times 10^{-3}$	0.51707617

From the results on the previous page it can be seen that the variables $\hat{r}$, $\hat{v}_r$, and $\hat{v}_n$ obtained with Sterne's equations are in agreement with the 0.2 step size constrained solutions to four significant digits.

B.1 Use of Sterne's Equations to Verify Correspondence of Constrained Solutions with Path Angle

In order to use Sterne's equations to show that the differences between the 0.8 step size and the 0.2 step size constrained solutions are primarily due to the differences in path angle u at corresponding computer output times, we can make use of the following method. Sterne's equations involve no numerical integration and hence, any differences in the variables $\hat{r}$, $\hat{v}_r$, and $\hat{v}_n$ obtained through the use of Sterne's equations with two slightly different values of u must be caused only by the differences in u. From the computer solutions of Chapter 6 we found that solutions obtained with two different integration step sizes resulted in slightly different values of u at corresponding values of computer output time. For the case of the constrained solutions, this difference in u was proposed to be the cause of the differences in the corresponding solutions for $\hat{r}$, $\hat{v}_r$, and $\hat{v}_n$ at the same computer output times. These differences are plotted in Figs. 6-1 and 6-2 of Chapter 6, and were obtained by subtracting the 0.2 step size constrained solutions for $\hat{r}$, $\hat{v}_r$, $\hat{v}_n$, and u from the 0.8 step size solutions at corresponding computer output times. If these differences in $\hat{r}$, $\hat{v}_r$, and $\hat{v}_n$ are indeed only due to the slight differences in u between the two different step size solutions, then we should be able to compute these same differences through the use of Sterne's equations.

As an example suppose we consider the 0.8 and 0.2 step size constrained solutions at a nondimensional computer output time of $\hat{t} = 32.0$. The 0.2 and 0.8 step size solutions for this value of $\hat{t}$ were as follows:

0.8 Step Size Constrained Solution

u	$\hat{r}$	$\hat{v}_r$	$\hat{v}_n$
5.8904631	1.5393033	-.12785493	.97443284

0.2 Step Size Constrained Solution

u	$\hat{r}$	$\hat{v}_r$	$\hat{v}_n$
5.8906127	1.5392750	-.12780900	.97445173

If the differences in the values of $\hat{r}$, $\hat{v}_r$, and $\hat{v}_n$ in the above computer solutions are only due to the difference in the values of u, then we should be able to obtain similar differences from Sterne's equations by evaluating them at the same two values of u given above. The solutions obtained from Sterne's equations for values of $u = \sigma + \omega$ of 5.8904631 and 5.8906127 radians are as follows:

Sterne's Method, u = 5.8904631

$\hat{r}$	$\hat{v}_r$	$\hat{v}_n$
1.5393131	-.12787113	.97442658

Sterne's Method, u = 5.8906127

$\hat{r}$	$\hat{v}_r$	$\hat{v}_n$
1.5392827	-.12782512	.97444582

The differences in the variables $\hat{r}$, $\hat{v}_r$, and $\hat{v}_n$ obtained from Sterne's method (variables corresponding to larger u subtracted from variables corresponding to smaller u) are as follows:

$$\Delta\hat{r}_{Sm} = + 30.4\text{x}10^{-6}$$

$$\Delta\hat{v}_{r_{Sm}} = - 46.01\text{x}10^{-6}$$

$$\Delta\hat{v}_{n_{Sm}} = -19.24\text{x}10^{-6}$$

where the subscript Sm refers to differences obtained with Sterne's equations. If we perform the same operation on the variables resulting from the constrained computer solutions listed on page 147, we obtain

$$\Delta\hat{r}_{Cs} = + 28.3\text{x}10^{-6}$$

$$\Delta\hat{v}_{r_{Cs}} = - 45.93\text{x}10^{-6}$$

$$\Delta\hat{v}_{n_{Cs}} = - 18.89\text{x}10^{-6}$$

where the subscript Cs denotes differences obtained from computer solutions.

From the above results, it is evident that the differences between the 0.8 and 0.2 step size constrained solutions at corresponding computer output times are the result of differences in u. The above procedure was applied at a number of points over the first orbit of the 0.5 eccentricity trajectory with comparable results to those shown above. These results are tabulated in Table B-1.

An interesting result is obtained if the above procedure is applied to the 0.8 step size unconstrained solutions for this same orbit. As an example, suppose we consider the 0.8 step size unconstrained solutions and the 0.2 step size constrained solutions for a computer output time of $\hat{t} = 4$. The computer solutions for these two cases were as follows:

0.8 Step Size Unconstrained Solution

u	$\hat{r}$	$\hat{v}_r$	$\hat{v}_n$
1.7857610	2.5155191	.32535791	.59611802

0.2 Step Size Constrained Solution

u	$\hat{r}$	$\hat{v}_r$	$\hat{v}_n$
1.7855802	2.5164035	.32546489	.59596583

As before, we can use Sterne's equations to evaluate the differences in the variables $\hat{r}$, $\hat{v}_r$, and $\hat{v}_n$ due to the small differences in u. The solutions obtained from Sterne's equations for values of u of 1.7857610 and 1.7855802 radians are as follows:

Sterne's Method, u = 1.7857610

$\hat{r}$	$\hat{v}_r$	$\hat{v}_n$
2.5168369	.32544263	.59586273

Sterne's Method, u = 1.7855802

$\hat{r}$	$\hat{v}_r$	$\hat{v}_n$
2.5165884	.32545543	.59592156

If we use the solutions from Sterne's method and subtract the solutions resulting from the larger u from those resulting from the smaller u we obtain the following differences:

$$\Delta\hat{r}_{Sm} = -248.5\times10^{-6}$$

$$\Delta\hat{v}_{r_{Sm}} = +12.8\times10^{-6}$$

$$\Delta\hat{v}_{n_{Sm}} = +58.83\times10^{-6}$$

These values represent the differences we should expect due to the small differences in u obtained with the computer solutions. If we now compute the differences in these same variables obtained from the constrained and unconstrained computer solutions listed above and on the preceding page we obtain (with 0.8 solutions subtracted from 0.2 solutions)

$$\Delta\hat{r}_{Cs} = + 884.4\text{x}10^{-6}$$
$$\Delta\hat{v}_{r_{Cs}} = + 106.98\text{x}10^{-6}$$
$$\Delta\hat{v}_{n_{Cs}} = - 152.19\text{x}10^{-6}$$

From the above results it is evident that the differences between the 0.8 step size unconstrained solutions and the 0.2 step size constrained solutions are not due solely to the small differences in u. If we use the results of Sterne's method to correct the 0.8 step size unconstrained solutions for the difference in u between it and the 0.2 step size constrained solutions we obtain the "corrected" values

$$\hat{r}_{.8_{corr}} = \hat{r}_{.8} + \Delta\hat{r}_{Sm} = 2.5152706$$
$$\hat{v}_{r.8_{corr}} = \hat{v}_{r.8} + \Delta\hat{v}_{r_{Sm}} = .32537071$$
$$\hat{v}_{n.8_{corr}} = \hat{v}_{n.8} + \Delta\hat{v}_{n_{Sm}} = .59617685$$

The above values now represent the 0.8 step size unconstrained solutions after correction for the deviation in u between the 0.8 unconstrained and 0.2 constrained solutions (i.e. these "corrected" values represent the values we should expect the 0.8 unconstrained solutions to have at the value of u obtained from the 0.2 constrained solutions or at u = 1.7855802 radians). If we now consider the 0.2 step size constrained solution to be exact, then the differences between the values $\hat{r}$, $\hat{v}_r$, and $\hat{v}_n$ obtained with the 0.2 step size constrained solution and the "corrected" values given above should represent the error in the 0.8 step size unconstrained solutions at the value u = 1.7855802 radians (i.e. u treated as the independent variable). These errors are as follows:

$$\hat{\epsilon}_r = \hat{r}_{.2} - \hat{r}_{.8_{corr}} = 2.5164035 - 2.5152706 = + 1.1329\text{x}10^{-3}$$
$$\hat{\epsilon}_{v_r} = \hat{v}_{r.2} - \hat{v}_{r.8_{corr}} = .32546489 - .32537071 = + .09418\text{x}10^{-3}$$
$$\hat{\epsilon}_{v_n} = \hat{v}_{n_{.2}} - \hat{v}_{n.8_{corr}} = .59596583 - .59617685 = - .21102\text{x}10^{-3}$$

The above results correspond to the differences between the 0.2 step size constrained solutions and the 0.8 step size unconstrained solutions at a value of u = 1.7855802. At this point, let us refer to Table A-4 in Appendix A. This table presents the values of the 0.8 step size unconstrained solutions and exact solutions at corresponding values of u for the case of the same 0.5 eccentricity orbit when no perturbing forces are present. From this table we can find exact and 0.8 step size unconstrained solutions for a value of u = 1.7850234 (i.e. a value of u very close to the value considered above). These values are as follows:

Non-Perturbed 0.5 Eccentricity Solutions for u = 1.7850234

Exact $\quad \hat{r} = 2.5176124 \quad \hat{v}_r = .32571367 \quad \hat{v}_n = .59580259$

$0.8_{uc} \quad \hat{r} = 2.5164803 \quad \hat{v}_r = .32561957 \quad \hat{v}_n = .59601337$

If the above 0.8 unconstrained step size non-perturbed solutions are subtracted from the exact solutions we obtain the following errors:

$$\hat{\epsilon}_r = + 1.1321 \times 10^{-3}$$

$$\hat{\epsilon}_{v_r} = + .09410 \times 10^{-3}$$

$$\hat{\epsilon}_{v_n} = - .21078 \times 10^{-3}$$

The agreement between these non-perturbed errors and those obtained on page 150 for the perturbed case is evident. This procedure was applied to several other points in 0.5 eccentricity orbit with oblate earth perturbations and similar results were obtained.

The results of this section verify that the differences between the 0.8 step size constrained solutions and the 0.2 step size constrained solutions at corresponding computer output times are primarily due to the slight variations in path angle between the two solutions. On the other hand, the differences between the 0.8 step size unconstrained solutions

and the 0.2 step size constrained solutions are not totally due to differences in path angle at corresponding computer output times.

B.2 Use of Sterne's Equations to Verify Linear Correction Technique

In Chapter 6, a simple linear techinque, developed in Chapter 4, was used to correct the computer solutions obtained with two different integration step sizes so that they could be compared at the same value of path angle. This technique was based on linear assumptions. From the previous section of this appendix we found that the more complicated equations of Sterne, which do not involve linear assumptions, can also be used to correct for differences in u. Therefore, if the linear technique is valid we should be able to obtain results comparable to those obtained with Sterne's equations.

Suppose we take as an example the 0.8 step size unconstrained solutions and the 0.2 step size constrained solutions at the computer output time $\hat{t} = 4$ considered in the preceding section of this appendix. The computer solutions for this case were as follows:

0.8 Step Size Unconstrained Solution

u	$\hat{r}$	$\hat{v}_r$	$\hat{v}_n$
1.7857610	2.5155191	.32535791	.59611802

0.2 Step Size Constrained Solution

u	$\hat{r}$	$\hat{v}_r$	$\hat{v}_n$
1.7855802	2.5164035	.32546489	.59596583

If we apply the linear technique as defined in Chapter 4 to obtain the corrections for the differences in u between these two computer solutions we obtain,

$$\Delta u = u_{.2} - u_{.8} = - .0001808$$

$$\Delta\hat{r} \simeq \left(\frac{\hat{v}_r\hat{r}}{\hat{v}_n}\right)_{.2}\Delta u = - 248.2\text{x}10^{-6}$$

$$\Delta\hat{v}_n \simeq \left(-\hat{v}_r\right)_{.2}\Delta u = 58.82\text{x}10^{-6}$$

$$\Delta\hat{v}_r \simeq \left(\hat{v}_n - \frac{1}{\hat{r}\hat{v}_n}\right)_{.2}\Delta u = 12.79\text{x}10^{-6}$$

The above results represent the predicted differences in the variables $\hat{r}$, $\hat{v}_r$, and $\hat{v}_n$ which should be present in the two computer solutions as a result of the differences in u. The differences given by Sterne's equations for this same case on page 149 were as follows:

$$\Delta\hat{r}_{Sm} = - 248.5\text{x}10^{-6}$$

$$\Delta\hat{v}_{n_{Sm}} = + 58.83\text{x}10^{-6}$$

$$\Delta\hat{v}_{r_{Sm}} = + 12.80\text{x}10^{-6}$$

From a comparison of these results it can be seen that the differences given by the linear technique are in very good agreement with those obtained by using Sterne's more complicated equations. This same trend was found to hold over several other points which were checked in the orbit. An additional example for a computer output time of 32.0 and a Δu between the 0.2 step size constrained solution and the 0.8 step size unconstrained solution of $\Delta u = u_{.2} - u_{.8} = - .0147581$ radians is shown below.

Sterne's Method

$$\Delta\hat{r} = 2921.5\text{x}10^{-6}$$

$$\Delta\hat{v}_n = - 1855.32\text{x}10^{-6}$$

$$\Delta\hat{v}_r = - 4550.65\text{x}10^{-6}$$

Linear Technique

$$\Delta\hat{r} = 2979.53 \times 10^{-6}$$

$$\Delta\hat{v}_n = -1886.22 \times 10^{-6}$$

$$\Delta\hat{v}_r = -4541.99 \times 10^{-6}$$

TABLE B-1

Comparison of Differences Between 0.8 and 0.2 Step Size Constrained Solutions and Those Obtained from Sterne's Equations at Corresponding Values of Path Angle

	t	$\Delta\hat{r}x10^6$	$\Delta\hat{v}_r x10^6$	$\Delta\hat{v}_n x10^6$
Cs*	.8	- 4.3	- 5.51	+ 2.59
Sm**		- 4.7	- 5.10	+ 2.86
Cs	1.6	-25.2	- 8.98	+12.33
Sm		-25.2	- 8.71	+12.37
Cs	2.4	-45.2	- 4.93	+17.12
Sm		-44.9	- 4.62	+17.03
Cs	3.2	-53.4	- 0.29	+15.69
Sm		-51.9	+ 0.03	+15.34
Cs	4.0	-53.9	+ 2.43	+12.65
Sm		-51.2	+ 2.64	+12.17
Cs	8.0	-36.9	+ 4.10	+ 4.12
Sm		-30.8	+ 4.11	+ 3.53
Cs	12.8	-17.7	+ 3.444	+ 1.34
Sm		-10.9	+ 3.307	+ 0.87
Cs	20.0	+ 3.3	+ 3.141	- 0.40
Sm		+10.8	+ 2.882	- 0.86
Cs	28.0	+24.7	+ 2.30	- 5.46
Sm		+28.5	+ 2.10	- 5.82
Cs	30.4	+34.5	- 5.51	-14.67
Sm		+37.4	- 5.39	-15.12
Cs	32.0	+28.3	-45.93	-18.89
Sm		+30.4	-46.01	-19.24

*Cs denotes the differences obtained by subtracting the 0.2 step size constrained computer solutions from the 0.8 step size constrained computer solutions

**Sm denotes differences obtained from Sterne's equations for path angles corresponding to constrained computer solutions

APPENDIX C

DEVELOPMENT OF EQUATIONS FOR THE DETERMINATION OF TRUNCATION ERROR OCCURRING OVER AN INTEGRATION STEP

For all of the cases in which the perturbing forces were either small or zero we found the large step size unconstrained solutions for $\hat{r}$, $\hat{v}_r$, $\hat{v}_n$, and u to be in considerable error when compared to the constrained solutions for these same variables. This was not unexpected as the unconstrained equations involve variables whose time rates of change are considerably larger than those of the variables contained in the constrained equations. In view of this, we could expect the errors in the large step size unconstrained solutions to be primarily due to truncation or discretization error. To verify that this is indeed the case, we can make use of unconstrained computer solutions obtained at two different step sizes and a method somewhat similar to Richardson's deferred approach to the limit[26]. The approach to be used here is approximate, but will be sufficient for the purpose of demonstrating that the errors contained in the large step size unconstrained solutions are of the same order as those which would arise from truncation. For a more detailed discussion on the estimation of error propagation in numerical integration the reader is referred to the treatments of this subject given by Sterne[24] and Zani[27].

C.1 Development of Equations

If we assume the only source of error in integrating over one step of width s with the fourth-order Runge-Kutta method to be that of truncation, and if in addition we assume the fifth derivatives of the state

variables to be approximately constant for a step size s and $\frac{s}{2}$, then we can write the expressions[26]

$$y_i(t,s) = y_i(t) + d_i s^5 \tag{C-1}$$

$$y_i(t, \tfrac{s}{2}) = y_i(t) + 2d_i(\tfrac{s}{2})^5 \tag{C-2}$$

In the above expressions $y_i(t)$ is the true value of the solution at time t; $y_i(t,s)$ is the value computed with step size s; $y_i(t, \frac{s}{2})$ is the value computed with step size $\frac{s}{2}$; and the terms involving d and s are the respective truncation errors occurring over the step s. The error term in Eq. (C-2) is doubled since this integration involves two steps. If we subtract Eq. (C-2) from Eq. (C-1) and solve for the term $d_i s^5$ we obtain

$$d_i s^5 = \frac{16}{15}\left[y_i(t,s) - y_i(t, \tfrac{s}{2})\right] \tag{C-3}$$

where the quantity $d_i s^5$ represents the truncation error incurred by the numerical solution obtained with step s over one step of integration. If we now substitute Eq. (C-3) into (C-1) and solve for $y_i(t)$ we obtain

$$y_i(t) = \frac{16y_i(t, \frac{s}{2}) - y_i(t,s)}{15} \tag{C-4}$$

The expression given by Eq. (C-4) is termed Richardson's deferred approach to the limit, or more simply "extrapolation to s = 0" since the term on the right, obtained through numerical solutions with two different step sizes, yields an "extrapolated" value which approximates the true solution $y_i(t)$.

Eqs. (C-3) and (C-4) are useful provided the numerical solutions are exact prior to taking the integration step s (that is to say exact at time = t - s). Therefore, if we think in terms of the unconstrained

computer solutions, Eqs. (C-3) and (C-4) in their present form would be of use only for the first step of integration since prior to this first step the numerical solutions would be exact by virtue of the initial conditions. At some point occurring later in the orbit, the numerical solutions obtained with two different step sizes would no longer be exact prior to taking the next step due to all of the errors accumulated prior to this step. Our problem is due to the way in which we defined the expressions given by Eqs. (C-1) and (C-2). In these equations we have assumed that the only differences existing between the numerical solutions and the exact solution at time t are the truncation errors which occurred over the step from t - s to t. In order to arrive at a set of more general expressions let us assume that we can write expressions of the form

$$y_i(t_2, s) = y_i(t_2) + \epsilon_i(t_1) + d_i s^5 \qquad \text{(C-5)}$$

$$y_i(t_2, \tfrac{s}{2}) = y_i(t_2) + \epsilon_i'(t_1) + 2d_i(\tfrac{s}{2})^5 \qquad \text{(C-6)}$$

where time t_2 is separated from time t_1 by the increment s or $t_2 = t_1 + s$ and the other variables are as follows:

$y_i(t_2, s)$ = numerical solution obtained with step size s at time t_2

$y_i(t_2, \frac{s}{2})$ = numerical solution obtained with step size $\frac{s}{2}$ at time t_2

$y_i(t_2)$ = true solution at time t_2

$d_i s^5$ and $2d_i(\frac{s}{2})^5$ = respective truncation errors incurred by the numerical solutions over the integration step $t_2 - t_1 = s$

$\epsilon_i(t_1)$ = accumulated error which exists at time t_1 in the numerical solution obtained with step size s

$\epsilon'_i(t_1)$ = accumulated error which exists at time t_1 in the numerical solution obtained with step size $\frac{s}{2}$

Next, let us define the accumulated errors $\epsilon_i(t_1)$ and $\epsilon'_i(t_1)$ in terms of the numerical solutions and the exact solution at time t_1 by the relations

$$\epsilon_i(t_1) = y_i(t_1, s) - y_i(t_1) \tag{C-7}$$

$$\epsilon'_i(t_1) = y_i(t_1, \tfrac{s}{2}) - y_i(t_1) \tag{C-8}$$

If we substitute Eq. (C-7) into Eq. (C-5) and Eq. (C-8) into Eq. (C-6) we obtain

$$y_i(t_2, s) = y_i(t_2) + y_i(t_1, s) - y_i(t_1) + d_i s^5 \tag{C-9}$$

$$y_i(t_2, \tfrac{s}{2}) = y_i(t_2) + y_i(t_1, \tfrac{s}{2}) - y_i(t_1) + 2d_i(\tfrac{s}{2})^5 \tag{C-10}$$

Following the same approach as we did for Eqs. (C-1) and (C-2), we subtract Eq. (C-10) from Eq. (C-9) and solve for the quantity $d_i s^5$ obtaining the expression

$$d_i s^5 = \frac{16}{15}\left\{\left[y_i(t_2,s) - y_i(t_1,s)\right] - \left[y_i(t_2, \tfrac{s}{2}) - y_i(t_1, \tfrac{s}{2})\right]\right\} \tag{C-11}$$

Eq. (C-11) is an expression similar in form to Eq. (C-3) in that it represents the predicted error due to truncation incurred by the numerical solution obtained with step size s over the integration step from time t_1 to time t_2. The above expression, however, will be more useful for our purposes since it is good for any two points in the orbit provided $t_2 - t_1 = s$. For simplicity, let us define a quantity ϵ_{P_i} such that

$$\epsilon_{P_i} = d_i s^5 = \frac{16}{15}\left\{\left[y_i(t_2,s) - y_i(t_1,s)\right] - \left[y_i(t_2, \frac{s}{2}) - y_i(t_1, \frac{s}{2})\right]\right\} \quad \text{(C-12)}$$

where ϵ_{P_i} is interpreted as the predicted truncation error incurred by the numerical solution obtained with step size s over the step t_1 to t_2. If we substitute Eq. (C-12) into Eq. (C-9) we obtain the expression

$$\left[y_i(t_2,s) - y_i(t_2)\right] - \left[y_i(t_1,s) - y_i(t_1)\right] = \epsilon_{P_i} \quad \text{(C-13)}$$

At this point, let us interpret the expression on the left of Eq. (C-13). The first term in brackets represents the total error existing in the numerical solution obtained with step size s at time t_2. The second term represents the total error in this same numerical solution at time t_1. Therefore, the difference between these two bracketed quantities must represent the actual error which is incurred by the numerical solution obtained with step size s over the integration step from time t_1 to time t_2. Again for simplicity, let us define a quantity ϵ_{A_i} such that

$$\epsilon_{A_i} = \left[y_i(t_2,s) - y_i(t_2)\right] - \left[y_i(t_1,s) - y_i(t_1)\right] \quad \text{(C-14)}$$

where ϵ_{A_i} is the actual error incurred by the numerical solution obtained with step size s over the step t_1 to t_2.

We now have two expressions for the error incurred by the numerical solution obtained with step size s over the step t_1 to t_2 (where $t_2 - t_1 = s$). The expression given by Eq. (C-12) gives us a predicted error for the numerical solution of step size s as a function of this solution and one obtained with a step size $\frac{s}{2}$. This predicted error was derived under the assumption that it was totally due to truncation. The expression given by Eq. (C-14) is the actual error incurred by the

numerical solution of step size s over the step t_1 to t_2 and is a function of this numerical solution and the exact solution. Therefore, if we have values for the unconstrained state variables ($\hat{r}$, $\hat{v}_r$, $\hat{v}_n$ and u) obtained at the computer output times $\hat{t}_1$ and $\hat{t}_2$ ($\hat{t}_2 - \hat{t}_1 = s$) with two unconstrained solutions (where one solution has a step size of s and the other a step size of $\frac{s}{2}$) and, if in addition, we have the exact solutions for the state variables at $\hat{t}_1$ and $\hat{t}_2$, we can perform the following test. If the quantity ϵ_{P_i} (where i denotes the variable $\hat{r}$, $\hat{v}_r$, $\hat{v}_n$, or u under consideration) computed from Eq. (C-12) is in good agreement with the actual error computed from Eq. (C-14), then we can conclude that the primary error existing in the unconstrained solution obtained with step size s is due to truncation. If the results obtained from both equations are not in good agreement, then the error in the unconstrained solution obtained with step size s is not primarily due to truncation.

C.2 Application of Truncation Error Test

During the computer program check-out of the unconstrained equations for the case of oblate earth perturbing forces, a 0.4 nondimensional step size solution was obtained for the 0.5 eccentricity orbit discussed in Chapter 6. This solution was obtained up to a nondimensional time of $\hat{t} = 20$ which represents slightly more than 1/2 of one orbit. In Chapter 6, we found the 0.8 step size unconstrained solutions for this same orbit to be in considerable disagreement with the 0.2 step size constrained solutions. Therefore, let us apply the truncation error test developed in the previous section to the large 0.8 step size unconstrained solutions.

In order to apply Eq. (C-14) we need exact solutions. For the case of oblate earth perturbing forces such solutions are not available. However, in view of the good agreement obtained between the 0.2 step size

constrained solutions and the exact solutions for this same orbit when no perturbing forces were present (Table A-1 in Appendix A), and the fact that the oblate earth perturbations are quite small for this orbit, we will take the 0.2 constrained solutions obtained for the 0.5 eccentricity orbit with oblate earth perturbations to be exact for the purposes of this example.

For purposes of demonstrating the method in which the computations are performed, let us consider the unconstrained state variable $\hat{r}$ (i.e. $y_i = \hat{r}$) and the solutions for this variable occurring over the integration step from $\hat{t}_1 = 5.6$ to $\hat{t}_2 = 6.4$. The pertinent computer solutions for this calculation are listed under the column $\hat{r}$ in Table C-2.

From Eq. (C-12) the predicted error over the integration step $t_1 = 5.6$ to $t_2 = 6.4$ is given by

$$\hat{\epsilon}_{P_r} = \frac{16}{15}\left\{\left[\hat{r}_{t_2} - \hat{r}_{t_1}\right]_{.8_{uc}} - \left[\hat{r}_{t_2} - \hat{r}_{t_1}\right]_{.4_{uc}}\right\}$$

$$= \frac{16}{15}\left\{\left[3.2286781 - 3.0079371\right] - \left[3.2297408 - 3.0089198\right]\right\}$$

$$= -.0000853$$

From Eq. (C-14) the actual error over this same integration step (taking 0.2 step size constrained solutions to be exact and rearranging bracketed terms) is given by

$$\hat{\epsilon}_{A_r} = \left[\hat{r}_{t_2} - \hat{r}_{t_1}\right]_{.8_{uc}} - \left[\hat{r}_{t_2} - \hat{r}_{t_1}\right]_{.2_c}$$

$$= \left[3.2286781 - 3.0079371\right] - \left[3.2298065 - 3.0089817\right]$$

$$= -.0000838$$

If the same procedure is applied to the other unconstrained variables ($\hat{v}_r$, $\hat{v}_n$, u) for this same integration step, similar results are

obtained. These results are summarized in Table C-1. This same technique was applied at two additional points in the orbit corresponding to integration steps occurring between times $\hat{t}_1 = 11.2$ to $\hat{t}_2 = 12.0$ (see Table C-3 for computer solutions) and times $\hat{t}_1 = 19.2$ to $\hat{t}_2 = 20.0$ (see Table C-4 for computer solutions). These results are also summarized in Table C-1.

From the results contained in Table C-1, it is evident that the primary source of error in the 0.8 step size unconstrained solutions for the 0.5 eccentricity orbit with oblate earth perturbations is due to truncation error.

TABLE C-1

Actual Per Step Error Compared to Predicted Per Step Truncation Error for the 0.8 Step Size Unconstrained Solutions for the 0.5 Eccentricity Orbit Under the Influence of Oblate Earth Perturbations *

	$\hat{r}$	$\hat{v}_r$	$\hat{v}_n$	u
	Integration Step $\hat{t}_1 = 5.6$ to $\hat{t}_2 = 6.4$			
$\hat{\epsilon}_P$	-.0000853	-.00000612	-.00000747	.0000755
$\hat{\epsilon}_A$	-.0000838	-.00000636	-.00000757	.0000752
	Integration Step $\hat{t}_1 = 11.2$ to $\hat{t}_2 = 12.0$			
$\hat{\epsilon}_P$	-.0001445	-.00001253	.00000579	.0000538
$\hat{\epsilon}_A$	-.0001442	-.00001257	.00000580	.0000535
	Integration Step $\hat{t}_1 = 19.2$ to $\hat{t}_2 = 20.0$			
$\hat{\epsilon}_P$	-.0002737	-.000021170	.00003055	.0001077
$\hat{\epsilon}_A$	-.0002732	-.000021178	.00003046	.0001072

* actual error computed assuming 0.2 step size constrained solutions to be equal to true solutions

TABLE C-2

Computer Solutions at Times $\hat{t}_1 = 5.6$ and $\hat{t}_2 = 6.4$
for 0.5 Eccentricity Orbit with
Oblate Earth Perturbations

	$\hat{r}$	$\hat{v}_r$	$\hat{v}_n$	u
		Time $\hat{t}_1 = 5.6$		
unconstrained .8 step size	3.0079371	.28729529	.49854423	2.1017595
unconstrained .4 step size	3.0089198	.28739385	.49842484	2.1014131
constrained .2 step size	3.0089817	.28739891	.49841828	2.1013836
		Time $\hat{t}_2 = 6.4$		
unconstrained .8 step size	3.2286781	.26439428	.46446546	2.2251888
unconstrained .4 step size	3.2297408	.26449858	.46435308	2.2247716
constrained .2 step size	3.2298065	.26450426	.46434708	2.2247377

TABLE C-3

Computer Solutions at Times $t_1 = 11.2$ and $t_2 = 12.0$
for 0.5 Eccentricity Orbit with
Oblate Earth Perturbations

	$\hat{r}$	$\hat{v}_r$	$\hat{v}_n$	u
		Time $t_1 = 11.2$		
unconstrained .8 step size	4.1668756	.12898804	.35990502	2.7449039
unconstrained .4 step size	4.1685708	.12915160	.35979016	2.7441612
constrained .2 step size	4.1686738	.12916176	.35978389	2.7441085
		Time $t_2 = 12.0$		
unconstrained .8 step size	4.2616380	.10798541	.35190345	2.8124225
unconstrained .8 step size	4.2634687	.10816072	.35178316	2.8116293
constrained .2 step size	4.2635804	.10817170	.35177652	2.8115736

TABLE C-4

Computer Solutions at Times $\hat{t}_1 = 19.2$ and $\hat{t}_2 = 20.0$ for 0.5 Eccentricity Orbit with Oblate Earth Perturbations

	$\hat{r}$	$\hat{v}_r$	$\hat{v}_n$	u
		Time $\hat{t}_1 = 19.2$		
unconstrained .8 step size	4.3861366	-.072589120	.34191643	3.3625149
unconstrained .4 step size	4.3896788	-.072278206	.34167049	3.3611260
constrained .2 step size	4.3899005	-.072258202	.34165576	3.3610347
		Time $\hat{t}_2 = 20.0$		
unconstrained .8 step size	4.3199234	-.092992114	.34715625	3.4257949
unconstrained .4 step size	4.3237222	-.092661353	.34688167	3.4243050
constrained .2 step size	4.3239605	-.092640018	.34686512	3.4242075

BIBLIOGRAPHY

1. Baker, R. M., Jr., and M. W. Makemson, An Introduction to Astrodynamics. New York: Academic Press, 1960.

2. Moulton, F. R., An Introduction to Celestial Mechanics, 2nd rev. ed. New York: The Macmillan Company, 1914.

3. Thomson, W. T., Introduction to Space Dynamics. New York: John Wiley and Sons, Inc., 1961.

4. Escobal, P. R., Methods of Orbit Determination. New York: John Wiley and Sons, Inc., 1965.

5. Danby, J. M. A., Fundamentals of Celestial Mechanics. New York: The Macmillan Company, 1962.

6. Brouwer, D., and G. M. Clemence, Methods of Celestial Mechanics. New York: Academic Press, 1960.

7. Goldstein, H., Classical Mechanics. Reading, Massachusetts: Addison-Wesley Publishing Company, 1950.

8. Synge, J. L., and B. A. Griffith, Principles of Mechanics, 3rd ed. New York; McGraw-Hill, Inc., 1959.

9. Greenwood, D. T., Principles of Dynamics. Englewood Cliffs, New Jersey: Prentice-Hall, Inc., 1965.

10. Baker, R. M. L., Jr., Astrodynamics Applications and Advanced Topics. New York: Academic Press, 1967.

11. Battin, R. H., Astronautical Guidance. New York: McGraw-Hill Book Company, 1964.

12. Conte, S. D., "An Evaluation of Special Perturbation Methods and Integration Routines for Space Trajectory Computations", Space Technology Laboratories Report 9850-66, 17 April 1961.

13. Pines, S., M. Payne, and H. Wolf, "Comparison of Special Perturbation Methods in Celestial Mechanics". Aero-Research Laboratory Report No. 60-281, Wright-Patterson Air Force Base, Ohio, August 1960.

14. Krause, H. G. L., "The Secular and Periodic Perturbations of the Orbit of an Artificial Earth Satellite", VII International Astronautic Congress, Rome, 17-22 September 1956.

15. Baker, R. M. L., Jr., et al., "Efficient Precision Orbit Computational Techniques", Los Angeles, California, University of California, Astrodynamical Report No. 3, 11 June 1959.

16. Pines, S., "Variation of Parameters for Elliptic and Near Circular Orbits", Astronomical Journal, Vol. 66, pp. 5-7, February, 1961.

17. Herrick, S., "A Modification of the Variation of Constants Method for Special Perturbations", Publ. Astron. Soc. Pacific, Vol. 60, pp. 321-323, 1948.

18. Space Systems Division of the Martin Company, "Orbital Flight Handbook", NASA SP 33 Part 1, Vol. 1, National Aeronautics and Space Administration, 1963.

19. Pitkin, E., "Integration and Optimization of Sustained-Thrust Rocket Orbits", Ph.D. Thesis, University of California at Los Angeles, 1964.

20. Fogarty, L. E., and R. M. Howe, "Flight Simulation of Orbital and Reentry Vehicles Part II - A Modified Flight Path Axis System for Solving the Six-Degree-of-Freedon Flight Equations", ASD Technical Report 61-171 (11), Wright-Patterson Air Force Base, Ohio, October 1961.

21. Kuiper, G. P., "The Earth as a Planet", The Solar System, Vol. II, Chicago, University of Chicago Press, 1954.

22. Jeffries, H., The Earth, 4th ed. Cambridge: The University Press, 1959.

23. MacMillan, W. D., The Theory of the Potential. New York: McGraw-Hill Book Company, 1930, p. 363.

24. Sterne, T. E., An Introduction to Celestial Mechanics. New York: Interscience Publishers, Inc., 1960, p. 38, pp. 116-126, pp. 188-198.

25. Ralston, A., A First Course in Numerical Analysis. New York: McGraw-Hill Book Company, 1965.

26. Henrici, P., Discrete Variable Methods in Ordinary Differential Equations. New York: John Wiley and Sons, Inc., 1962, pp. 66-83.

27. Zani, R. C., "A Computer Study of the Estimated Propagation of Errors in the Numerical Integration of Ordinary Differential Equations", Masters Thesis, Air Force Institute of Technology, Wright-Patterson Air Force Base, Ohio, 1967.

28. Van Putte, R. E., "The Use of Constraint Equations to Improve Trajectory Calculation on a Digital Computer", Professional Degree Thesis, University of Michigan, 1964.